THE RISE OF *ENDOCLADIA MURICATA*: PUNCTUATED CHANGE AT AN ABRUPT RANGE EDGE

A DISSERTATION

SUBMITTED TO THE DEPARTMENT OF BIOLOGICAL SCIENCES

AND THE COMMITTEE ON GRADUATE STUDIES

OF STANFORD UNIVERSITY

IN PARTIAL FULFILLMENT OF THE

REQUIREMENTS

FOR THE DEGREE OF

DOCTOR OF PHILOSOPHY

Luke John Hoot Hunt

June 2006

I certify that I have read this dissertation and that, in my opinion, it is fully adequate in scope and quality as a dissertation for the degree of Doctor of Philosophy.

Mark W. Denny (Principal Adviser)

I certify that I have read this dissertation and that, in my opinion, it is fully adequate in scope and quality as a dissertation for the degree of Doctor of Philosophy.

George N. Somero

I certify that I have read this dissertation and that, in my opinion, it is fully adequate in scope and quality as a dissertation for the degree of Doctor of Philosophy.

Fiorenza Micheli

I certify that I have read this dissertation and that, in my opinion, it is fully adequate in scope and quality as a dissertation for the degree of Doctor of Philosophy.

Judith Connor

Approved for the University Committee on Graduate Studies

ABSTRACT

Species borders are centrally important to ecology, and their dynamics are key to understanding how ecosystems respond to environmental changes. Range boundaries of habitat-forming species are especially important, because (by definition) these borders correspond to a shift in habitat type that impacts an entire community. Datasets of sufficient duration and resolution to identify non-linear biological responses to climate change are extremely rare. Because of the lack of data, and despite theoretical results to the contrary, it is commonly implied that biotic responses to changing climate will occur gradually and over similar timescales as changing climate. Here I report a detailed history of the strikingly sharp ecotone that is formed by the upper limit of the intertidal alga *Endocladia muricata* at Hopkins Marine Station (Pacific Grove, CA). The upper range limit of *Endocladia* tracks a high-temperature isotherm where lethal temperatures are experienced infrequently (once every few years). Thallus desiccation provides a nearly-complete refuge from lethal temperatures for fronds near the periphery of a clump. However, periods of growth are also reduced for these fronds, and this tradeoff may lead to intriguing patterns, including the fairy rings that are common in this species. Using historical photographs spanning the last century, I show that the upper range limit of *Endocladia muricata* has followed rising sea level up the shore. However, unlike the gradual increase of sea level, *Endocladia's* range-extension occurred in a single jump, that connected periods of relative range stability. Using computer simulations, I demonstrate that density-dependent facilitation between individuals can lead to both 1) sharply-defined species' range boundaries and 2) punctuated range shifts. Field experiments show that facilitation is important for *Endocladia* survival at the upper limit. In addition, the range edge persists in disequilibrium with environmental constraints, and this disequilibrium is a necessary condition for gradual environmental changes to generate punctuated range expansions. Facilitation between individuals has often been observed in canopy-forming species, such as many tree species. These feedbacks may lead to abrupt range shifts that have, so far, been overlooked because the empirical data are difficult to obtain. To this end, I present a new use of GIS tools that greatly assists with historical photographic comparisons. The final chapter develops a thermal model for calculating thallus temperatures from measured meteorological conditions.

TABLE OF CONTENTS

LIST OF FIGURES

LIST OF TABLES

ACKNOWLEDGEMENTS

I am so thankful for all the people who helped stoke me through grad school. First, Mark Denny has been an amazing teacher, deftly walking the line between advisor and best friend. He is always the first person I want to share a new idea with, and he expertly keeps me on the straight and narrow. Somehow Mark teaches people to think *better* –not just new ideas, but ones that cut closer to the crux. The Denny Lab thrives because of his leadership. And I try not to imagine being anywhere else.

Hopkins Marine Station is also an amazing place. The staff is replete with key people. Judy, John, Chris, Barbara, Freya, Bob and Peter each do the work of 10, and as a result, I have never been so immune from red tape in my life. In the library, Joe, Suzy and Jeanine make a crackerjack team. I was continually amazed by Joe, who would routinely find the most apropos articles in the greyest corners of the literature. Esther Trosow at the P.G. Museum was also a crucial contact and she allowed me to access some early photographs, while they were in the early stages of being archived.

The emeriti and former students of HMS were also a wealth of insight. Chuck Baxter pointed me to crucial references that would never have crossed my radar, and with John Pearse, he helped me place ideas in a long-term perspective. Peter Glynn provided much needed support, when I was trying to decipher conflicting lines of historical evidence. Chris Kitting kept me abreast of the required technology. And further a field, Art and Chris DeVries helped to keep my interests broad and my toolbox full.

My committee was totally, full-on super. Wow. Fio Micheli provided laser-like critiques with the perfect amount of optimism, and her lab has been a great crucible for refining nascent ideas. George Somero used his celebrity to unearth crucial photographs for the historical record. Furthermore, he always came up with new twists that broadened my scope, on everything from philosophy to methods. Judith Connor taught me to love my seaweed. She is so energetic and positive and everything seems to run more smoothly in her presence. I hope I grow up to teach like she does. Jim Watanabe is also an inspirational teacher, and while not officially on my committee, he was a prime advisor through it all. I am very grateful for the kindness of my advisors.

Upon arrival at Hopkins, Lorretta Roberson and Josh Rosenthal helped me settle in and they introduced me to the local edible fungi. George Leonard immediately got me into the field and thinking about ecological questions, while dodging waves in a flack suit. From the get go, Ben Hale was an essential sounding board and unique source of goofy brilliance. Elizabeth Nelson championed every alternative perspective (even substituting string beans for noodles) and her thoughtfulness balanced out the rest of the lab's propensity for "ready-fire-aim".

Nonetheless, hair-brained schemes and free ranging minds seem to be the backbone of the Denny Lab's genius. To the point, Luke Miller was a staid accomplice when mayhem looked promising, and the Mikes eagerly supplied this essential ingredient. Mayhem aside (and atop my desk) I don't know anyone more versatile and more game to help than Moose—no matter how many interests he was juggling, Moose always welcomed one more. Likewise, Patrick Martone was always available when I needed help. I could count on Martone to radiate contagious joy whenever I mentioned seaweed. When I needed cheering on, Katie was there, and she helped me to write more clearly. In the field, Tad Finkler, Joanna Nelson and Lisa Walling were all aces when I was in Antarctica. In particular, Lisa skirted many catastrophes that I set up for her, and the 1.9 million iButton data would be worthless without her help. Numerous friends and most of my family also helped out in the field. Early tides and headlamps enabled them to make the most out short vacations. Of special note, Vince Suich and Timothy Hunt have left their indelible mark, as masters of the hammer drill.

Steve Palumbi took a neophyte under his wing and demystified genetics in the style of Penn and Teller. In the Palumbi lab, Tom Oliver, Julie Alipaz and Adam McCoy all gave generously of their time and used small words. Tony DeTomaso and Will Luddington did the same, with more expletives. Jim Coyer proved that it was possible. Thanks you guys; I feel empowered like someone gave me a shiny new cheater bar.

I am grateful for the close-knit community at Hopkins. In the Fio Lab, Carrie Kappel infused us all with vision beyond grad school, Kim Heiman was always on my same wavelength, and Becca's energy never failed to provide some vicarious coffee. Steve Litvin

and Cheryl Logan fueled our bike rides and Kevin Weng was always catalyzing an adventure (more, more!).

Among of my favorite people to talk science with are Chris Harley, Christian Reilly and Brian Gaylord. Harley helped me see that everything needs an energized context. Moreover, he taught me that science is the most fun when belly-laughing counterpoints quality ideas. Talks with Christian always spiral fantastically out of control and make me read some new book, or at least plan to. Mostly we like to watch the ideas build and feel the sutures in our skulls spreading. Brian has a knack for asking the right question at the right time, and I only wish he were around more.

A strong cadre of friends and family was always ready to help wrangle slippery ideas, while hard at play. The ringleaders are Ginny, Larry, Ben and Heather Hunt, Aaron Solomon, Tad Finkler, Christian Reilly, and the Denny Lab. I could write an epic about all these guys. Most of "my" best ideas are theirs. One point I can't resist: Aaron cut down the run time of some of my programs by a factor of 10-100!

Finally, Heather is a saint in the order of Ph.D. spouses. She is my dream gal. She can jackhammer in a miniskirt by the light of a headlamp, she thrived aboard our 31-foot sloop, and with her I can pretty much do anything.

With people like these in my life, it's all good as gold. Thank you!

.

INTRODUCTION

"The most conspicuous landmark on the sheltered rocks near Pacific Grove is the upper limit, sharply marked in many places, of the turf of short seaweeds covering the lower parts of the shore."

– T.A. and Anne Stephenson (1972) summarizing observations from 1947.

Life's complexity largely results from connectivity across an interface. Fluxes across membranes cause biochemical and neural patterns that are the foundation of an organism's functioning. Similarly, at the community scale, where nature is often described as a mosaic of interacting patches (e.g., Kimura and Weiss 1964; Paine and Levin 1981; Hanski 1998), behavior at the range edge is critically important for ecosystem functioning. This central importance of species borders in ecology has been emphasized repeatedly, most recently by two working groups devoted to the subject (Laurance et al. 2001; Holt and Keitt 2005). In contrast to small-scale biological borders that are convenient for experiment (e.g., at the organ or cellular level), ecological interfaces often occur at large spatial and temporal scales that are unwieldy for the experimentalist. Consequently there is an abundance of theoretical insight on ecological borders and a relative paucity of experimental evidence.

The Problem

A large and growing literature highlights, on theoretical grounds, the possibility that species' ranges may respond abruptly and non-linearly to driving factors such as changing climate (Wilson and Agnew 1992; Wilson et al. 1996; Davis et al. 1998). Nevertheless, the accepted

mode of interpretation remains the gradualist model: small environmental changes cause proportionally small biotic changes, and the timescale of the biotic response mimics the timescale of the environmental change. When this assumption is used to set conservation and management policies, deviations from linearity (e.g. abrupt responses to gradually changing conditions) could drastically undermine our ability to make effective conservation and management decisions in the face of a changing climate.

Species that create habitat by forming a canopy or by aggregating together (e.g., rainforest trees, intertidal mussels, and turf algae) exemplify this difficulty. These species are especially important for achieving conservation and management goals because their survival is ecologically leveraged: canopy survival may determine the survival of an entire community association. However, ecological theory cautions that strongly mutualistic systems such as these are the very ones predisposed to having surprising dynamics (Wilson and Agnew 1992; Gurney and Lawton 1996).

Here I present a long-term biotic history of a canopy-forming species that shows profoundly non-linear behavior at the range edge, both in distance (see the quote at the beginning of this chapter) and in time (see Chapter 1, in which I discover an abrupt range extension). The historical record I present is unique in its combination of length and resolution, and the rest of my dissertation work takes advantage of the available history to better understand this sharply defined and ecologically significant border.

The Study System

The red turf seaweed *Endocladia muricata* (Post. & Rupr.) J. Ag. forms a prominent habitat on high intertidal rocks between Alaska and Southern California (Abbott and Hollenberg 1976). Hopkins Marine Station (HMS, Pacific Grove, CA), is near the center of *Endocladia's* latitudinal range, and is an ideal study site for a number of reasons. (1) Virtually all the relevant work on this species was done at HMS: In 1965, Glynn described the *Endocladia* ecosystem in minute detail, yielding a valueable "before range extension" snapshot of the community. In 1996 Hopkins Marine Station undergraduates Ashley Simons and Erin Leydig repeated Glynn's survey, and their work provides a "post-range-extension" view of this community. Furthermore, Susan Britting (1993) conducted the first in-depth

physiological experiments on *Endocladia* at HMS. (2) The intertidal zone is a reserve and working laboratory, where long-term field manipulations are possible. (3) The rocks offshore have a distinctive appearance and are particularly photogenic, which enabled me to construct the long-term photographic history. (4) The Gilbert Smith Herbarium at HMS contains specimens from before the range extension, thus a genetic perspective on this change is available from samples collected before and after the range extension. (This project is in progress, and it does not appear in my dissertation.) (5) Finally, HMS is close to long-term weather and tidal observatories (within 10 km) that provide essential context for understanding this history.

The Conclusions

In Chapter 1, I use historical photographs to reconstruct the history of *Endocladia's* upper range limit over the past century. Over the last 104 years, the climate has changed more-or-less gradually, with the most noteworthy change being a 24 cm increase in the sea level at HMS. The upper limit of *Endocladia* rose in conjunction with the rising sea level. However, most of *Endocladia's* range increase happened during the 7 years between 1963 and 1970. Thus, the history of the range edge consists of three periods: the range was relatively stable between 1897 and 1963; then between 1963 and 1970, the range extended upward dramatically; and since 1970, the range has again remained constant. This history prompts one of the major questions addressed in later chapters: why did the range extend suddenly, even though climate change occurred more gradually?

In Chapter 2, I show the possibility that abrupt spatial and temporal patterns may be causally linked. I use a computer simulation to show that density-dependent facilitation (or safety in numbers) can generate an abrupt range edge within a constant environmental gradient (Wilson and Nisbet 1997). I extend this model to show that density-dependence can also lead to punctuated range changes because it enables a range to persist out of equilibrium with environmental constraints. I refer to this as a state of *persistent disequilibrium*, which can give rise to step-like range changes if recruitment (i.e. successful dispersal) is episodic.

Chapter 3 is devoted to field experiments designed to test the ideas presented in Chapter 2. Field manipulation demonstrate that density-dependent facilitation is indeed important for

Endocladia clump survival at the upper limit. Frond mortality is significantly greater in small clumps than in large clumps, and this size-dependent mortality causes small clumps to die out at a much greater rate than larger clumps. This is the premise of the models in Chapter 2. Also following the predictions of Chapter 2, I show that the upper limit is in persistent disequilibrium with environmental constraints. I artificially triggered a range expansion, by transplanting *Endocladia* clumps higher than the current range limit. Transplanted clumps survived up to the elevation predicted from the sea level rise that has occurred since the last range extension of 1963-1970.

These first three chapters together suggest that gradual response to climate change should not necessarily be expected for habitat-forming species which have strong density-dependent interactions and episodic recruitment. Management policies for habitat-forming species should build in safeguards that acknowledge the importance of rare periods of range extension for these key ecological players.

Chapters 4 and 5 examine the thermotolerance and the temperature climate at the upper limit of *Endocladia.* Chapter 4 shows that lethal temperatures are only experienced when the thallus is hydrated, but not when it has dried. The protective role of desiccation in intertidal algae has not yet been considered by intertidal ecologists, and it is likely an important aspect of the turf "strategy" (Hay 1981) for *Endocladia.* At HMS, the upper limit retains its sharply delimited character, while undulating more than a meter vertically (60% of the tidal range). Chapter 5 explains the significance of these undulations: the upper limit changes elevation to track a high-temperature isotherm. Here, the response of the habitat-forming species reduces thermal variability for the associated community and provides ecological homeostasis. The thermotolerance of associated organisms can be plotted atop the risk curves for lethal temperature exposures to determine which durations of temperature stress are most likely to cause mortality in the field.

Chapter 6 presents a thermal model that makes it possible to use historical weather observations to hindcast the temperature and desiccation state of *Endocladia* simultaneously. This model estimates temperatures for fronds near the edge of an *Endocladia* clump, where temperatures could not be measured directly. Direct measurement was impossible because it was infeasible to set up data loggers with probes small enough to track frond

temperatures, yet sturdy enough to withstand the surf zone. These peripheral temperatures are compared to temperatures measured at the clump center in Chapter 5.

As a whole, this dissertation examines the remarkable range boundary and threshold in biodiversity that occurs at the upper limit of *Endocladia muricata*. I point out areas where the current work can be expanded, and I suggest opportunities for using *Endocladia* as a model system for studying range-edge phenomena and expanding ecological theory for habitat-forming species.

Chapter 1

PUNCTUATED BIOLOGY IN A GRADUALLY-CHANGING ENVIRONMENT: TRACKING THE UPPER LIMIT OF *ENDOCLADIA MURICATA* THROUGH THE 20TH CENTURY

1.1 Introduction

A large and growing literature highlights, on theoretical grounds, the possibility that species' ranges may respond abruptly and non-linearly to driving factors such as changing climate (Wilson and Agnew 1992; Wilson et al. 1996; Davis et al. 1998). In addition, theorists have pointed out general features, such as the presence of strong feedback cycles that predispose a system to nonlinear dynamics (Holling 1973; May 1977; Wilson and Agnew 1992; Schroder et al. 2005). Nevertheless, the accepted mode of interpretation remains the gradualist model: small environmental changes beget proportionally small biotic changes on a coherent timescale. When this assumption is used to set conservation and management policies (because there is no data to the contrary) deviations from linearity may drastically undermine our ability to make effective conservation and management decisions in the face of changing climate.

Species that create habitat by forming a canopy or by aggregating together (e.g., rainforest trees, intertidal mussels and turf algae) may exemplify this difficulty. These species are especially important for achieving conservation and management goals because their survival is ecologically leveraged: canopy survival may determine the survival of an entire community association. However, ecological theory cautions that strongly mutualistic systems such as these are the very ones predisposed to having surprising dynamics (Wilson and Agnew 1992; Gurney and Lawton 1996).

Here I present a long-term biotic history of a canopy-forming assemblage that shows profoundly non-linear behavior at the range edge, both in distance and in time. In central California, the upper range limit of intertidal turf-forming algae is an abrupt border, only a few centimeters wide, between a habitat of thick canopy [one that supports a rich fauna (Glynn 1965)], and a habitat that is, by comparison, bare rock (Figure 1-1). No sharp

environmental threshold is known to exist at the height of the range limit (Doty 1946; Underwood 1978), and it appears that this abrupt transition occurs within a smoothly-varying environmental gradient (see Chapter 5). Likewise no sharply-defined threshold in physical performance (Chapter 6) is known. Computer simulations (see also Chapter 2) have shown that sharp range boundaries such as the one seen here may develop within a smooth environmental gradient when performance is strongly density-dependent (Wilson et al. 1996; Wilson and Nisbet 1997), and this is likely the case for turf-forming seaweeds (Hay 1981; Scrosati and DeWreede 1998). Thus, a probable "sharpening" mechanism exists by which the punctuated biological pattern may form in the absence of a concomitant pattern in a physical driver. I will explore this mechanism of density dependence further in later chapters, but I introduce it here because it is one context in which the history of this upper limit must be considered.

Figure 1-1. The upper limit of turf algae (here *Endocladia muricata*) is often sharply marked on the intertidal rocks offshore of Hopkins Marine Station, Pacific Grove, CA.

I assembled a historical photographic record to document the upper range limit of this turf assemblage over the past century at Hopkins Marine Station, Pacific Grove, CA. In

combination with weather and climate records, the duration and resolution of this history makes for a unique perspective on an ecological border, and it provides an opportunity to question expectations based on shorter records. The upper limits of intertidal species are thought to be set by abiotic stresses associated with out-of-water periods during low-tide (Connell 1961), and consequently the expectation is that these intertidal range limits will change with local climate and with rising sea-level. Indeed, over the last century, the upper limit of intertidal turf algae rose approximately 35 cm (in comparison, sea level rose 25 cm). However, the range shift was unusual. While sea-level rose relatively gradually, the turf experienced a single brief episode of range expansion: 83% of the expansion occurred during a single 7-year period (between 1967 and 1970), and for the last 35 years the Endocladia upper limit has been remarkably stable. The cause of this range extension remains a mystery. There does not appear to be a concomitant step-like change in environmental conditions, nor is a probable environmental trigger evident.

I will conjecture that this punctuated range shift may be in response to gradually-changing sea level (see also Chapter 2). Between range shifts, the upper limit persists at a near-constant elevation that is in disequilibrium with environmental constraints. This disequilibrium may be sustained by density-dependent interactions that limit recruitment outside the extant range, except during unusual periods when the range "corrects." The result would be a series of punctuated corrections as the biotic upper limit tracks gradually-rising sea level.

1.2 Methods

1.2.1. Measurement of the Upper Limit

The upper limit of intertidal macroalgae appears as a line of high visual contrast on the rocks offshore of Pacific Grove, CA. This visual contrast makes it possible to clearly discern the upper limit in historical photographs and to compare past and present upper limits. I assembled a biological chronology using historical photographs from a wide range of sources (from personal collections to university archives, see Table 1-1) that showed the upper limit of canopy-forming macroalge on the rocks offshore of Pacific Grove, CA. Since 1947, the upper limit visible in the historical photographs can be identified as the

upper limit of the turf alga *Endocladia muricata.* Except where noted (2 photographs near Lovers Point, 1.5 km to the northwest) all of the photographs are from a 300-meter-long section of shoreline immediately offshore of Hopkins Marine Station. Details of the photographs used to construct this record are shown in Table 1-1.

Date	Source	Location	UL Species	Elevation Method
1895	Tuttle Collection, Pacific Grove Museum of Natural History (PG Museum)	Lovers Point	Turf	S
1897	HMS Archives	HMS	Turf	S
1900	Tuttle Collection, PG Museum	Lovers Point	Turf	S
1900	Tuttle Collection, PG Museum	Lovers Point	Turf	S
1920	HMS Archives	HMS	Turf	W
1929	HMS Archives	HMS	Turf	W
1930-34	Hewatt (HMS Thesis)	HMS	*Turf/Fucoid*	S
1947	V. Standish Mallory (1947 U.C. Berkely unpublished student papers on file at HMS)	HMS	*Endocladia*	W
1947	John Johnston (1947 U.C. Berkely unpublished student papers on file at HMS)	HMS	*Endocladia*	S
1949	Marcia White & Gerson Rosenthal (1949 U.C. Berkely unpublished student papers on file at HMS)	HMS	Turf	W
1956	Howard Feder (HMS Thesis)	HMS	*Endocladia*	W
1958	Margaret Bradbury	HMS	*Endocladia*	W
1962	Peter Glynn (HMS Thesis)	HMS	*Endocladia*	W
1962	Peter Glynn (HMS Thesis)	HMS	*Endocladia*	W
1963	Isabella Abbott	HMS	*Endocladia*	W
1963	David Egloff	HMS	*Endocladia*	W
1965	David Egloff	HMS	*Endocladia*	W
1966	Margaret Bradbury	HMS	*Endocladia*	W
1966	Simeon Baldwin	HMS	*Endocladia*	W
1974	Christopher Kitting	HMS	*Endocladia*	W
1975	Christopher Kitting	HMS	*Endocladia*	W
1976	Christopher Kitting	HMS	*Endocladia*	W
1977	Christopher Kitting	HMS	*Endocladia*	W
1978	James Watanabe	HMS	*Endocladia*	W
1984	HMS Archives	HMS	*Endocladia*	W

Table 1-1. For each photograph the table shows the sources, the location, the species forming the upper limit, and the method used for computing elevation changes, either water-level-derived contours (W), or size standards (S). Continued on the next page

1987	Christopher Kitting	HMS	*Endocladia*	W
1988	Christopher Kitting	HMS	*Endocladia*	W
1988	Emily Carrington	HMS	*Endocladia*	W
1991	Emily Carrington	HMS	*Endocladia*	W
1994	Christopher Kitting	HMS	*Endocladia*	W
2000	Luke Hunt	HMS	*Endocladia*	W
2001	Luke Hunt	HMS	*Endocladia*	W
2002	Luke Hunt	HMS	*Endocladia*	W
2003	Luke Hunt	HMS	*Endocladia*	W
2004	Luke Hunt	HMS	*Endocladia*	W
2005	Luke Hunt	HMS	*Endocladia*	S

Table 1-1 (continued from previous page).

To extract quantitative information about the historical upper limit, a current photograph was taken from the same location as each original photograph. The two photographs were then overlaid using the georeferencing tool in ArcGIS 8 (ESRI, Redlands, CA), which automates the rotation, translation, and scale adjustments (including those for non-parallel photographic planes) needed to precisely overlay the images. The upper limits were digitized in both the historical and current photographs and compared, to give a difference in upper limit elevation between the two timepoints.

In order for precise elevations to be gleaned from the oblique photographs, it was necessary to standardize the vertical scale throughout the depth of field. For example, in order to use a photograph of a crowd to measure heights of people, one must correct the vertical scale so that people farther do not appear smaller. In addition, if the photograph is taken from slightly above the crowd, heights will be underestimated, unless they are compared with a nearby vertical standard.

In this study, one of two methods for scaling elevations was employed for each photograph. This first method was used for 80% of the photographs (Table 1-1). Lines of constant elevation were determined as follows: photographs were taken on an incoming tide during extremely calm weather, when the flat surface of the sea intersected the rock in a horizontal contour line. The precise tide height of the water was measured by a pressure gauge (Sea-Bird Instruments, Bellevue, WA) approximately 50 m from the site. The pressure gauge was calibrated each day to water heights measured from a nearby benchmark at known tidal

elevation. Calibration was necessary to remove any changes in pressure that were not due to water depth. For each photograph of the site, during the incoming tide, the shoreline was digitized. The digitized shoreline provided a line of constant elevation on the photograph. The elevation lines and digitized upper limits were printed out on graph paper at a scale where one square represented approximately 1 to 2 meters horizontally. Therefore computing the elevations at each vertical grid line resulted in an approximately standard spacing between measurements. The distance between the upper limits was measured with calipers at each vertical grid line and scaled to the distance between contour lines, to yield an elevation difference. This method was useful for making a large number of comparisons in close proximity because a single set-up (placing and calibrating the pressure gauge) could be used, and photographs from different locations that matched different historical photographs, could be taken in a sequence. The time at which each photograph was taken was recorded, so the water level visible in the picture could be determined from the pressure records, and the elevation of the resulting contour line was known. Using this method, field measurements took one day for about 20 photographs. However, when comparing a single pair of photographs, or for widely spaced samples that could not be conveniently photographed in a timely sequence, it was impractical to wait for the extremely rare calm day and then spend many hours photographing the rising tide.

In these cases, I used a second method that employed a number of vertical size standards placed throughout the photograph (orange-painted sticks of known size nailed into seams in the rock or balanced vertically with modeling clay and braces). The number of references varied depending on the depth of field, but a size reference was placed for every few meters of horizontal (depth of field) offset. This method was time consuming, so one, or at most 2 photographic comparisons were possible during a low tide, and this method was best suited for comparing a few photographs.

Using GIS software for precisely overlaying historical photographs is likely to be useful in a variety of other long-term monitoring applications. It is quick (5-10 minutes per image), it allows precise indexing of images, and it does not require permanently-marked quadrats with framing standards. Only the photographer's position needs to be matched, and this can be determined from the original photograph.

Briefly, to find the original photographer's position, one stands so a landmark visible in the photograph is aligned with the same landmark in real life. Walking directly toward the chosen landmarks will keep them in line, and matching up a second landmark determines where along this line the original photographer stood. Once in the approximate area, fine tuning progresses by repeating this procedure for additional landmarks.

1.2.2. Environmental Records

The upper limits of intertidal organisms are thought to be set largely by physical environmental stresses, so a historical environmental record was essential for comparison with the upper limit history. Fortunately, Pacific Grove is close to sources of long-term environmental data (within 10 km) at the Monterey Tide Gauge and coastal weather stations in Monterey, CA.

Sea Level

Rising sea level decreases the time algae at the upper limit spend out of the water and at risk of extreme environmental conditions. In addition, rising sea level increases the amount of time turf algae at a given elevation are hydrated and potentially engaged in photosynthesis.

Monthly sea level in Monterey (relative to Mean Lower Low Water NTDE 1983-2001) was obtained from tide gauge records for 1974-2004. Before 1974, Monterey monthly sea levels were estimated from a linear fit to San Francisco levels (Monterey Tide Level=1.02 x San Francisco Tide Level - 0.041, $R^2 = 0.91$, for the period 1974-2004).

Benchmark survey data (National Geodetic Survey) indicate negligible vertical movement between Monterey and San Francisco prior to 1974.

Air Temperature

Extreme physiological temperatures are likely important in setting the upper range limits of a number of intertidal species (Schoenbeck and Norton 1978; Tomanek and Helmuth 2002), and air temperature is an important driver of body temperature in high intertidal marine algae (Bell 1995, Chapter 6).

Daily air temperature data were obtained from the National Climate Data Center (NCDC) for the Monterey station (about 9 km from the study site. Lat/Long/Elevation: 36° 35' N / 121° 55' W / 117 m above sea level). Missing data between April 1, 1963, and September 24, 1963, were filled using a linear fit between the Monterey station and the station at the Monterey Naval Airfield (approximately 7 km from the study site. Lat/Long/Elevation: 36° 36' N / 121° 52' W / 50m). The fit between the 2 locations for January 1, 1961, through December 31, 1963, is summarized as follows: for maximum daily temperatures $y=0.849x+0.757$, $R^2 = 0.85$, and for minimum daily temperatures, $y=1.078x+0.795$, $R^2 = 0.83$ (y=Monterey, x= Monterey Naval Airfield). The missing months of March, 1955, and December, 1950, were not filled. No missing data occur after September 24, 1963, and prior to that date (excluding the periods already discussed) 2.2% of the data are missing with a maximum number of 10 consecutive missing days in May, 1957.

The weather stations are somewhat inland from the coast (<3 km), and daily maximum temperatures at these sites are warmer than temperatures measured locally at Hopkins Marine Station. Moreover, between 1999 and 2005, temperatures at the two sites do not correlate as well as one might think ($R^2<0.5$ for days exceeding 25 ºC, Figure 1-2). The presence of a strong environmental gradient from the coast inland and the fact that weather data were not made at the precise location of the intertidal study site are unavoidable caveats in all of these weather records. In fact, the assumption that Monterey weather data match those at the study site is untestable in any records besides temperature because locally-measured data do not exist for comparison. Therefore, conclusions based on the minute details in these records are problematic, and I will limit discussion to their general features.

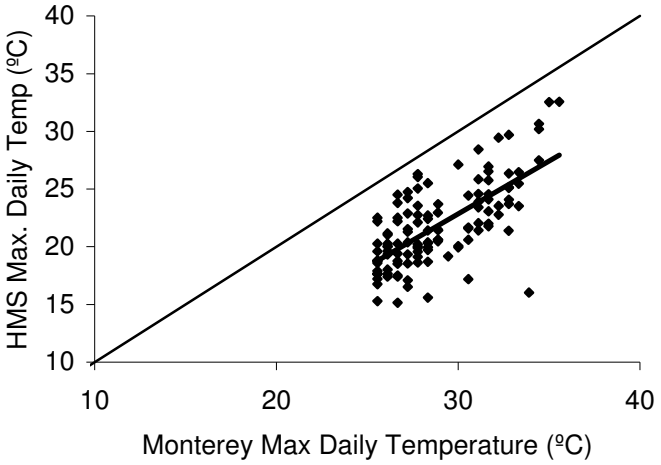

Figure 1-2. Comparison of maximum daily temperatures at a local weather station (~200 m from this site [HMS]) and temperatures (for days exceeding 25 ºC) at a long-term weather observatory in Monterey (<10 km from this site) for the period Aug. 1999 – Aug. 2005. HMS=0.92 x Monterey - 4.6, R^2=0.47. The line of unity is shown as reference.

Fog

Likewise, solar insolation is important in setting the body temperature of marine algae (Bell 1995, also see Chapter 6), and although no direct irradiance data are available, the presence of fog is a clue to potential irradiance. In addition, the fog record also provides an indication of the regional conditions that produce fog in Monterey.

The proportion of foggy days (visibility less than 6 miles for one hour) per month was obtained from Dr. Robert Renard (pers. comm.) for the period October 1963 through March 2004. In addition, the NCDC weather record notes days with fog. However, in the NCDC record no distinction is made between "no fog observed" and "nobody observing," and the definition of a "foggy day" appears to have been left up to the observer. Despite this seemingly fundamental problem, the NCDC data appear to be salvageable. The monthly number of fog days calculated from NCDC data align well with Renard's monthly data for the period of overlap (1985-2004) (Figure 1-3), and I have used early NCDC data to supplement Renard's observations for dates before October, 1963. In addition, the NCDC

data provide a daily record, and while I have not used the data in this manner, they appear to provide a nearly continuous daily fog record from 1983 until the present.

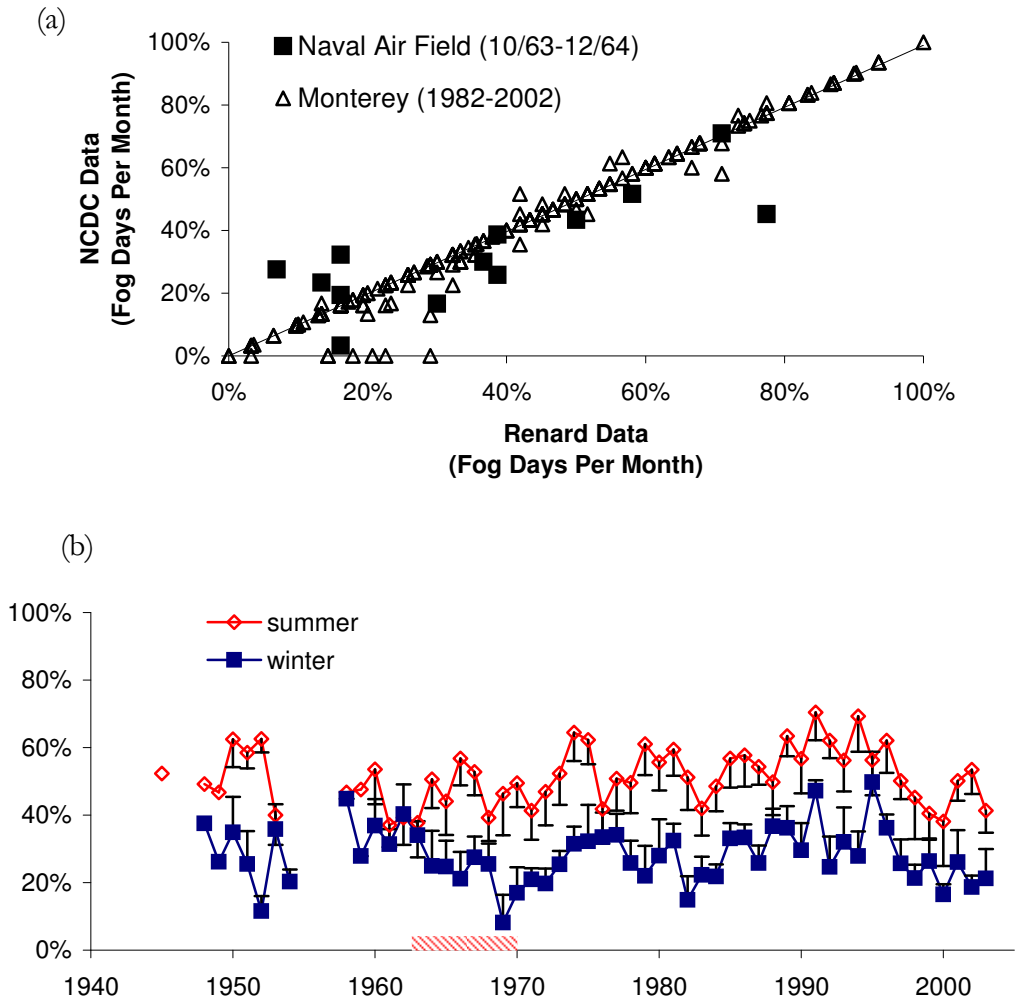

Figure 1-3. (a) Comparing data sources for Monterey Fog. The 2 questionable National Climate Data Center (NCDC) records related to Renard's Data. The line of unity is shown as reference. (b) Average proportion of fog days for summer (April-September) and winter (October-March). See text for details. Error bars = 1 S.E. The hatched red bar on the x-axis marks the period of *Endocladia* range extension.

Rainfall

Hypo-osmotic stress is another potential risk associated with high intertidal life and daily rainfall amounts were also obtained from the NCDC Monterey weather records.

Sea Surface Temperature

Sea surface temperature has been implicated in geographic range shifts in intertidal species (Barry et al. 1995). The daily surface water temperature at Hopkins Marine Station was obtained from long-term measurements.

Other Environmental Correlates

In addition to the above environmental factors, where direct stresses are implicated, two other sources of long-term data provide possible correlations: First, the El Niño/Southern Oscillation (ENSO) is a Pacific Ocean oscillation that results in increased summer tide levels and water temperatures in Pacific Grove, CA, with a period of approximately 7 years. ENSO conditions have likely triggered numerous biotic changes in marine communities (Tait and Dipper 1998). Second, the Pacific Decadal Oscillation (PDO) is a 10-30 year oceanographic cycle which has also been correlated with ecological changes in the Northeast Pacific Ocean (Francis et al. 1998).

The El Niño/ Southern Oscillation (ENSO) index used is the ICOADS 2.0 ENSO Index available at http://tao.atmos.washington.edu/data_sets/globalsstenso.

The Pacific Decadal Oscillation (PDO) index data are from http://jisao.washington.edu/pdo/PDO.latest (see Mantua et al 1997 for index details).

1.3 Results

1.3.1. Seasonality: Short-Term Stability of the Endocladia Upper Limit

The elevation of the upper limit showed little seasonality between 2002 and 2005 (Figure 1-4), and between 1974 and 1978 (photos from Dr. Chris Kitting, not shown). Clumps at the upper limit are seen to thin seasonally, but this does not affect the elevation of the upper limit. In addition, in many places the upper limit has not moved since 1970. A photographic comparison from 1978 is shown in Figure 1-5. This lack of short-term variability of the upper-limit (seasonal to a few decades) provides a necessary context for

interpreting historical pictures. For example, this constancy greatly simplifies the methods because comparisons can be made independent of season (and in some cases the month of the historical photograph is unknown) and low temporal variability enabled the characterization of the upper limit history with relatively few photographs.

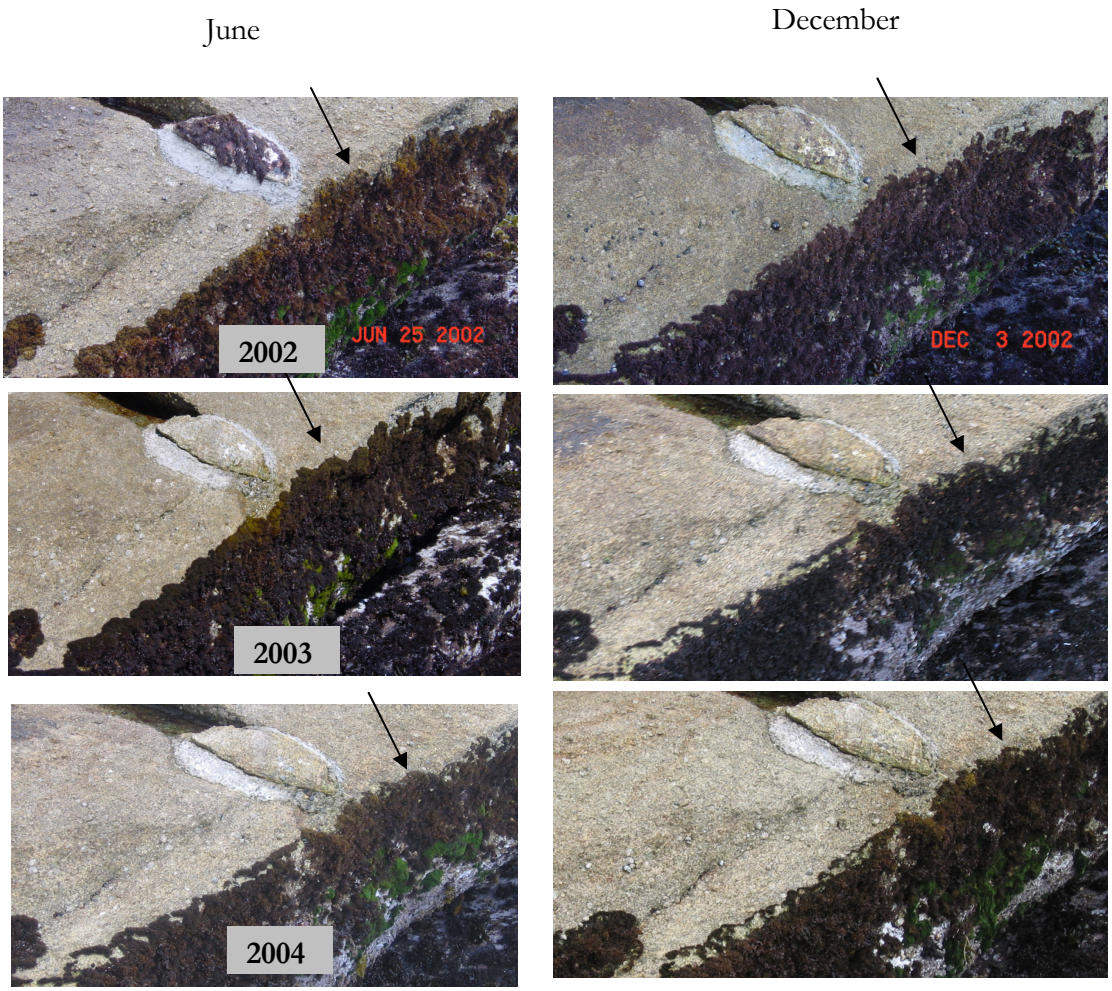

Figure 1-4. Seasonal variability at the *Endocladia* upper limit. Pictures from June (left) and December (right) between 2002 (top row) and 2004. Arrows indicate the same location in each photograph.

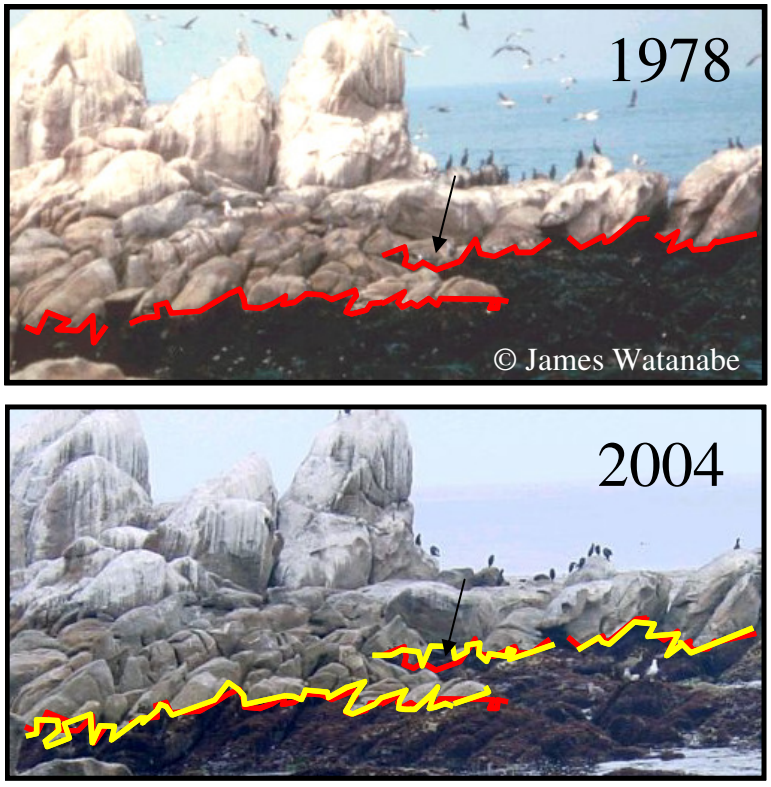

Figure 1-5. The upper limit of intertidal turf seen in 1978 (top) and in 2004. Both the present upper limit (yellow) and the 1978 upper limit (red) are shown. The upper limit retains its site-to-site patern of undulation between the two periods. The arrow marks a site where a rock has moved, and the upper limit has changed.

1.3.2. The Endocladia History

The historical timecourse for the upper limit of Endocladia is shown in Figure 1-6. The Endocladia upper range limit rose 36 cm over the last 107 years (from the difference between the average of the first three years and average of the last three years of the record). However 30 cm, or 83%, of that increase occurred during the seven years between 1963 and 1970.

Accordingly, there appear to be three distinct periods in the upper limit history: Between 1897 and 1962 the upper limit rose at an average rate 1.0 cm/decade (± 0.78 cm/decade, 95% confidence interval). Over this first period the slope was significantly different from zero ($p<0.011$). However, the slope is largely dictated by the first two points, and between

1900 and 1963 the slope (0.50 ± 0.87 cm/decade) was not significantly different from zero ($p>0.23$). During the period of upper limit change, between 1962 and 1970, the upper limit rose at 35 ± 18 cm/decade, and in the third period, between 1970 and 2004, the upper limit did not change significantly (-0.1 ± 0.03 cm/decade).

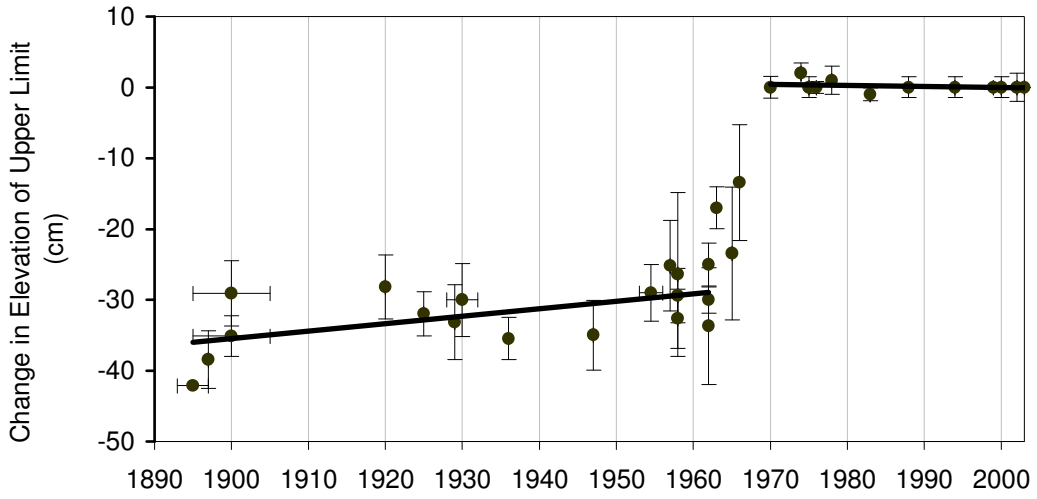

Figure 1-6. The Upper Limit (UL) of Endocladia muricata rose 30cm between 1962 and 1970, abruptly switching between elevations at which the upper limit was constant for decades. Slope= 1.0 cm/decade ± 0.74 (95% CI, $p<0.02$) for 1895-1960. However, between 1900 and 1970, the slope= 0.5 ± 0.87 cm/decade (non-sig.). For 1970-2004 slope=-0.17 cm/decade ± 0.34 (non-sig.). Endocladia vertical error bars are 1 S.E. for 10-30 point comparisons over 40-100m of shoreline. Horizontal error bars are maximal date uncertainty for undated photographs.

Figure 1-6 shows the *difference* in elevation between the current upper limit and the historical upper limit. Consequently, the standard errors shown do not indicate the variation in the upper limit elevation, but rather the variation in the upper limit *change* in elevation, relative to 2004. When the upper limit rose 30 cm, sites changed microhabitats. For example, at some sites, the upper limit may have moved up and into a crevice where it was shaded and experienced a more benign habitat, and at this site the change in elevation would likely be greater than at a site where the upper limit moved up and onto an exposed prow. Because

the change in Figure 1-6 is measured relative to 2004, only the error bars before the range shift include this site-to-site variation in range extension. Those afterward do not. The error bars after 1970 do not include the variability of the range shift because the upper limit in these years is compared to 2004, which is also after the shift. Therefore, since 1970, the small error bars indicate that the upper limit has remained quite constant at all locations, in addition to being constant in an average sense (see also Figure 1-5). In contrast, the large error bars before 1970 indicate that the upper limit rose different amounts at different sites, but because of the intervening change in range, they do not provide information about the site-to-site variability of the elevation of the upper limit at earlier times, nor do they indicate interannual variability during the period before 1970.

1.3.3. The Environmental History

The sea level in Monterey has been rising at an average rate of 24 cm per century over the last 104 years (Figure 1-7, Table 1-2). The three periods shown are the three periods of *Endocladia* upper limit history: stasis, rise, and stasis. Approximately 50% of the residual variation about the linear trend in sea level is due to the annual and semi-annual tidal cycles (frequencies in the range 0.988 to 1.017 years and 1.986 to 2.0144 years). The average rate of sea level rise remains unchanged when this known variability is removed [by subtracting these frequencies from the spectrum (Levine et al. 2002)], and upon removing this variability, significant variation in the rate of sea-level rise is detectable among the three putative periods ($p<0.04$). Although the rate of sea-level rise is significantly greater during the period of *Endocladia* rise, the overall change in sea-level during this period is 6 cm, if calculated from the regression slope, and 4 cm, if calculated as the difference in sea-level elevation between the five years before and the five years following the period of change. In other words, even though there may have been a period of more rapid sea-level rise between 1963 and 1970, the 4 to 6 cm change in sea-level is nowhere near the 30 cm needed to keep pace with the *Endocladia* movement during its range transition.

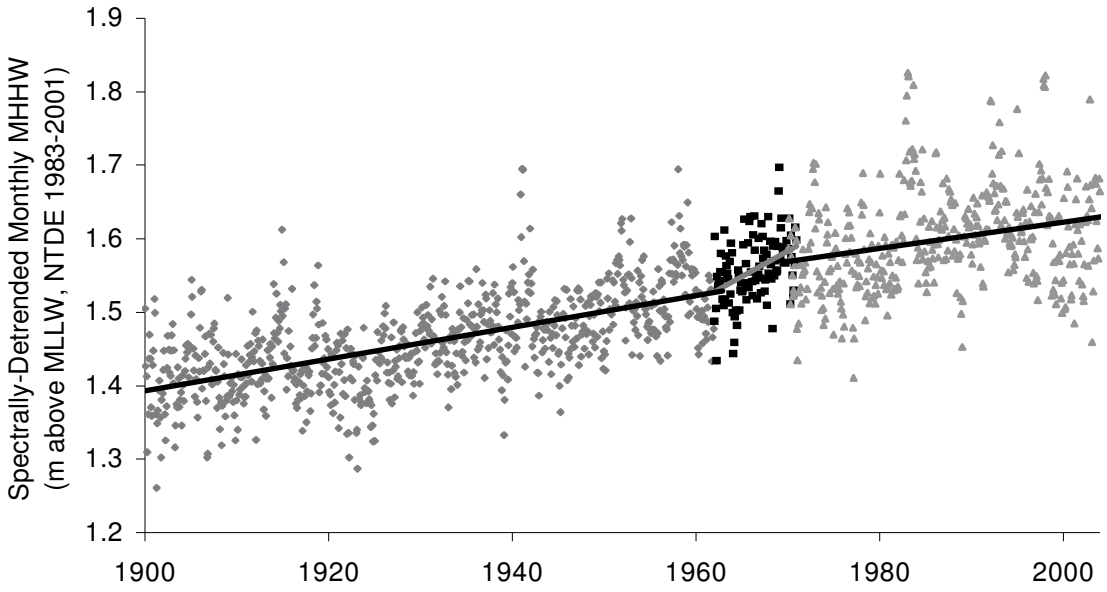

Figure 1-7. Monthly Mean Higher High Water (MHHW), in Monterey, CA, has been rising at an average rate of 24 cm per century over the last 100 years. Lines show the regression for the various periods in the Endocladia history: the first period of relative stasis (grey), the rapid UL increase (black) and the second period of stasis (grey). Slopes are significantly different during the 3 periods ($p<0.04$, see also Table 1-2). However the magnitude of the rise (4 to 6 cm) during the period of *Endocladia* range extension is much less than the UL rise (30 cm). Because *Endocladia* inhabits the upper intertidal zone, MHHW is chosen as a more ecologically relevant reference than the chart datum, Mean Lower Low Water (MLLW).

A further well-known pattern is visible in Figure 1-7: ENSO years appear in the tide record as periods of temporarily increased sea levels, which occur when the ENSO-produced wave of warm water arrives (for example, the ENSO year of 1983 is particularly visible).

No step-like changes that parallel the Endocladia record are evident in any of the weather records for Monterey (Figure 1-8). These data are difficult to interpret quantitatively in light of *Endocladia*'s range shift, and I relegate further description to the discussion.

Period	Monthly MHHW	Spectrally-Detrended MHHW	Summer MHHW (Apr.-Oct.)	Winter MHHW (Nov.-March)
1900-1962	2.2 ± 0.30	2.1 ± 0.19	2.3 ± 0.37	2.0 ± 0.54
1962-1970	8.0 ± 6.1	**7.4 ± 3.5**	3.7 ± 6.3	10.0 ± 7.5
1970-2004	1.9 ± 0.87	1.8 ± 0.65	2.0 ± 1.3	1.6 ± 1.8
0verall (1900-	2.4 ± 0.15	2.4 ± 0.10	2.3 ± 0.2	2.5 ± 0.29
19-yr running avg.	2.6 ± 0.0			

Table 1-2. Comparing average rates of sea level rise (slope ± 95 % confidence limits in cm/decade) for periods suggested by *Endocladia's* history. Slopes are less certain for the short period of *Endocladia* rise (1962-1970) than in the longer periods on either side. The significantly-increased slope in the spectrally-detrended tide record (cycles near annual and semi-annual removed, see text) is in bold. All others are non-significant.

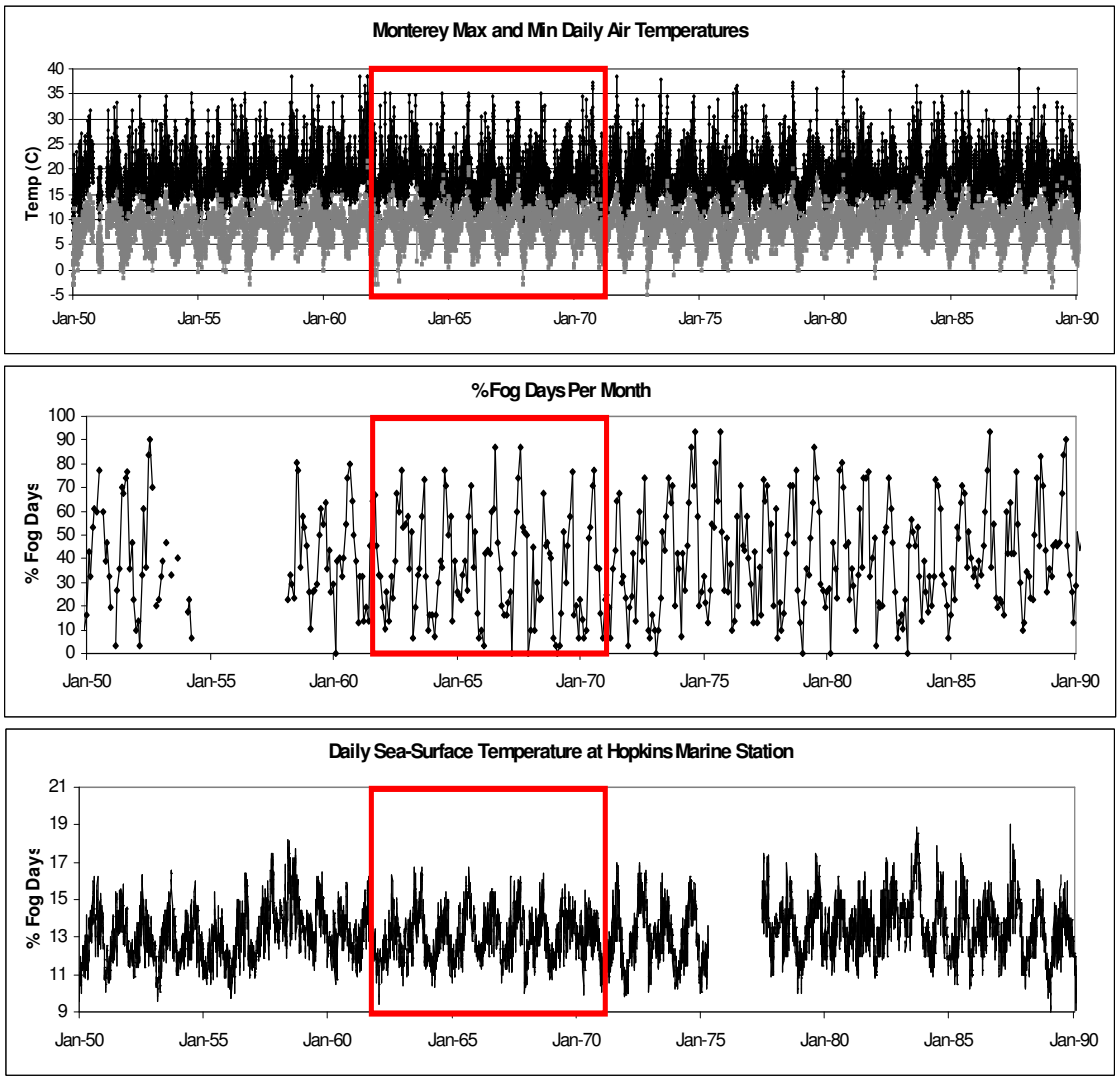

Figure 1-8. Monterey environmental data around the period of the *Endocladia* range-shift (in red box). Figure 1-8 is continued on the following page.

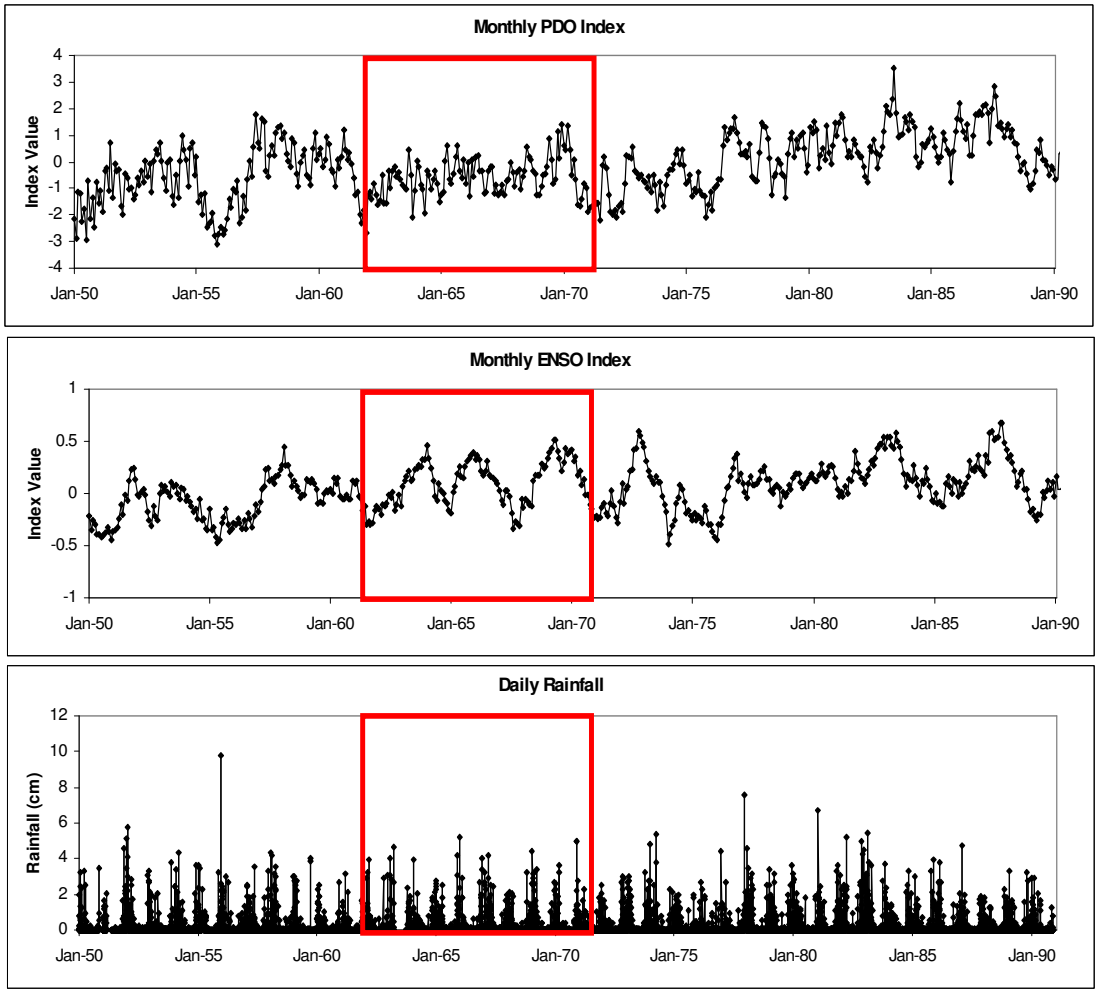

Figure 1-8 Continued

Otters

Following its near extinction by early fur hunters, the range of the California Sea Otter expanded northward from the Big Sur coast where a small population was re-discovered in 1938 (Kenyon 1969; Woolfenden 1979). The repopulation of the kelp beds near Hopkins Marine Station (HMS) coincided exactly with the range extension of *Endocladia:* 1963 was the first year otters were again found in Monterey Bay, and by 1970, 140 animals inhabited the kelp beds offshore of HMS (Judson Vandiver pers. comm.). As many as 18 otters were seen foraging in the intertidal mussel beds of HMS, and researchers at the marine station noticed that these groups decimated the mussel beds in a matter of days (Judson Vandevere, Alan Baldridge pers. comm.). Otters are significant predators and keystone species of the kelp-forest community (Estes and Palmisan 1974), and because they prey on large grazers,

their presence markedly affects subtidal algal abundance (Estes and Duggins 1995). However, otters do not frequently forage in the *Endocladia* habitat at HMS, and Kovnat (1982) failed to show any ecological effect of otters on the intertidal community at HMS. In addition, Sagarin et al. (1999) repeated a pre-otter intertidal survey (1931-1933) and found no significant decrease in any of the moluscan grazers (from the genera *Littorina* and *Lottia)* of *Endocladia*. Rather, when abundances changed, these authors found that grazer populations had *increased*. One final comparison suggests that otters are an unlikely candidate for provoking the range extension of *Endocladia*. Glynn (1965) described the community in the mid-*Endocladia* zone prior to the otters' arrival in 1963, and in 1996 HMS undergraduates Ashley Simons and Erin Leydig (1996) re-surveyed the community near Glynn's sites, and did not find a significant difference in the number of limpet grazers (as a pooled group). In summary, although otters are important for structuring subtidal communities, in this case, their serendipitous arrival appears to be a red herring, and so far I have been unable to link their arrival to any likely mechanism of *Endocladia* change.

1.4 Discussion

The upper limit of turf algae was largely stable for 93% of the last century. However this is not the "average" trend of the upper limit. Two periods of relative range stability (the first at least 66 years long, the second presently 34 years long) were linked by an abrupt upper-limit rise between 1963 and 1970. The magnitude of this shift greatly exceeds the inter-annual variability (> 44 standard errors of the between-year mean upper limit change over the last 34 years), and represents 18 percent of the tidal range (diurnal range, Monterey Tide Gauge).

The climate record during 1963-1970 appears "normal," and I see no likely event in the environmental history that would trigger a range expansion. For example, between the beginning of 1963 and September, 1970, there were no days during which the air temperature exceeded 35ºC. This might be remarkable, but for the occurrence of a similar period in the 1950's. And similarly, 1961 was a year with four unusually high temperatures (>35ºC), three of which exceed 38ºC and two of these were on consecutive days. However, 1978 and 1980 were also unusually hot. 1970 had three days above 35ºC and 1980 had two

consecutive days above 38ºC. Thus I find it difficult to regard the period 1963-1970 as unusual in terms of the environmental data available.

The sea-level rise (24 cm) is similar in magnitude to the *Endocladia* rise (36 cm); however, the sea level rise was gradual in comparison. If the *Endocladia* rise was a "correction" event triggered by unusual circumstances (such as a banner recruitment year, see Chapter 2) one would expect a trigger today to lead to a range shift corresponding to the sea level rise since 1970, or 8.75 cm. In Chapter 3, I artificially triggered an *Endocladia* range extension by transplanting large clumps upwards. In this case, the average upper limit was elevated an average 9.5 cm, which is similar to that expected by extrapolation from the sea-level trend.

One possibility that I have not yet examined is that the upper-limit rise was due to a genetic change, for example a cryptic invasion. Preliminary data (Hunt and Coyer unpublished) suggest that there is substantial sequence variability in the ITS-1 and ITS-2 loci among populations of *Endocladia*. This variation could be used to "map" sequences from herbarium specimens collected in Pacific Grove, CA before and after the range shift onto their current distributions. If the range shift coincided with a genotypic change that implicated an invasion (for example, the colonization of HMS by a southern genotype); the relative performance (e.g., the thermotolerance) of the hypothetical populations before and after the change could be investigated by utilizing extant populations However, to date I have been unable to obtain adequate sequence data from herbarium specimens.

The historical record I present here is unique among range limit data sets because of its remarkable length and resolution. The record is unusual because it documents a punctuated range shift with a surprisingly long time scale—the pattern only emerges at a timescale longer than those typically considered. For example, manipulative studies in the intertidal zone seldom last longer than ten years (notable exceptions include Denny and Paine 1998; Connell et al. 2004) and twenty years is considered long-term monitoring (Dye 1998; Menconi et al. 1999; Foster et al. 2003). In the few cases where studies are of adequate duration to detect long-term nonlinearities of the sort observed here, (Barry et al. 1995; Sagarin et al. 1999; Munda 2000), the comparison is based on very few points in time, and therefore the timescale of any intervening change remains largely unknown. Thus, the usual

experimental frameworks could discover either the stability of the upper limit or the shifting range, but not both.

If the range limit shifts rapidly in one direction, the tendency is to look for a concomitant threshold in a physical driver. That is, the location of the upper limit is presumed to be proportional to some factor(s) of the environment unless there are data suggesting otherwise. Or in a more extreme interpretation, discontinuous ranges may be considered *de facto* evidence for discontinuous environmental conditions (Caughley et al. 1988). The upper limit of *Endocladia* challenges this assumption on two fronts. The historical data show that the range changed in a punctuated manner, but so far, there is no candidate for a rapidly changing cause. The *Endocladia* range rapidly transitions in space, as well as through time, and experiments in later chapters will focus on the abrupt nature of the current upper limit (because this pattern is experimentally tractable on the timescale of a thesis and the historical pattern is not).

The assumption of coherent proportional response is most often made out of necessity, when insufficient data are available. However, there is both long-standing and growing evidence from the theoretical literature (see Chapter 2) that points out exceptions on theoretical grounds. Thus, the possibility of discontinuous range dynamics is well documented. The occurrence of such events is less well accepted by the scientific community (Schroder et al. 2005) and largely unknown outside that community (Walker and Meyers 2004), where management decisions are being made. In this context, the upper limit of *Endocladia* provides a good case study, and I suggest that for canopy-forming species (where individuals are strongly interdependent), inferring punctuated dynamics is at least as strongly supported as inferring a proportional response. Furthermore, the boundaries that are most conducive to study are those that are sharply defined (such as the border of *Endocladia*), and therefore at a greater likelihood of having feedback loops (see also Chapter 2) which lead to rapid switching (Wilson and Agnew 1992; see also Bella et al. 1994). Since communities are often limited by canopy-forming species (removing the canopy removes the community) I suggest that gradualist thinking must seriously be questioned when considering range boundaries for these communities.

Chapter 2

GRADUAL CHANGE AND PUNCTUATED RESPONSE: SIMULATING DISEQUILIBRIUM AT THE UPPER RANGE LIMIT OF *ENDOCLADIA MURICATA*

2.1 Introduction

2.1.1. A Conceptual Framework

Whether a species range limit is perceived as a static "line" or as a moving front largely depends on the time scale considered. These static and dynamic viewpoints have led to two different conceptualizations of the range edge: the static view considers the range as a feature to be mapped, while the dynamic view regards the range edge as the current state of a propagating invasion (Kinlan and Hastings 2005). The literature largely reflects this split. Ecological physiologists consider the range to be a more-or-less static feature, and this viewpoint emphasizes the importance of physiological constraints in setting species borders. In contrast, "invasion biologists" emphasize moving borders and the population-level phenomena that set these borders, when the environment is not limiting and further habitable space is left unoccupied. The essence of the split, however, is not between dynamic and static viewpoints, but rather between cases where range limits are largely in *equilibrium* with environmental conditions [e.g., a "zone", (Stephenson and Stephenson 1949; Terborgh 1971; Caughley et al. 1988)], and cases where range limits are *not* in equilibrium with environmental conditions [e.g., an invasion or a transient patch (Levin 1974; Keitt et al. 2001; Holt et al. 2005)].

On one hand are the biotic "zones" of montane and intertidal systems, which are perceived to be in equilibrium with environmental conditions; that is, survival (or carrying capacity) is zero outside the extant range. On the other hand, the range of a species that is invading pre-existing habitable area is not limited by environmental constraints. Rather, survival outside the current range is possible (this can be demonstrated by artificially seeding populations beyond the range limit), but in nature, historical constraints limit the species' distribution.*

* This is, of course, a generalization that can be pressed too far, and to insist that species which have yet to colonize the greenhouse at McMurdo Station , Antarctica are in disequilibrium, would eliminate the utility of this heuristic.

For example, the range may be expanding from a source population and be limited by a finite rate of dispersal.

The distinction between equilibrium and disequilibrium range limits is important when considering species' response to climate change. An equilibrium response occurs when a species' range extends at the same rate as new habitable area is created. In this case, the range is always environmentally constrained. Alternatively, if successful dispersal (i.e. recruitment) is episodic the range may sometimes be dispersal-limited and periodically "correct," expanding to the environment limits during periods of high dispersal. In this case, the range may experience periods of both equilibrium and disequilibrium, depending on the magnitude of dispersal.

Equilibrium ranges are intuitive: the range ends where the species can no longer survive. Disequilibrium ranges are more conceptually interesting, and there is a rich literature devoted to modeling species invasions in which suitable habitat is left unoccupied (May 1977; Keener 1987; Wilson and Agnew 1992; Lewis and Kareiva 1993; Wilson and Nisbet 1997; Keitt et al. 2001; Holt et al. 2005). These models universally incorporate density-dependent terms (e.g., Allee effects decrease population viability at low densities and facilitation increases survival at high densities). Under the proper conditions, density dependence may lead to ranges that are locally stable (Wilson et al. 1996; Keitt et al. 2001), even though they are not in equilibrium with environmental constraints. Here local stability differs from my definition of a range in equilibrium with environmental conditions: a range in equilibrium fills all the habitable space, whereas a locally stable range may end, leaving suitable habitat beyond the range edge.

Stability, however, is not necessary for a range to persist for long durations in disequilibrium with environmental conditions. A slow rate of range extension (e.g., slower than the rate of climate change) is sufficient to produce disequilibrium range boundaries (Okubo 1980; Lewis and Kareiva 1993; Taylor et al. 2004) because habitable area is formed faster than it is filled. In fact, in the field, it is often difficult to distinguish stability from slow rates of change (Schroder et al. 2005). Furthermore, natural variation works to eliminate local stabilities. (For example, consider balancing a marble on an upside-down bowl. This may be

possible if the bowl is stationary, but not if the bowl is randomly jiggled. In this case, random perturbation eliminates the locally stable, balanced state). Holling (1973) emphasized that, in a fluctuating environment, stability per se does not assure the persistence of an established state. Rather the *robustness* of the stability (ecological resilience) is crucial to the persistence of stable states in the real world. To date, models of species ranges have seldom included environmental stochastisticy (Keitt et al. 2001; Dennis 2002), and conditions of robust range stability have not yet been well-characterized. Therefore, the model I present does not attempt to generate range stability in a changing environment. It is sufficient here to demonstrate the existence of persistent states of disequilibrium.

2.1.2. Modelling Endocladia's Upper Limit

This simple simulation exhibits two threshold-like features that I have observed at the upper range limit of *Endocladia muricata* and that do not appear to be linked to environmental discontinuities. First, the upper range limit of *Endocladia* is sharply defined; however, there is no known environmental threshold that co-occurs at the range edge, and the sharp range edge appears to exist within a smooth environmental gradient. This case is identical to that studied by Wilson et al. (1996) and Wilson and Nisbet (1997), and the model I present is similar to that studied by these authors.

The second simulated feature of the *Endocladia* upper limit is that it persists in disequilibrium with current conditions. This is shown in Chapter 3 by experiments in which *Endocladia* transplanted above the current range limit continues to survive more than 4 years after transplantation. In a changing environment, Allee effects could slow the potential response of a range edge (Lewis and Kareiva 1993; Taylor et al. 2004) and lead to a range boundary that is in persistent disequilibrium with environmental constraints. Chapter 3 also shows a strong Allee effect: small clumps (or equivalently low-density populations made up of small clumps) suffer higher mortality than do larger clumps.

In this light, the simple simulation I present combines the results of Wilson et al. (1996, 1997) and Taylor (2004) to demonstrate that density-dependence, coupled with a smooth environmental gradient that shifts through time, (e.g., rising sea level) is sufficient to explain the perplexing history of *Endocladia's* upper range limit (Figure 1-6). If dispersal is episodic,

the range may sometimes be dispersal-limited and periodically "correct," by expanding to the environmental limits. In this case, the range may experience periods of both equilibrium and disequilibrium, depending on the magnitude of dispersal, and as long as colonization episodes are sufficiently rare (approximately once per century), the upper limit would track gradually rising sea level in the discontinuous manner seen in Chapter 1.

2.2 Methods

This simulation is a cellular automaton similar to that in Wilson et al. (1996,1997), which was also used to simulate the estuarine invasion of the grass *Spartina alterniflora* through a uniform environment (Taylor et al. 2004). The main feature is density dependent growth and mortality, and except for different "rules," the simulation is similar to Conway's game of life (Gardner 1970). The simulation is performed on a square lattice of 100 x 100 cells. When determining local density, diagonal cells are not counted; therefore an occupied cell can have between 0 and 4 occupied neighbors (Figure 2-1). Cells at the edge of the lattice (the edge of the "universe") do not have a full complement of neighbors, and these edge cells are maintained in their initial, randomly-assigned state throughout the simulation.

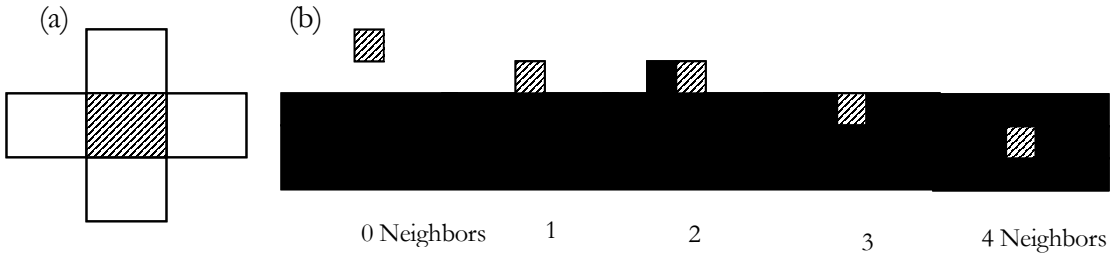

Figure 2-1. (a) Possible neighbors around a central (hatched) cell. (b) Cell positions showing 0-4 neighbors. In order for a border to become established, the death rate must exceed the birth rate for < 2 neighbors (patches above the upper limit), while for > 2 neighbors (patches below the upper limit), the birth rate must exceed the death rate. Once the border is established, it will remain stationary only where the birth rate equals the death rate given 2 neighbors. Otherwise random births (or deaths) at the range edge will expand horizontally and eventually lead to changes in the range.

The survival of an occupied cell is determined by both a vertical mortality gradient (suggestive of the intertidal zone, highest mortality is at the top of the lattice [Figure 2-2]) and the density-dependent mortality term (Figure 2-1, Table 2-1), which depends on the number of neighboring cells occupied. The density-dependent mortality of a cell is added to the local value of the mortality gradient to determine the mortality of a cell at a particular location. For example, if a cell has 2 neighbors, the corresponding density-dependent mortality is 0.1 (Table 2-1). At an elevation of 80 units, (Figure 2-2a) the density-*independent* mortality is 0.5; therefore the combined mortality for a cell with 2 neighbors at an elevation of 80 units is 0.6, or 60%.

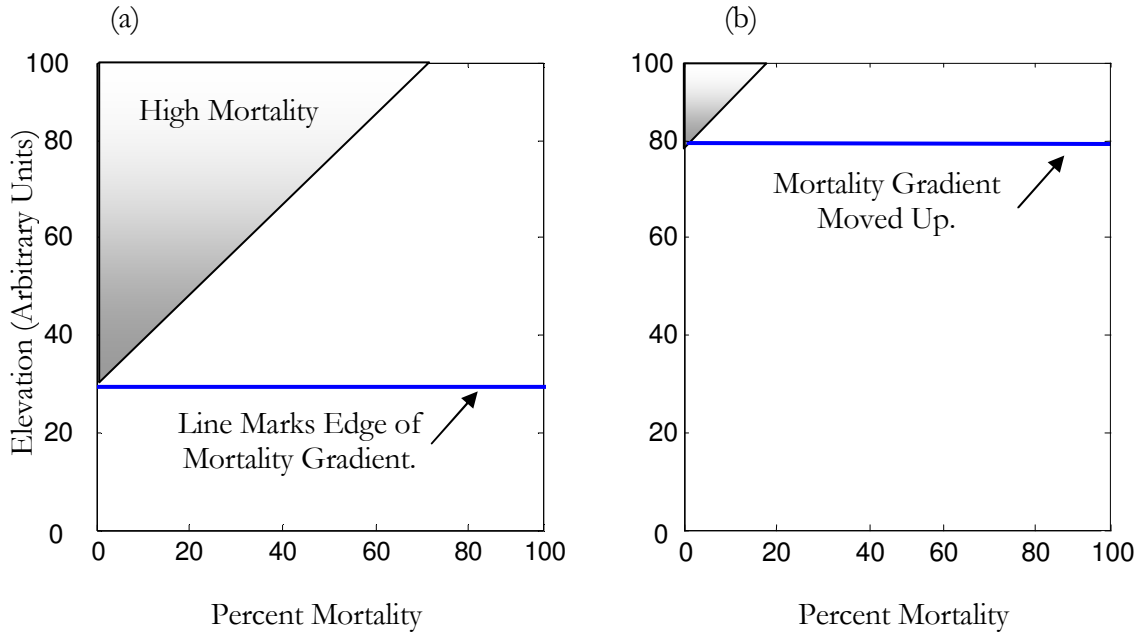

Figure 2-2. The mortality gradients used in these simulations are shown. The blue line marks the edge of the mortality gradient, where the overall mortality equals the density-dependent mortality plus zero (the gradient contribution). Panel (b) shows the mortality gradient in (a) shifted upwards, for instance mimicking sea-level rise after a number of years.

Unoccupied cells are filled at a rate solely determined by the density of neighbors, which is independent of elevation. I define "birth" as filling an unoccupied cell, and "mortality" as

clearing an occupied cell. Possible mechanisms for density-dependent birth rates are clonal growth and very local dispersal. Self-shading within a clump and resistance to wave scouring (i.e., mechanical removal) are mechanisms for density-dependent survival. The density-dependent mortality and birth rates used are shown in Table 2-1.

Number of Neighbors	0	1	2	3	4
Fast Birth Rate	0.001	0.01	0.1	0.3	0.8
Slow Birth Rate	0.0001	0.001	0.01	0.3	0.8
Mortality Rate	0.2	0.05	0.1	-0.5	-0.8

Table 2-1. Values used in the simulation for birth and mortality rates given 0-4 neighbors. "Fast" birth rates are 10 times "Slow" birth rates for patches at or above the range edge. Rates within the range remain constant. Density-dependent mortality rates are added to the local value within the mortality gradient (Figure 2-2) to calculate the overall mortality rate for a given cell.

During each iteration, a random number between 0 and 1 is drawn for each cell. This random number is either compared to a cell's birth rate (if the cell is unoccupied) or death rate (if the cell is occupied), and if the number is less than the cell-specific rate, the cell changes state. For example, on a given iteration, if an empty cell has a birth rate of 0.6, and the random number drawn for this cell is 0.5, the cell will be filled. However, if the random number were 0.8, the cell would remain empty. On average the cell would be filled 60% of the time.

2.3 Results

2.3.1. A Feel for General Model Behavior

In order for a border to become established, two conditions are necessary: The death rate must exceed the birth rate for < 2 neighbors (patches above the upper limit, Figure 2-1b); otherwise, the range will not die back above the upper limit. And the range will not fill in below the upper limit unless the birth rate exceeds the death rate for > 2 neighbors. Once the border is established, it will remain stationary only if the birth rate equals the death rate, given 2 neighbors. If the 2-neighbor rates are unequal, random births (or deaths) at the range edge (leading to cells with 2 neighbors, see Figure 2-1b) will gradually expand horizontally and eventually lead to changes in the range. For example, "holes" in the range edge will grow if the 2-neighbor birth rate is less than the 2-neighbor death rate.

2.3.2. Simulation Results

Figure 2-3 shows the development of a sharp species border within a smoothly varying environmental gradient. The initial lattice is randomly filled with 20% occupied cells. Under conditions of "high" birth rate (Table 2-1), the transient accretion patterns (Figure 2-3a, 50 iterations) are rapidly filled in. However, reducing the birth rate slows the rate of filling. These transient patterns are suggestive of patterns on low-intertidal rocks (Figure 2-3b). The patterns seen in the field have changed little in the last four years (indicating low dispersal), and these patterns are being tracked with periodic photographs to determine their permanence.

(a)

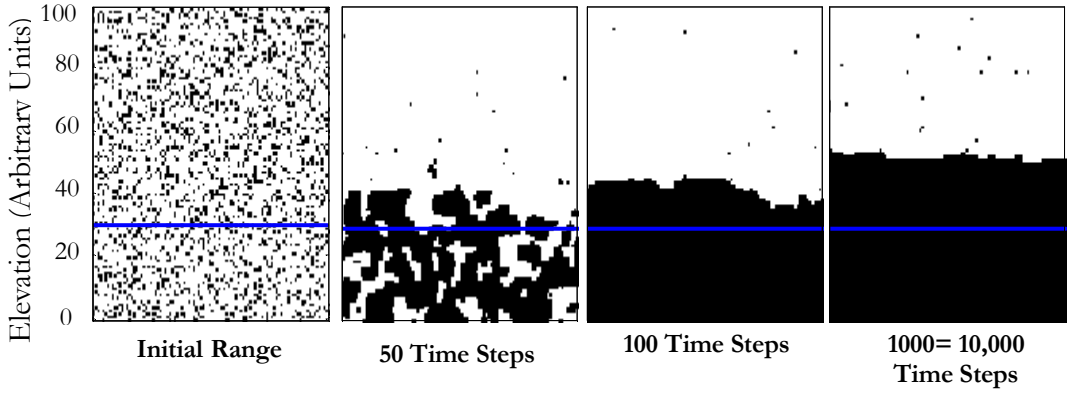

(b)

Figure 2-3. (a) A sharp upper limit develops within the constant environmental gradient above the blue line [see also Wilson and Nisbet (1997)]. The range has stabilized within 1000 iterations under "high" dispersal (values in Table 2-1). The transient pattern after 50 iterations is similar to the natural pattern shown in (b). The pattern in (b) has changed little between 2002 and 2006, which suggests that 50 iterations under "high" dispersal conditions is substantially longer than 4 years under current natural dispersal conditions (in the simulation the pattern is filled between 50 and 100 iterations, while in the field, there is little change in 4 years).

Once a sharp upper limit is established, the range responds rapidly to changes in environmental conditions (Figure 2-4a) as long as dispersal remains high. However, slowing the dispersal rate (Figure 2-4b) results in a slow response of the upper limit to environmental changes and persistent disequilibrium. This model is insufficient to generate an upper limit that is stable in a changing environment.

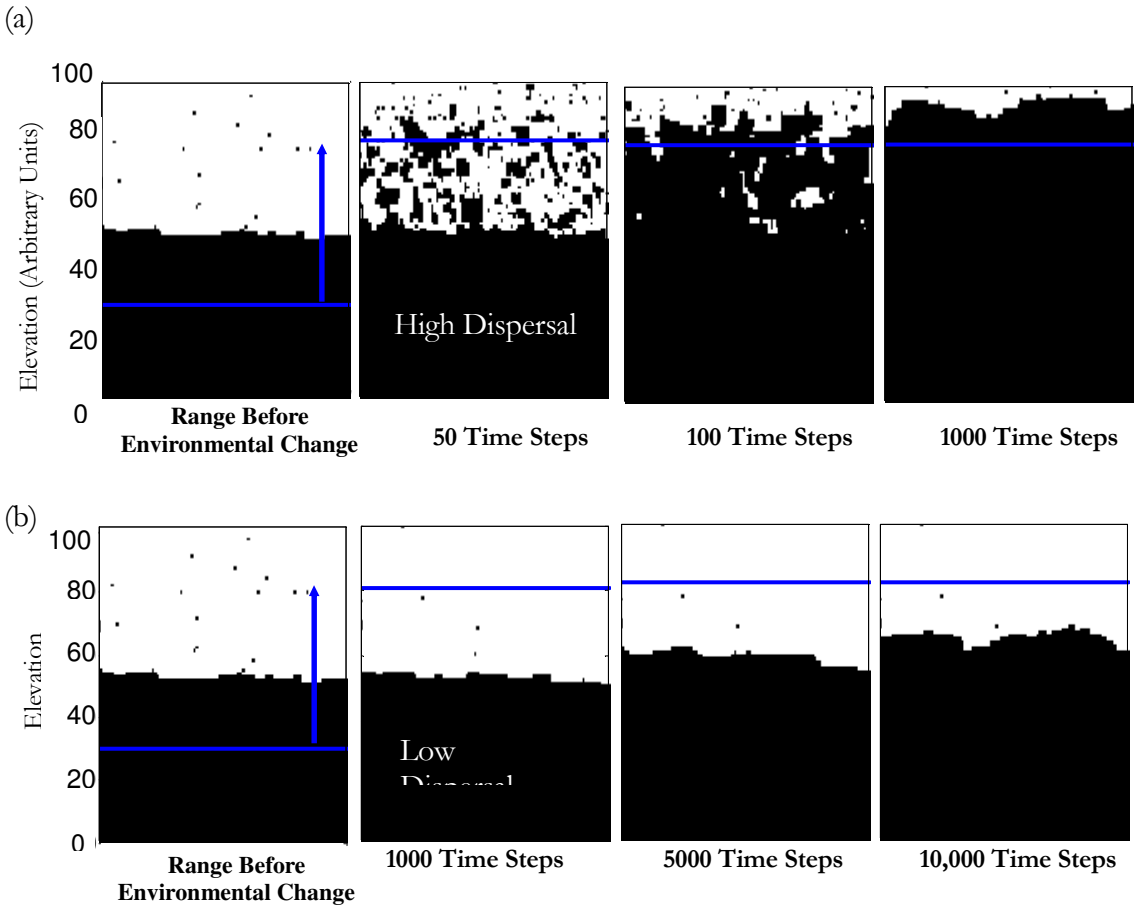

Figure 2-4 Following a change in the elevation of the mortality gradient (e.g., a change in sea level) the rate at which the upper limit responds depends substantially on the dispersal rate. And under conditions of "low" dispersal, the upper limit remains in disequilibrium for a large number of iterations. The natural rates of dispersal are too small to be measured in this study: no range extension has been measured in 5 years of study (Figure 1-6).

2.4 Discussion

In this chapter I have shown that episodic recruitment and simple density-dependent coupling is sufficient to cause punctuated biotic patterns, even in the absence of environmental thresholds. In Chapter 1, I presented a historical record of the *Endocladia* upper limit that showed a punctuated response to gradual climate change, and then I unsuccessfully searched for a corresponding change in environmental conditions. The purpose of this chapter is to demonstrate that a corresponding step-like environmental change is unnecessary to explain this history. Extremely low rates of colonization above the upper limit are suspected from field experiments (Figure 3-13), and a rare episode of increased recruitment occurring at the time of range extension, in combination with density dependence and rising sea level, could explain the perplexing history of the upper limit. There is no evidence for or against an episode of recruitment between 1963 and 1970. However, episodic recruitment is well known in marine and intertidal species (Keough 1983; Caffey 1985; Connell 1985; Reed et al. 1988; Roughgarden et al. 1988). Moreover, I have shown that artificial "dispersal", via transplantation (Chapter 3), can successfully raise the upper limit under current conditions, and that the magnitude of the rise matches the increase predicted from the hypothesis that the *Endocladia* range tracks sea-level rise in a punctuated manner (Chapter 1). In later chapters I will address environmental gradients, physiological constraints, and density dependence. Although these topics are interesting in their own right, they also bear on the hypothesis of gradual change and punctuated response presented as a numerical simulation in this chapter.

POSITIVE INTERACTIONS AND RANGE STABILITY IN THE INTERTIDAL ALGA *ENDOCLADIA MURICATA*

3.1 Introduction

Species range boundaries are critical breakpoints, and their dynamics are key to understanding ecology in a changing environment (Brown et al. 1996; Gaston and Chown 1999; Warren et al. 2001; Parmesan et al. 2005). From species invasions and global change to evolution and physiology, research at the range edge is proving crucial for placing ecological findings into a dynamic context (Stillman and Somero 2000; Sakai et al. 2001; Via 2001; Tomanek and Somero 2002; Walther et al. 2002).

Interactions between biological and physical factors determine important range traits such as the location of the border, its sharpness, stability and resilience following disturbance (Tirado and Pugnaire 2005). Theory indicates that, where strong feedbacks exist in the form of biological interactions (e.g., density dependent survival), it is possible for sharp range boundaries to develop, even in the absence of environmental thresholds (Lewis and Kareiva 1993; Wilson et al. 1996). Species that form canopies provide an important example. By definition, the canopy coverage must be between zero and 100%. However, if survival is strongly density-dependent (e.g., if neighboring individuals provide mutual shading and reduce environmental stresses), individuals may not survive without the protection of neighbors. If low-density aggregations die off, then the only densities that remain are complete cover and complete absence, and at the range edge, coverage abruptly transitions between these two extremes, without a region of intermediate density.

Because the result is nearly a binary decision (there will either be thick canopy or no canopy) the result has been called an ecological "switch" (Wilson and Agnew 1992). In the above example, I described a switch operating across distance. The same dynamics could also create a switch that operates through time. Gradual colonization is impossible if intermediate densities are not viable. In this case, any movement of the range edge would necessarily be an abrupt switch between no canopy and thick canopy because the transition

state is not viable. So, by analogy, punctuated range shifts are the temporal equivalent of an abrupt range edge. It does not matter whether one looks across space or follows a single region through time, only thick canopy or no canopy is possible, and changing between states requires throwing a switch. The exogenous agent that throws the switch is often called a "catastrophe" (after Thom 1975). In the context of this study, the identity of the catastrophe is less important than the dynamics that underlie the switching [and in most cases, the catastrophe is usually a *post hoc* inference (Holt et al. 2005)]. It is particularly important to understand that temporal and spatial switches may be a result of the same ecological process, for instance density dependent survival.

Here I examine the relative importance of feedbacks and environmental constraints and their interaction in setting the upper range limit of the intertidal alga *Endocladia muricata*.

The stability and resilience of this sharp border is important in two different contexts. First, in light of history and the punctuated range shift presented in Chapter 1, I ask, "Could a range shift as dramatic as the one in the 1960's happen at other times?" Second, species borders are currently sparking intense interest, and the need for empirical evidence has recently been highlighted by two separate working groups (Laurance et al. 2001; Holt and Keitt 2005). In this context, *Endocladia's* upper limit provides a much-needed example of how community feedbacks and environmental conditions interact to set a biological boundary.

The upper limit of *Endocladia* is a superb system for experimentation at a range edge because the range spans only a few vertical meters and can be easily manipulated. These features enabled me to test the ideas presented above experimentally in the field. First I test for the presence of a switching mechanism: density-dependent survival near the upper range limit of *Endocladia*. To assess density-dependance I trimmed the upper limit into patches of different sizes and compared the performance of different size clumps. In addition, because I predict that density-dependance is due to self-shading and the resulting habitat amelioration, I artificially shaded clumps to determine if artificial shading could "rescue" clumps that would otherwise die, once its neighbors were removed.

I then "throw the switch" by transplanting *Endocladia* up above its existing range and clearing areas below its range limit and monitoring the stability of this new state. If *Endocladia* reverts to its natural state following manipulation, this indicates that the switch between states does not overcome environmental limitations. Either the transplant is too small for the switching mechanism to be important, or the environmental constraint is too strong. Thus it is possible to determine the relative importance of density-dependent factors and environmental factors near the range limit by assessing the resilience of the upper limit to perturbation. For example, a transplanted canopy of *Endocladia* survives, on average, 9.5 cm above its current upper limit. The range extended 9.5 cm following an artificial catastrophe, which allowed colonization in mass, but above 9.5 cm, the environmental constraints overwhelmed density-dependent facilitation, and transplanted *Endocladia* died. Interestingly, the response to the transplant "catastrophe" was less than the historical range shift of the 1960's (9.5 cm versus 30 cm in the 1960's). Because the transplant sizes are much larger than the size where strong density-dependent survival was observed, it appears that the scale of the catastrophe (the size of the transplants) is sufficient to confer facilitative interactions within a clump. In this case it is likely that the potential range is more constrained by the environment now than it was before the range shift of the 1960's.

3.2 Methods

Sites for all experiments were spread haphazardly throughout the upper intertidal zone at Hopkins Marine Station, Pacific Grove, CA. The upper limit of *Endocladia* is usually 1 to 2 meters above MLLW at this site. The size requirements of the sites and the high rugosity of the terrain prevented completely random site selection. Site locations are shown in Figure 3-1.

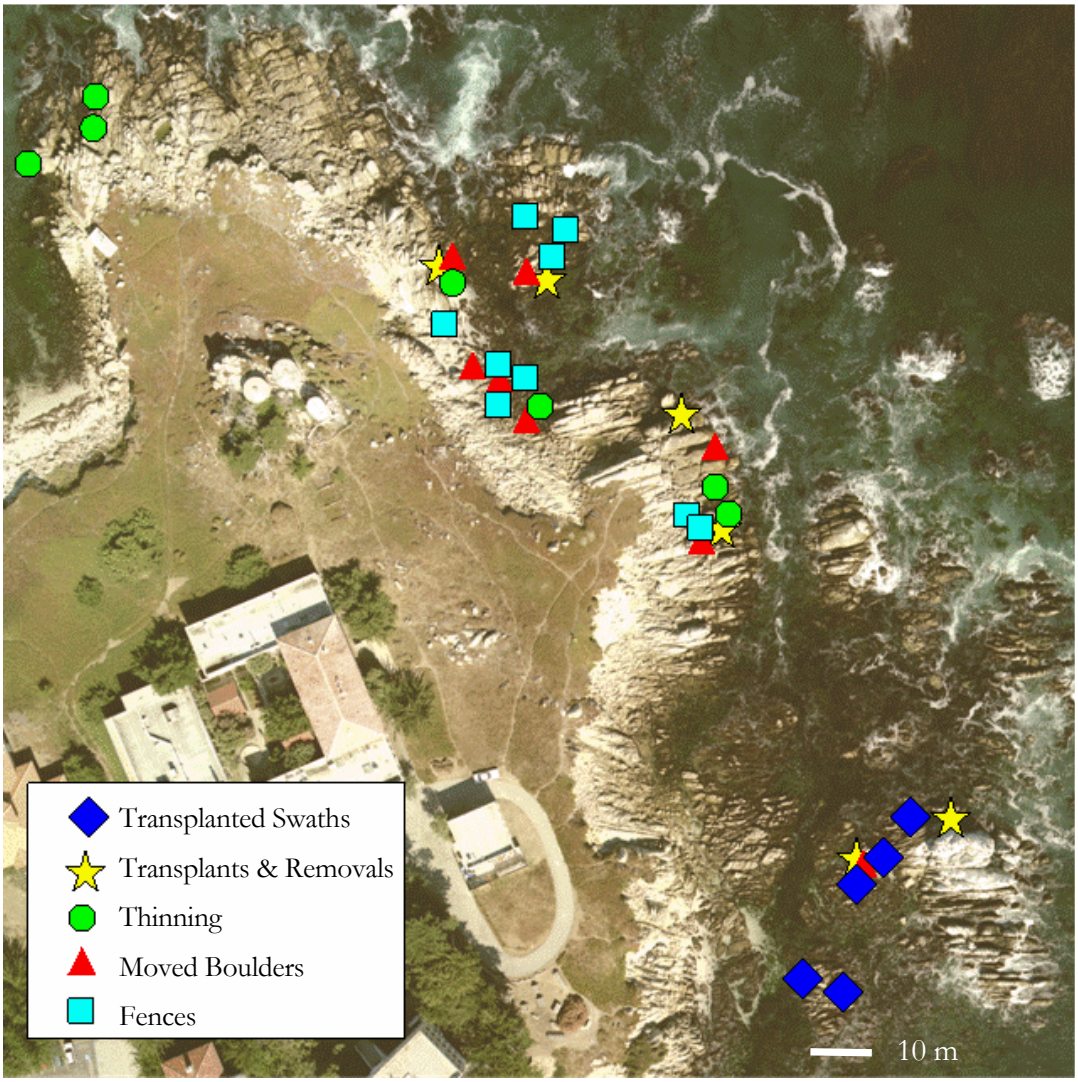

Figure 3-1. Aerial view of Hopkins Marine Station showing the location of the study sites.

3.3 Results

3.3.1. Thinning: Testing Density Dependent Performance

The upper turf of *Endocladia* was thinned using forceps and a Dremel-tool-mounted wire wheel to produce circular patches of thalli (or clumps) in 4 different size classes (areas of 0.2, 0.8, 7, and 16 cm^2. Size class "1" is smallest, and "4" is largest.). Figure 3-2 shows the experimental set-up. At 10 different sites, a set of patches from all 4 size classes was paired with a similar set of clumps over which an artificial shade was erected to determine if

artificial shading could "rescue" clumps that would otherwise die once neighboring individuals were removed. Shades (29 X 46 cm) were made of 14 gauge, vinyl-coated wire mesh and covered with a replaceable layer of plastic mesh (2 squares per cm, Vexar, NSW, Roanoke, VA) held in place with zip ties. The shades were secured with 6 large polycarbonate washers and bolted into plastic dry wall anchors placed in holes drilled in the rock (Figure 3-2). An iButton temperature logger was placed in the center of each set of clumps (see Chapter 5). Two shades were ripped out of the rock by large waves and lost, and these sites are excluded from analysis, leaving a total of 8 paired sites.

The practical size of the shade prevented replication of the larger size classes within a site, but it was possible to replicate the smaller size classes, so a set of clumps consisted of: 3 of the smallest clumps, 2 of the next larger size, and a single clump of each of the 2 largest size classes. Size classes within a site were randomly ordered from right to left along the upper limit. A size standard was glued into place (Z Spar Splash Zone Compound) near each clump size, and image analysis (Image J, U. S. National Institutes of Health, Bethesda, MD) was used to determine clump areas from digital photographs taken approximately monthly between June 18th, 2003, (the date of set up) and April 27th, 2004. The unshaded portion of the experiment, which examined density dependence under natural field conditions, was repeated between April 27th, 2004 and January 26th, 2005.

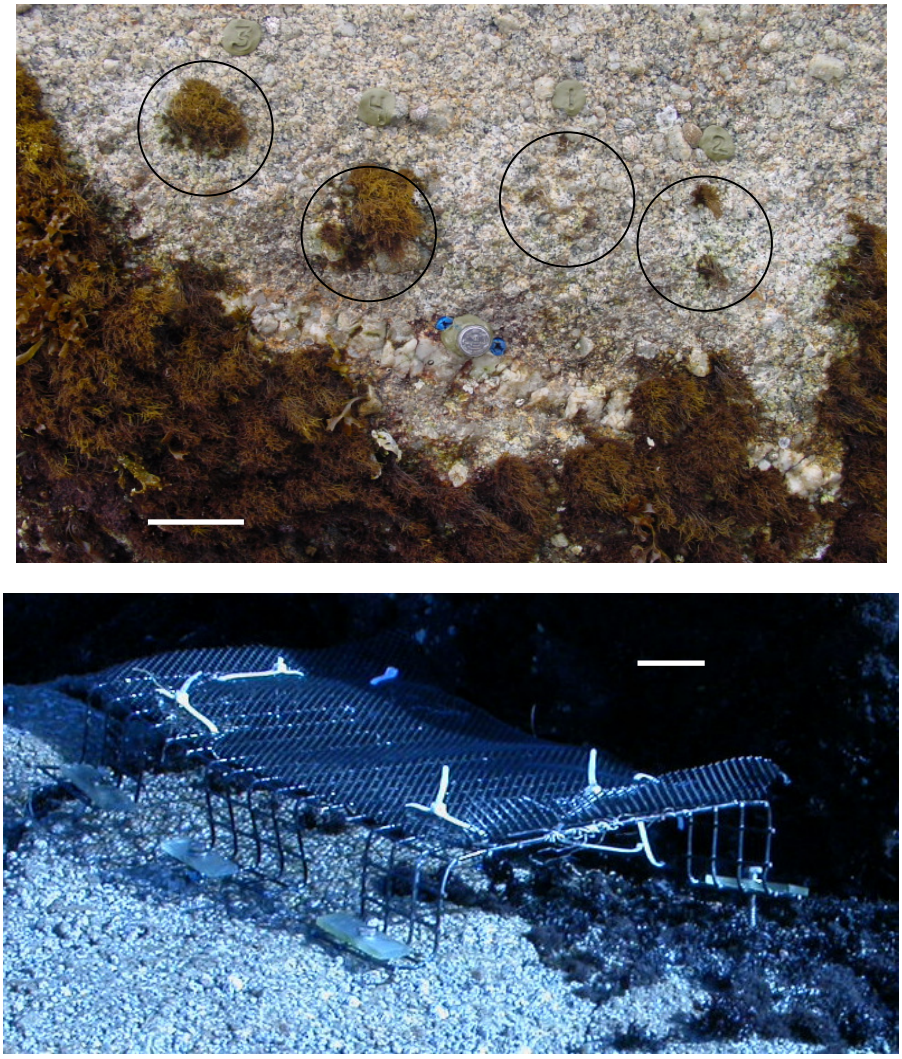

Figure 3-2. The experimental set-up for year-1 thinning experiments. At each of 8 sites, an unshaded group of thinned clumps in 4 size classes (above) was paired with a shaded group of clumps (below). The unshaded group was replicated without the shaded group during year 2. Scale bars are 5 cm.

To compare changes in clump area, the measured area was normalized by the initial area to give a proportional change. This is also the clump's relative growth over the period , and for the thinning experiments, I will use growth and relative area interchangeably. Growth less than 1 means the clump has died back to a fraction of its initial size. The relative area data is skewed right (because negative ratios are impossible) and the variances differ substantially between shaded and unshaded treatments (Chochran's test $p<0.01$, see also Figure 3-7). Under these conditions, a non-parametric test (distribution-free and based on ranks) is

preferable, and the effect of shade was compared for each size classes using Wilcoxon's matched pairs test with a one-tailed Bonferroni-adjusted significance of 0.0125 (=0.05/4 comparisons). For size classes with multiple samples per site (sizes 1 and 2), the average growth rate per site was used, so that all size classes would have the same number of values (one sample per site).

Data for unshaded sites were log(x+1) transformed and compared assuming equal variances (Chochran's test P>0.3) using a 2-way mixed-model ANOVA, with site as the random factor. Differences between sites are unimportant in this experiment (and impossible to test, for the unreplicated larger size-classes), so results focus on size effects.

Overall clump survival (presence/absence at the end of the experiment) was also analyzed. Significance testing for survivorship followed the method described in Zar (1999 p. 563), which is Tukey testing, modified for proportions. Clump survival was analyzed for year 1, for year 2, and because data are similar between years, for both years pooled together.

3.3.2. Transplants: "Throwing the Switch, Part 1"

To determine the stability of the *Endocladia* range following a range extension (here it was artificially-induced), I transplanted *Endocladia* above its natural range in 3 ways: as isolated transplants (part 1, this section), as swaths of cover extending above the range (part 2, below) and as entire boulders with attached *Endocladia* (below).

Transplanted *Endocladia* was taken from a common location (Figure 3-1) where the alga covered thick hummocks of the barnacle *Balanus glandula*. A sharp wood chisel cut the barnacle shell plates just above the basal plate, and a barnacle patch with *Endocladia* attached was removed as a unit. Most of the barnacle tissue was cleaned from the shell plates with a pressurized stream of seawater, and the shell plates (with attached *Endocladia*) were glued (Z-Spar Splash Zone Compound) back onto the rock in 10 cm X 10 cm patches.

Arrays of transplants were repeated at 6 sites (Figure 3-1). At each site, 9 total transplants were made as follows: 3 replicate transplants were placed at 3 different elevations, relative to the upper limit of *Endocladia* (Figure 3-3). One set of 3 replicates was transplanted at the elevation of the upper limit, into clearings that allowed a buffer of 5 cm between the

transplants and the existing turf. A second set was transplanted 20 cm above the upper limit and the third set, 40 cm above the upper limit. Note that these elevations are relative to the *Endocladia* upper limit at that point on the shore. Absolute tidal elevations are shown in Figure 3-3. Transplant elevations were surveyed from a nearby U. S. National Geodetic Survey Benchmark (PID GU3971, 6.81 m above Monterey MLLW, NTDE 1983-2001) with a total station (Topcon 1100D).

(a) (b)

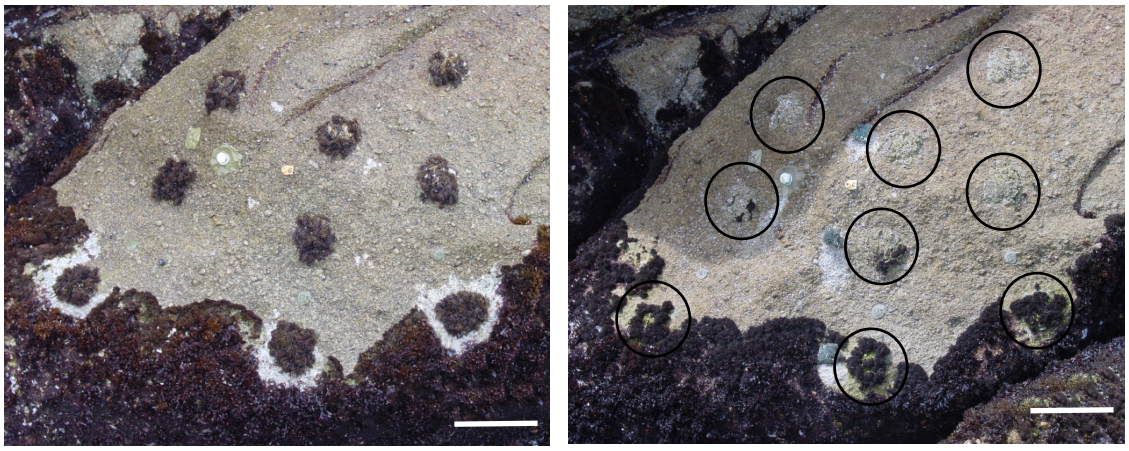

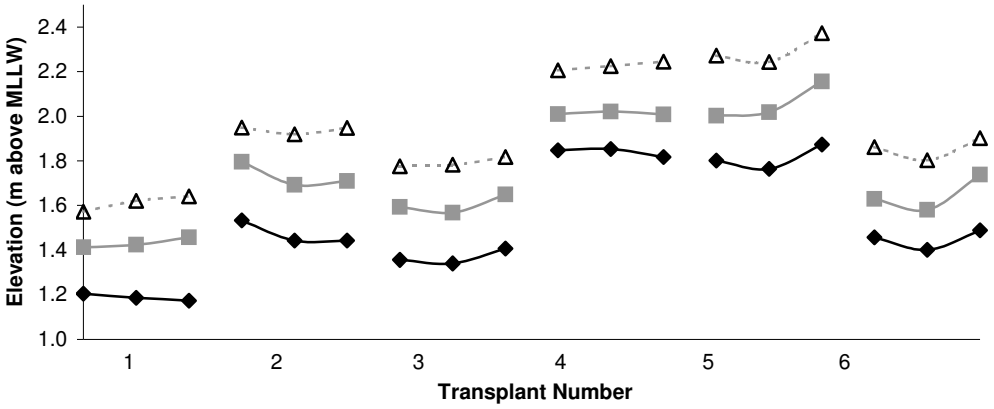

(c)

Figure 3-3. Transplants #6 is shown on June 25th, 2002 in (a) and on April 27th, 2003 in (b). Transplants are located at the elevation of the upper limit, and 20 cm and 40 cm above the upper limit. Absolute transplant elevations are shown in (c). Scale bars are 20 cm.

At each elevation, an iButton temperature logger was placed near the center transplant. Percent cover of living *Endocladia* within the transplants was assessed with image analysis (Image J) approximately monthly between July 9th, 2002 and February 22nd, 2003. The transplants were left in place, and after February 22nd, 2003, I noticed little subsequent change in transplant cover during the following 3 years (until December 12th, 2005, the final date of photography).

Endocladia survival was measured as transplant cover in January, 2003, (all sites started with 100% cover when first established, between June 25th and June 28th, 2002). Survival among sites at the three heights above the *Endocladia* upper limit was compared following log (x+1) transformation, using a mixed-model 2-way ANCOVA, with the transplant tidal elevation (above MLLW) as the covariate.

Only one iButton was placed at each elevation per site (see above). Consequently, the cover of the 3 replicate transplants at an elevation was averaged and the average cover regressed against the maximum temperature measured for the site at that elevation.

3.3.3. Transplanted Swaths: "Throwing the Switch, Part 2"

Endocladia was transplanted into swaths [30 cm X 10 cm vertically-oriented patches (Figure 3-4)] using the methods described above for isolated transplants. Swaths extended 25 cm above the upper limit and 5 cm below the upper limit, and the turf was removed around the part of the swath that extended below the upper limit. 3 swaths were constructed at 5 sites (Figure 3-1). Percent cover of *Endocladia* was monitored with digital photography between March 21st, 2003 (the date of transplantation, 100% cover) and December 13th, 2005. Cover was measured on December 13th, 2005 at three elevations: at the upper limit of *Endocladia*, 10 cm above the upper limit and 20 cm above the upper limit. Following log(x+1) transformation, a mixed-model 2-way ANOVA tested elevation and site effects. Again, only the elevation effect and the non-significant interaction are important for this experiment.

(a) (b)

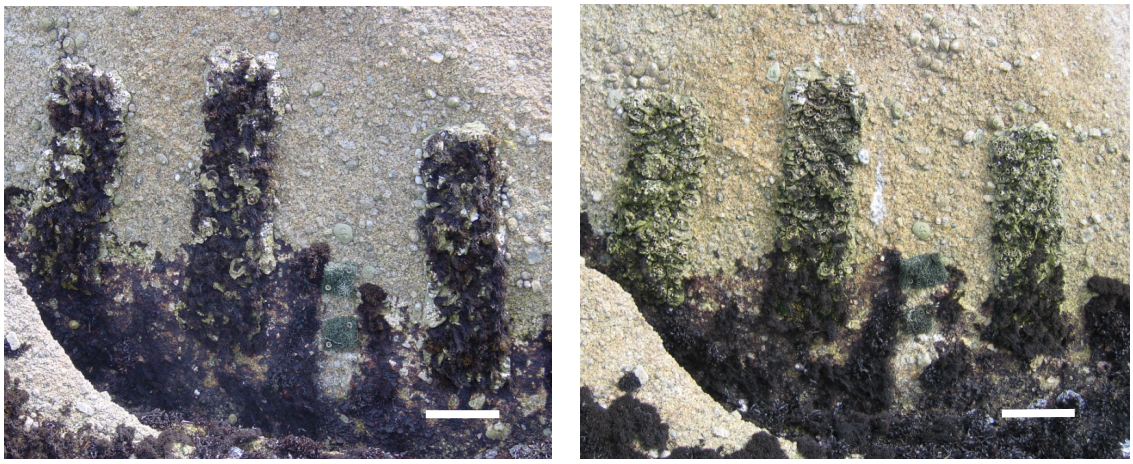

Figure 3-4. Transplanted swaths (a) on April 23rd, 2002 and (b) August 3rd, 2004. Scale bar is 15 cm long. The cleared area around the swath base is difficult to see because the encrusting bases of *Mastocarpus papillatus* remain.

In addition, the elevation of the highest clump was measured December 13th, 2005. Clumps in the interstices between transplanted barnacle tests were excluded if they had summer-ephemeral fronds and were not visible in the photograph taken September 4th, 2005.

3.3.4. Clearings

The resilience of the range edge following artificial clearing was also tested. Vertical clearings 15 cm wide were cut out of the Endocladia turf using a drill-mounted wire wheel. The cleared surface was then sterilized with two treatments (on consecutive days) of lye-based foaming oven cleaner (Easy Off, Reckitt and Benckiser). Oven cleaner was sprayed onto clearings after the area was exposed by low tide and the cleaner was allowed to soak until high tide washed it away, at least 6 hours. The sterilization extended 40 cm above the upper limit and at least 50 cm below the upper limit (Figure 3-5). Three clearings were made at 4 sites, and 2 clearings were made at 2 additional sites, where there was no space for a third clearing (Figure 3-1). Recruitment and vegetative growth inward from the sides of the clearing were monitored with digital photographs from June 25th, 2002, (the date of clearing) until December 13th, 2005.

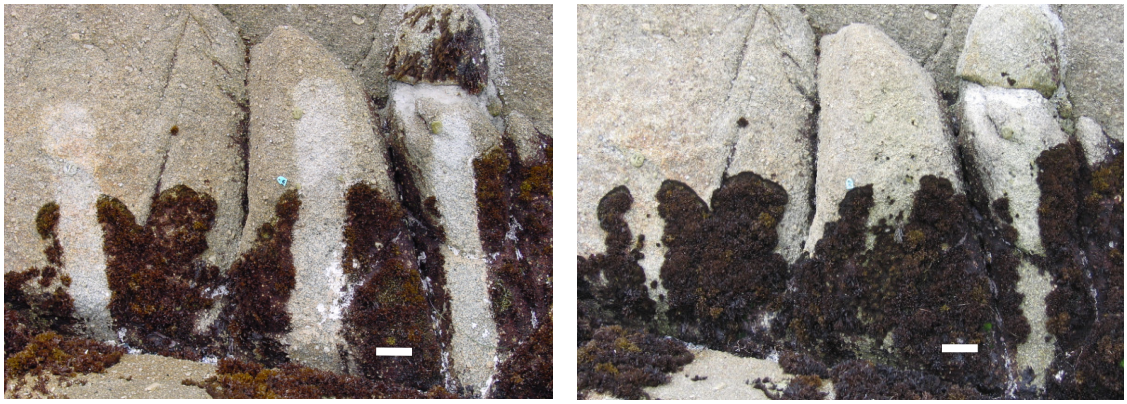

Figure 3-5. Removals shown on July 15th, 2002 (left) and August 3rd, 2004. Note also the rock atop the right-most clearing, which was moved from below the upper limit and cemented in place. Recruitment above the upper limit is visible in the center clearing, and an isolated clump of *Mastocarpus papillatus* survives well above the upper limit in a seam between the two left-hand removals. The left and right clearings narrowed due to lateral growth inward from the edge of the clearing. The "V" shape visible in the left clearing is caused by more rapid lateral growth at lower elevations; this pattern was common. Scale bar is 15 cm.

The cover of turf that had successfully recruited into the clearings (distinct from that due to growing inward from the edges) was measured on December 13th, 2005, by counting squares in a quadrat made of 1.5-squares-per-cm wire hardware cloth and converting the result to a percent-of-area covered. This cover was measured at the upper limit, 20cm below the upper limit, and 40 cm below the upper limit. Percent cover was also measured above the upper limit, but because successful recruitment was so scarce above the upper limit (occurring only in 2 out of 16 treatments), maximal percent cover was measured by centering the quadrat at the elevation of highest cover. This sampling method biased the above-upper limit measurements toward higher percent-cover, but the bias is acceptable because it results in higher likelihood of accepting the null hypothesis (equal recovery regardless of height), which does not affect conclusions in this case. Furthermore, because the height of maximum density was sampled, conclusions about recruitment above the upper limit apply

for all elevations (0 to 40cm) above the upper limit, rather than a single sampled elevation. Analysis was by ANOVA as described above for swaths.

3.3.5. Boulders

In addition to the carefully arrayed transplants and removals, entire boulders and their associated communities were skidded up or down within the intertidal zone. Transplanting the entire community of *Endocladia* as a unit was more "natural" in the sense of a community-wide re-location, but it was impossible to place boulders very carefully, as was required for a quantitative analysis. Thus the boulders serve as a qualitative validation of transplant methods that manipulated only *Endocladia* (transplants and swaths above) and where areas were poisoned (clearings).

Boulders were skidded using a come-along hand winch and two high-lift jacks in combination. Boulders were moved as fortune would have it. The largest boulder moved was approximately 6 tons (moved to a lower elevation). *Endocladia* recruitment and survival on these boulders was monitored qualitatively with photographs from June 2002, through December 2005.

3.3.6. Fences

In addition to experiments testing the response of the upper limit following manipulations of density (via thinning) and the physical environment (via transplantation at different elevations, I monitored the response of the upper limit following exclusion of limpets, suspected grazers on *Endocladia* (Carefoot 1977; Luning 1990). Limpet grazers were removed and excluded from a 23 X 23 cm square fenced area and each fenced area was paired with a partially-fenced area used as a procedural control (Figure 3-6). Fences were made from 3-squares-per-centimeter stainless steel hardware cloth folded into a square "C" cross section. The upper part of the "C" added rigidity to the wall and provided an overhang that was difficult for limpets to surmount. The lower part of the "C" was bolted into plastic anchors placed into holes drilled in the rock. Closed-cell foam was cut in strips and compressed between the mesh and the rock, overlapping in the corners, to seal the bottom of the fences. Any limpets that entered the cages were removed monthly (about 10 total, none of these occurred during the summer months, when *Endocladia* was most reproductive).

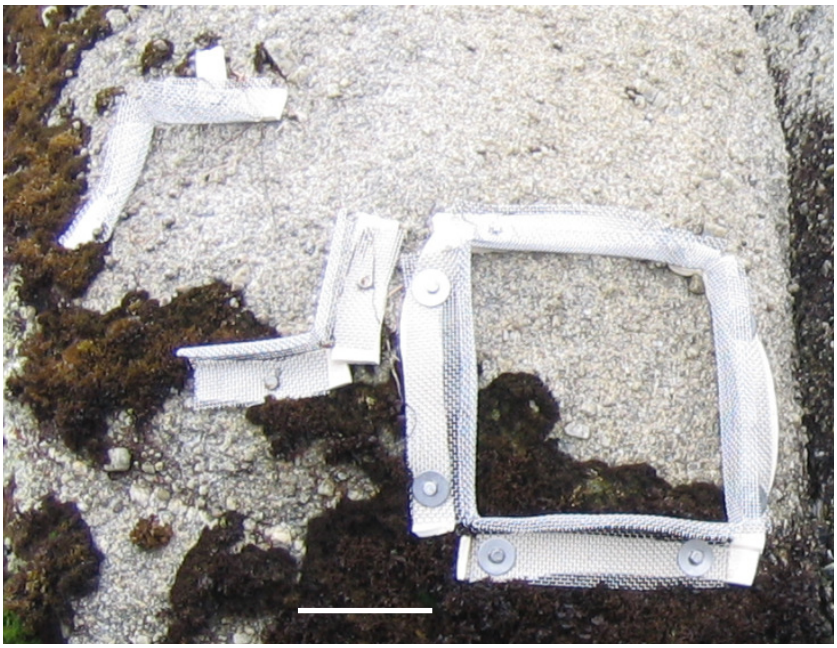

Figure 3-6. Fence paired with a partial fence at the upper limit of *Endocladia*. Scale bar is approximately 15 cm.

This experimental unit was repeated at 9 sites, and monitored for changes in elevation of the *Endocladia* upper limit between July 28th, 2004 and December 13th, 2005. The change in upper limit elevation was averaged for 5 equally-spaced points at each site, leaving a 3.5cm margin between the edge samples and the fence, and compared between fenced and partially fenced regions using a paired t-test.

3.4 Results

3.4.1. Thinning

Shades decreased the maximum temperature in the *Endocladia* clumps underneath them by 2.8 ± 1.8 °C (mean ± 95% confidence interval).

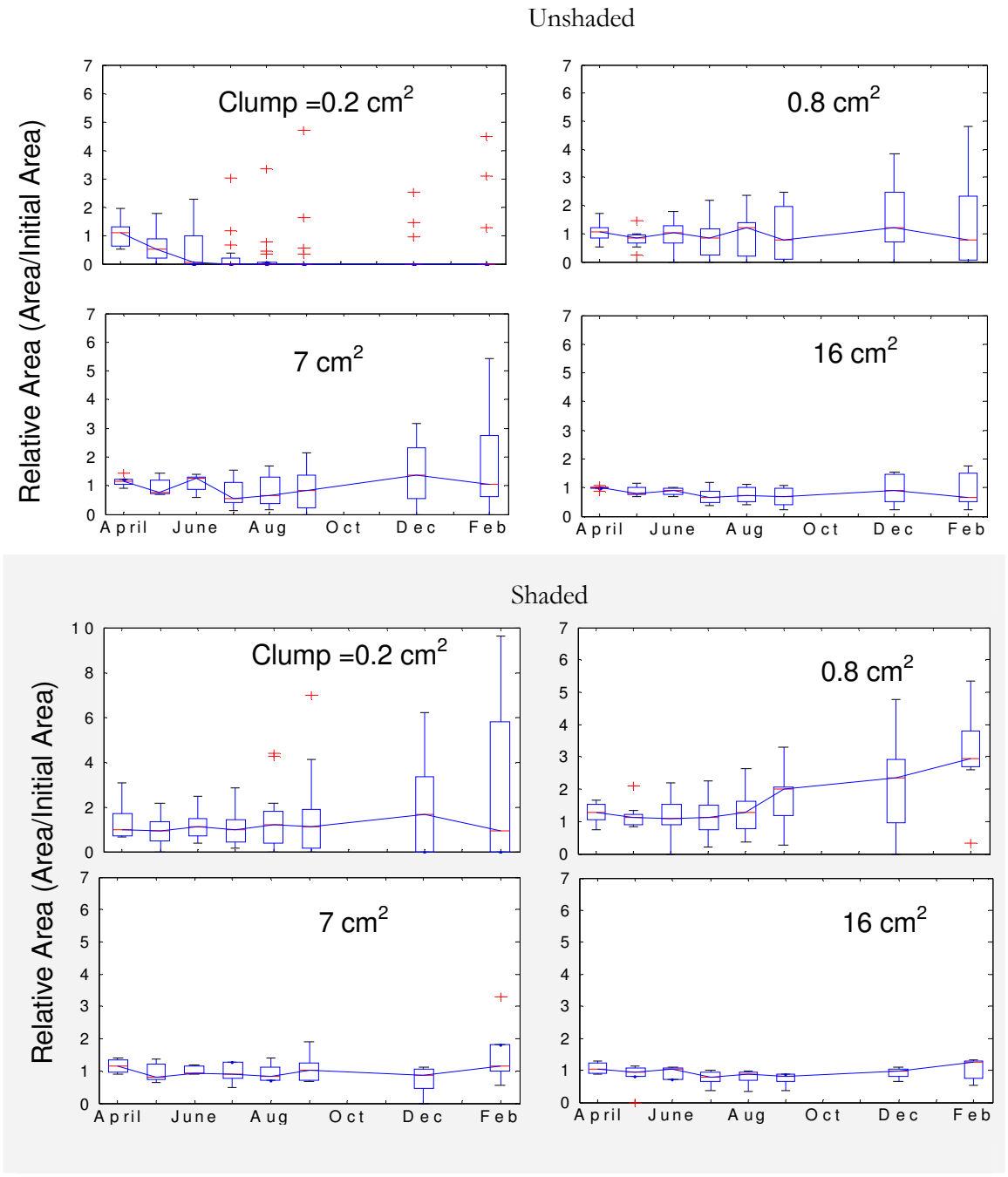

Figure 3-7. Time course for relative growth (die-back if <1) of 4 clump sizes for unshaded (top) and shaded (bottom) treatments. Lines connect medians at each date. The box extends from the lower to upper quartiles. Whiskers extend 1.5 times the interquartile range, and data outside this range are marked (+). Note the expanded y-axis scale for size 1, when shaded.

The relative area in both the shaded and unshaded treatments of 2003-2004 is shown for each size class in Figure 3-7. Shades significantly increase the growth (and decrease the die-back) of the smallest size-class (Table 3-1). Shades also increased the growth rates of the other size classes, but the effect was not significant for larger sizes.

Size	n	Z	p
0.2 cm^2	8	2.366	**0.036**
0.8 cm^2	8	1.820	0.136
7 cm^2	8	2.240	0.052
16 cm^2	8	1.820	0.068

Table 3-1. Wilcoxon's matched pairs test for shade effect among different sizes. P-values are one-tailed and Bonferroni corrected for 4 comparisons. In all cases, shades increased the final percent cover of clumps. The effect was only significant for the smallest size class.

In 2003-2004, clump size significantly affected algal growth ($p<0.001$, Table 3-2a). Ordered by growth rate, the size classes are 2,3,4,1 and the only significant differences in relative growth rates are between size class 1 and sizes 2 and 3. (Tukey Test $p<0.04$, Table 3-2a).

The following year, in 2004-2005, the results were similar, with more power to differentiate between size classes (Table 3-2b). Average growth of size class 1 was significantly below all the larger size classes (Tukey test $p<0.01$, Table 3-2b). Growth of size classes 2 to 4 were indistinguishable with $p>0.35$.

(a)

2003-2004 (unshaded)	df	MS	F	p
Size	3	0.192	9.415	**<0.001**
Site (random)	9	0.044	1.52	0.186
Size X Site	27	0.02	0.701	0.823
Error	30	0.029		

Tukey Test for Growth within Unshaded Clumps (2003-2004)

	1	2	3
2	**<0.001**		
3	**0.039**	0.96	
4	0.16	0.71	0.96

Result: 1 4 3 2

(b)

2004-2005 (unshaded)	df	MS	F	p
Size	3	0.756	14.617	**<0.001**
Site (random)	16	0.124	2.703	**0.004**
Size X Site	48	0.052	1.123	0.341
Error	51	0.046		

Tukey Test for Growth within Unshaded Clumps (2004-2005)

	1	2	3
2	**<0.001**		
3	**0.002**	0.54	
4	**0.005**	0.36	0.99

Result: 1 < 4=3=2

Table 3-2. The rate of growth (final area/initial area) within unshaded clumps analyzed separately for 2 years: June 18, 2004 through April 27th, 2004 (a), and April 27th, 2004, through January 27th, 2005 (b). The smallest size class (0.2 cm^2) died back (growth <1) more than the 3 larger size classes (≥0.8 cm^2) Growth of clumps of size >1 was indistinguishable. Matrices for Tukey tests show comparisons between size classes.

In unshaded conditions, the smallest-size clump suffered more mortality than all the other size classes ($p<0.001$, Figure 3-8). When artificially shaded, however, survival of the smallest size clump was indistinguishable from all of the other size classes, either shaded or unshaded.

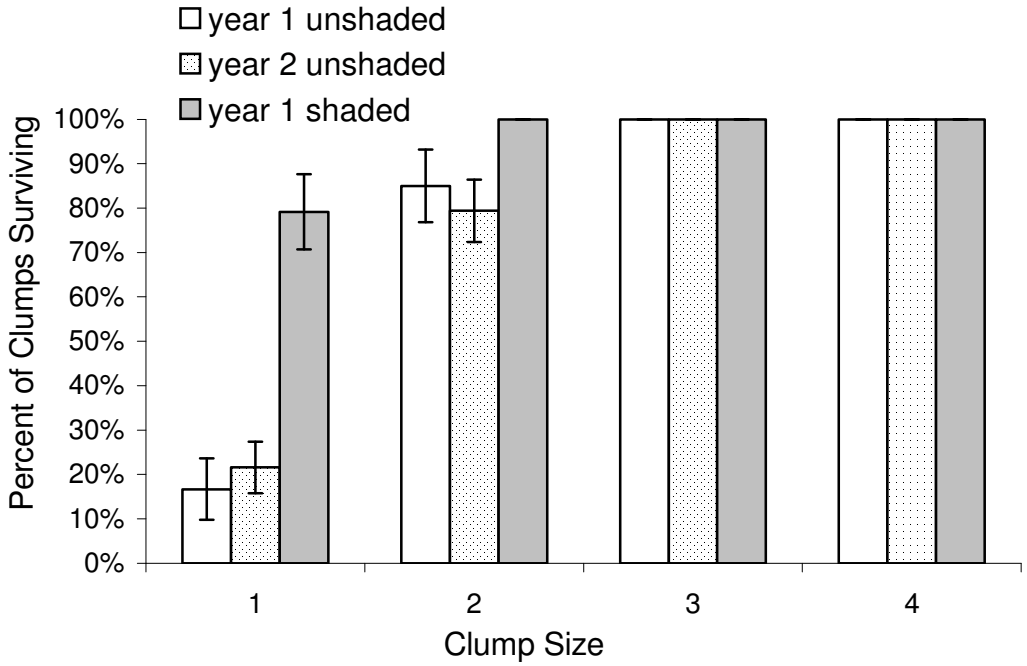

Result: 1 < 1s = 2s = 3 = 3s =4 = 4s

Figure 3-8. Comparison of whole-clump survival (clump persistence through the experimental period) for 4 size classes for shaded and unshaded treatments. Year 1 was June 18th – April 27th, 2004. Year 2 was April 27th, 2004 – January 27th, 2005. Highest clump mortality occurred in the smallest size class, when it was not shaded. When shaded, the mortality of the smallest size class was indistinguishable from the larger size classes both shaded and unshaded. Unshaded data for years 1 and 2 were pooled for the multiple comparison (Table 3-3). However, results are unchanged if the 2 years are analyzed separately.

	n1	n2	p2'-p1'	SE	q	p
1 vs 2s	81	16	56.332	5.4685	10.301	**<0.001**
1 vs 4=4s=3=3s	81	8	53.615	7.3015	7.343	**<0.001**
1 vs 2	81	54	37.448	3.5446	10.565	**<0.001**
1 vs 1s	81	24	35.401	4.6673	7.5848	**<0.001**
1s vs 2s	24	16	20.931	6.4513	3.2445	>0.2

Table 3-3. Multiple comparisons between surviving proportions for thinned clumps (see Figure 3-8).

3.4.2. Transplants

Survival within a transplanted clump initially decreased during summer and recovered only in the lowest transplant. The time course of survival is shown at each elevation for the average of 3 randomly selected sites: sites 3,4 and 6 (Figure 3-9). Three sites were chosen because it took many hours to digitize percent cover (even after partial automation in Image J), and the time-course was not crucial for further analyses, as analyses only considers the final sample on February 23rd, 2003. By this time the transplant cover had stabilized and there was little change over the following 2 years.

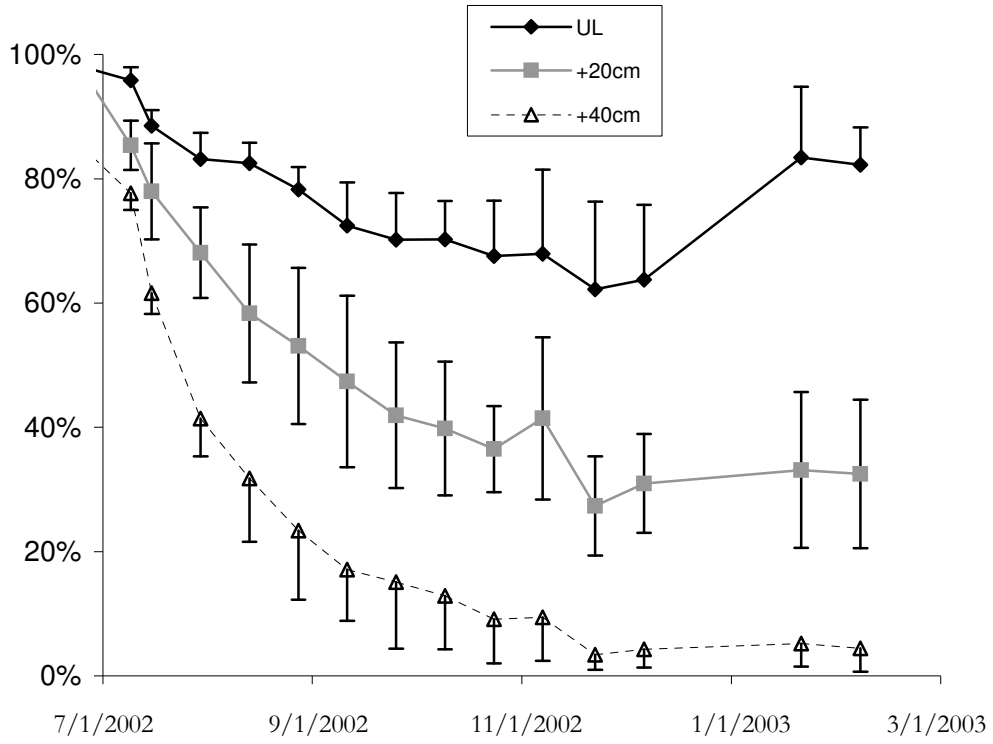

Figure 3-9. Survival time course for the three transplant heights. Data are mean percent cover at each height averaged from 3 randomly selected sites (3, 4, 6). Error bars are 1 standard error.

Endocladia survivorship decreased as transplant height increased above the upper limit (Figure 3-10). Transplants 40 cm above the upper limit had significantly more mortality than those 20 cm above the upper limit, and these had significantly more mortality than transplants at the upper limit ($p<0.001$ for all comparisons). The actual elevation above MLLW was not a significant factor and explained only 14.5% of the variance in *Endocladia* survival ($p>0.48$, Figure 3-10).

Maximum temperature significantly predicted 40% of the variation in transplant survival (Figure 3-11). Site was also a significant effect. However, this was not related to the tested hypothesis, and because elevations behaved similarly at all sites (no site-height interaction), the significant site effect was not analyzed further.

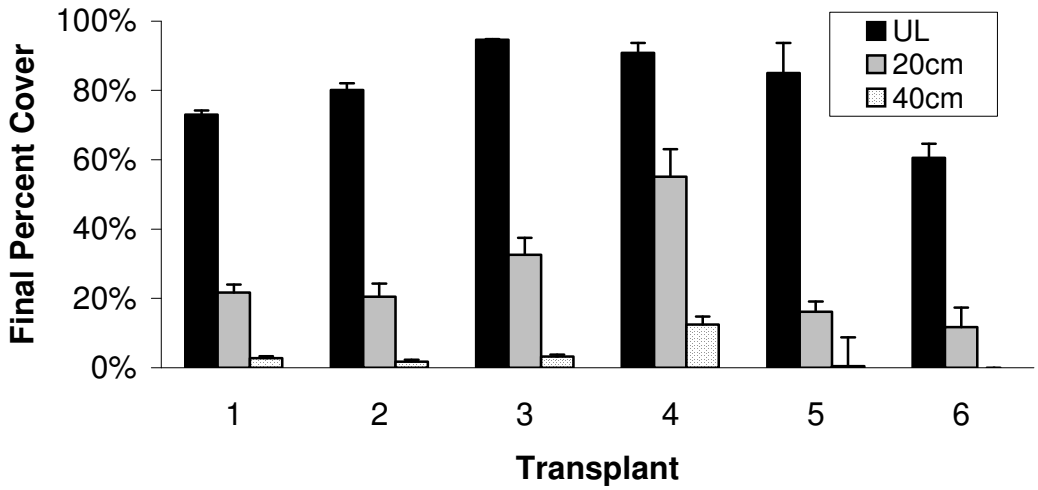

Result: Surviving Cover 40 cm above UL < 20 cm above UL< at UL

Figure 3-10. Survival within transplants was predictable from the height above the local upper limit but not by the absolute tidal elevation (Table 3-4). Survival 40 cm above UL was less than 20 cm above the UL, which was less than survival at the UL.

ANCOVA Results for Transplant Cover

Source of Variation	df	MS	F	p
Height	2	0.0227	14.5856	**0.0011**
Site	5	0.0060	2.7455	**0.0346**
Height X Site	10	0.0016	0.7122	0.7070
Error	34	0.0022		
Regression for Absolute Tidal Elevation				
Tidal Elevation	1	0.0022	1.0362	0.3157
Error	35	0.0021		

Tukey Test for Survival at Elevations Above UL

Elevation	At UL	20 cm above UL
20 cm above UL	**0.0001**	
40 cm above UL	**0.0001**	**0.0001**

Result: 40 cm above UL < 20 cm <UL

Table 3-4. ANCOVA and multiple comparisons for transplant cover. Elevation above the local UL predicted survival within transplants. Absolute tidal elevation was not a significant predictor of within-transplant survival.

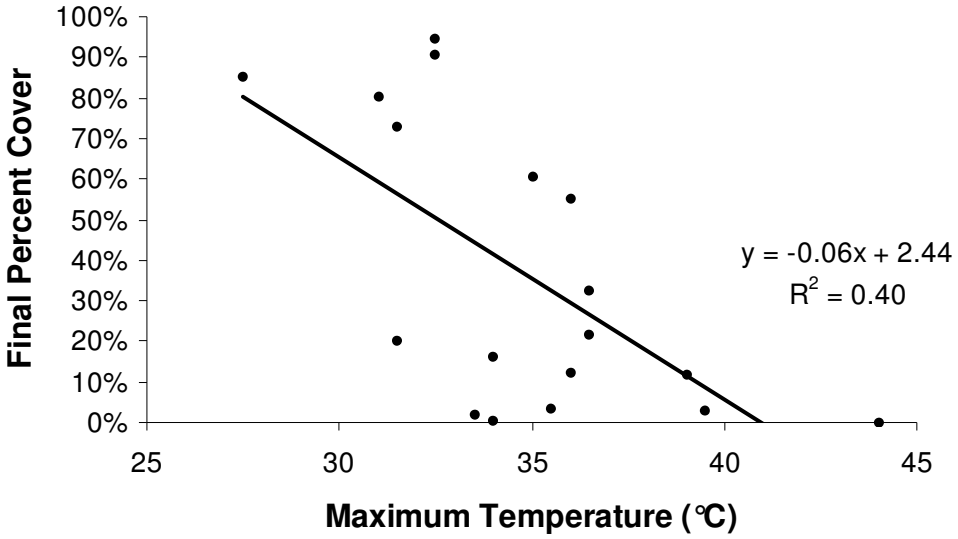

Regression for Maximum Temperature

Source or Variation

	df	MS	F	p
Max. Temperature	1	0.0798	10.61	**0.0049**
Error	16	0.00753		

Figure 3-11. Regression of temperature and transplant survival (final percent cover). Percent cover data were averaged across the 3 replicates at each height above the upper limit (2 replicates for the lowest elevation at site 5). Data were log(x+1) transformed before regression analysis. Un-transformed data are plotted.

3.4.3. Swaths

The results for the transplanted swaths are similar to those for isolated transplants: mortality increased with increasing elevation above the *Endocladia* upper limit (Figure 3-12). Mortality was significantly greater 20 cm above the upper limit than 10 cm above the upper limit and significantly greater 10 cm above the upper limit than at the upper limit ($p<0.001$, Figure 3-12).

The average elevation above the upper limit at which transplanted *Endocladia* survived for 33 months was 9.47 ± 3.70 cm (95% confidence limits from 15 swaths).

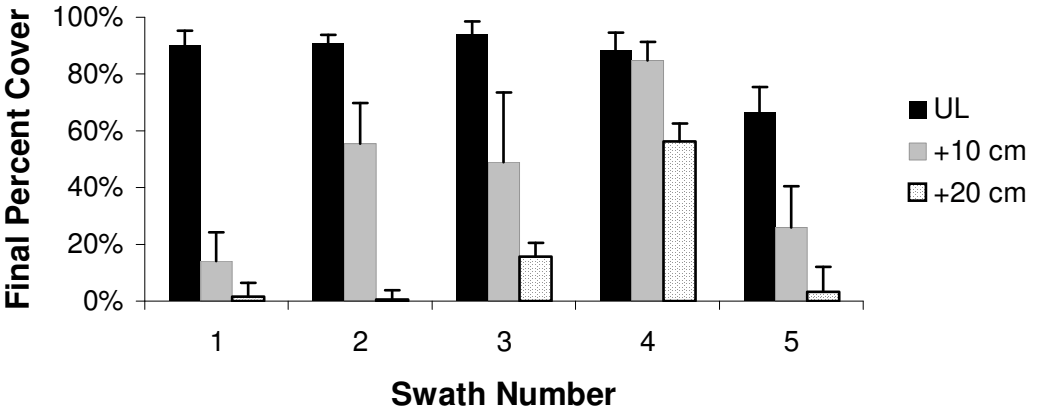

Figure 3-12. Survival within transplanted swaths as final percent cover. Survival 20 cm above the UL was lower than 10 cm above the UL (see Table 3-5). Survival at the elevation of the UL was highest. These results are similar to the transplant experiment conducted the previous year (see Figure 3-10).

Source of Variation	df	MS	F	p
Height	2	1.872	24.898	**<0.001**
Site	4	0.280	7.033	**<0.001**
Site X Height	8	0.075	1.886	0.100
Error	30	0.040		

Tukey Test for Survival at Elevations above the UL

Elevation	UL	10 cm above UL
10 cm above UL	**0.0001**	
20 cm above UL	**0.0001**	**0.0008**

Result: 20 cm above UL < 10 cm <UL

Table 3-5. ANOVA results comparing survival within swaths at different elevations. Survival declined as elevation above the local UL increased.

3.4.4. Removals

Successful recruitment into new sites depended on elevation ($p<0.001$, Figure 3-13). The area re-covered by *Endocladia,* from recruitment and subsequent growth, was statistically indistinguishable at and below the upper limit ($p>0.25$). The re-covered area above the upper limit was significantly less than below the upper limit ($p<0.02$, Figure 3-13).

(a)

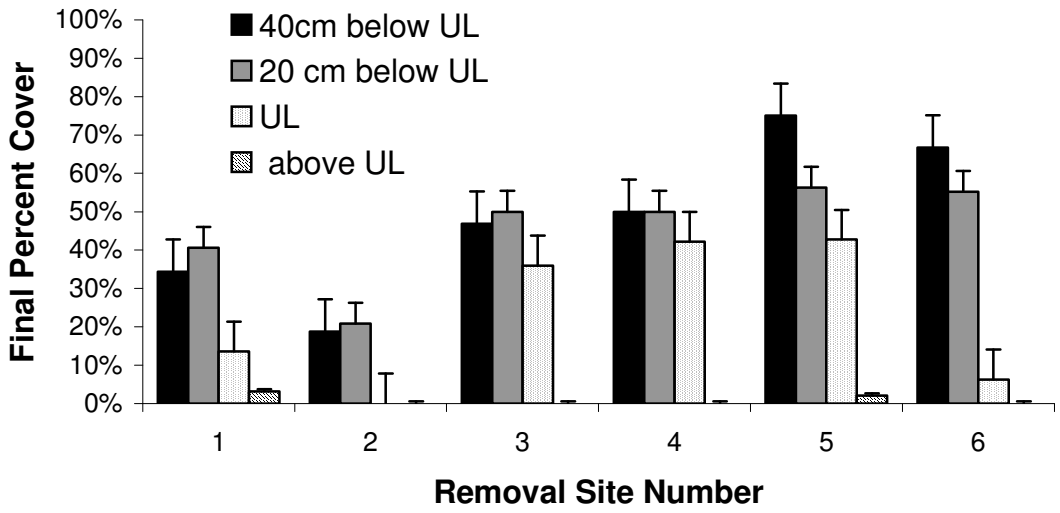

(b)

Result: Above the UL | **at UL** | **20cm below UL** | **40cm below UL**

Figure 3-13. (a) Recruitment above the UL was significantly less than below the UL (see Table 3-6). Recruitment at the UL was not significantly different than for sites above or below the UL. Sites above the UL were measured at the location of maximum percent cover. Sites below the UL were at a constant elevation. Plotted data are site averages ± 1 SE. (b) Treatments that are not significantly different are grouped with a contiguous underline.

Source of Variation	df	MS	F	p
Height	3	0.760	19.773	**<0.001**
Site	5	0.162	1.120	0.366
Site X Height	15	0.038	0.265	0.996
Error	40	0.145		

Tukey Test for Recruitment at Elevations Below the UL

	40 cm below UL	20 cm below UL	at UL
20 cm below UL	0.996		
UL	0.257	0.370	
above UL	**0.005**	**0.010**	0.350

Result: Above the UL at UL 20cm below UL 40cm below UL

Table 3-6. ANOVA results for recruitment at 4 elevations relative to the local UL. Recruitment above the UL was less than below the UL.

3.4.5. Boulders

Endocladia living on the manipulated boulders behaved similarly to that in transplant and removal experiments. One out of 3 rocks moved below the upper limit had significant recruitment, and none of the boulders moved above the upper limit had any survival (see Figure 3-14). The one exception was a small clump in a concrete seam below one of the boulders, but above the upper limit, which supported a seasonally ephemeral clump of *Endocladia* that only had visible fronds during the winters of 2002 - 2005. These fronds had bleached white and disappeared by each July.

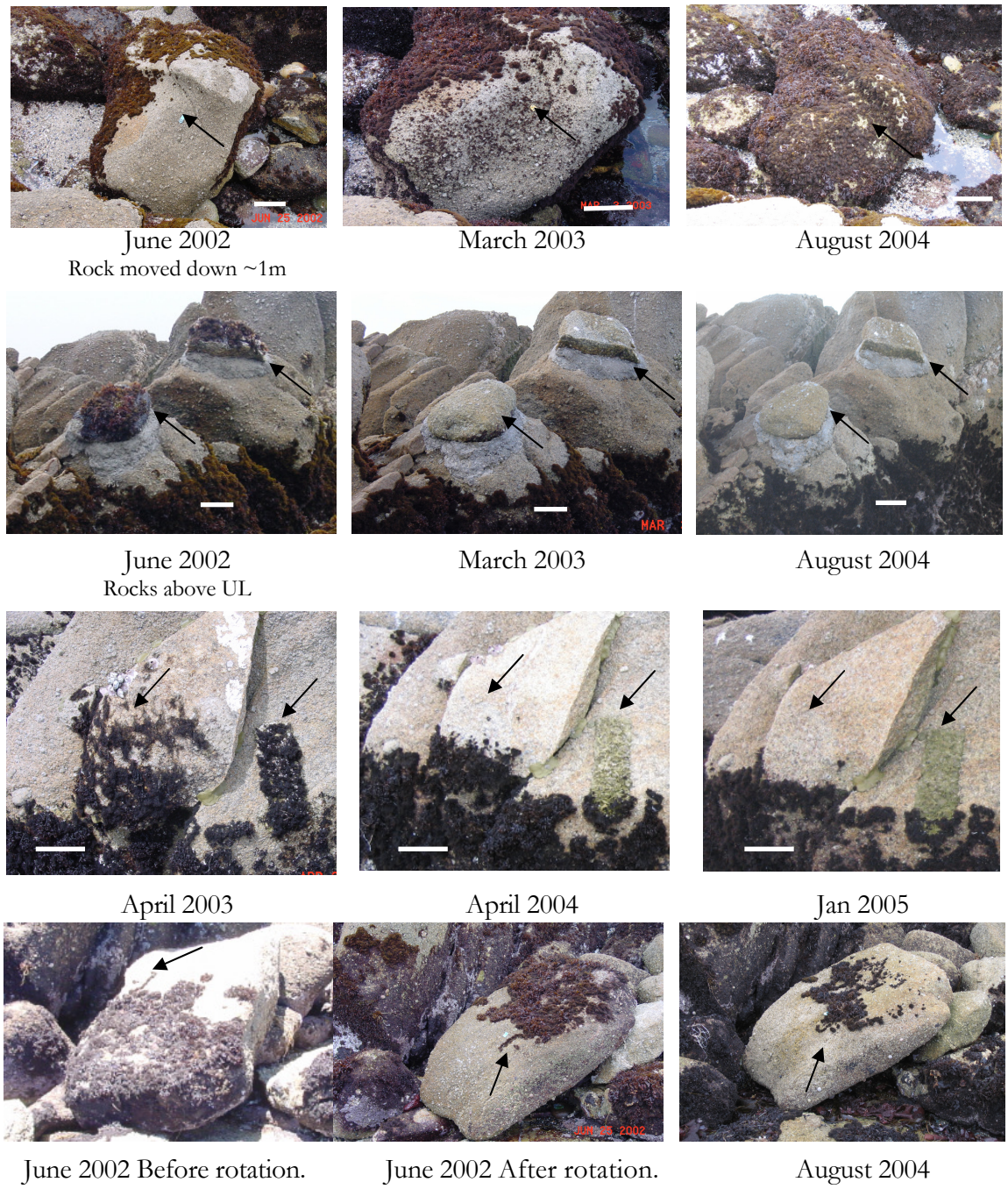

Figure 3-14. Boulders moved with attached *Endocladia* community show similar patterns of mortality and re-colonization as the smaller manipulations. Arrows for reference. Note the swath transplant visible to the left of the boulder in row 3 corresponds well with the boulder in the same photograph. Scale bars are approximately 20 cm.

3.4.6. Fences

The upper limit did not shift significantly in the fenced areas, or the fenced controls; see Figure 3-15.

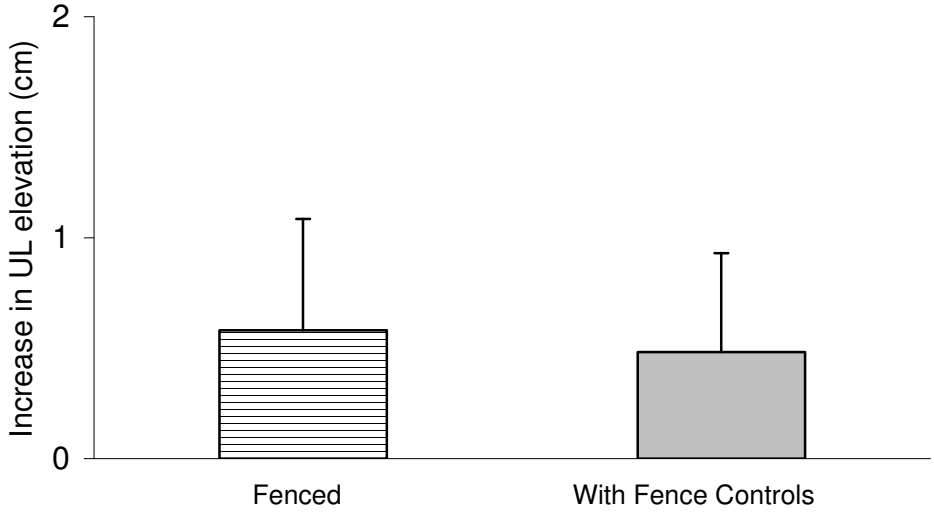

Figure 3-15. Values are averages for 9 sites ± 1 SE. The upper limit did not move significantly in either the fenced or fence-control areas (see error bars), and a paired t-test detected no difference between the treatment and the controls ($p>0.75$).

3.4.7. Summary of Results

I predicted that artificial shades would mimic some of the effects of the neighbors that had been removed during thinning (such as increased shading and decreased maximum temperatures), and thus I expected shades to enhance survival for the size classes that were most impacted by the removal of neighbors. Shades did decrease the maximum temperatures experienced by the clumps below them, and shading also rescued small clumps, to the point that survival was no longer distinguishable from the survival of larger size classes (Figure 3-8). Shades also significantly decreased the rate at which the smallest clumps lost area to frond die- back. Under natural, unshaded conditions, the smallest size class suffered more mortality and frond die-back than the larger size classes. These larger

size classes were statistically indistinguishable ($p>0.35$). While large clumps can persist once they become established, small clumps at the upper limit (and presumably above the upper limit) experience significantly higher mortality.

Height above the local upper limit was a significant predictor of survival within transplants. However, absolute tidal elevation was not. Maximum temperature was also a significant predictor of transplant survival. Although transplanted *Endocladia* generally died back above the upper limit, transplanted clumps survived 9.5 ± 3.7 cm above the local upper limit.

Recovery within clearings was less above the upper limit than below the upper limit, and excluding limpets from sites at the upper limit had no effect on the elevation of the upper limit.

3.5 Discussion

Manipulations at the upper limit show that the position of the range boundary is stable to large perturbations. The upper limit regressed towards its initial state after it was artificially moved lower or higher. Transplants 40 cm above the upper limit died back to the point that they remained only in the sheltered interstices created during transplantation, and transplants 20cm higher than the upper limit lost approximately 75% of their *Endocladia* cover over the first summer (Figure 3-9). Similar trends were seen in the swath transplanting experiment (Figure 3-12) and when entire boulders were moved (Figure 3-14). In other words, a 30-cm range shift upward, a range extension similar in magnitude to the one documented in Chapter 1, could not have happened during this study, although a 9.5cm range shift is demonstrably possible.

Clearings in the *Endocladia* zone were repopulated back to the elevation of the upper limit but seldom higher (Figure 3-13). However one-third of the clearings had no recolonization at all during 3.5 years of observation regardless of elevation. This low level of recruitment in *Endocladia* is consistent with the observation of others who documented rare and sporadic recruitment in this species (Northcraft 1946; Dayton 1971; Farrell 1991; Foster et al. 2003), including one removal study, which documented no recovery of Endocladia after 5 years post-treatment (Northcraft 1946).

Endocladia also extends vegetatively (Woodward 1988), so the question arises: what keeps the upper limit from extending upward via vegetative growth? I did not test this directly (for example by shading a region for an extended period) due to time limitations and the logistical hurdles of keeping shades functioning and unfouled for multiple years. However, observations of the clearings provide some insights. Vegetative growth appears to be slow at the upper limit and increase at lower elevations. This forms a characteristic "V" shape, as clearings fill in from the edges at lower elevations, while at the upper limit, inward growth is minimal. This may be a result of clump morphologies. Fronds at the edge of *Endocladia* turf, whether at the upper limit or adjacent to a cleared area, are typically short and erect with few branches, while fronds in the interior are usually more heavily branched and much longer. Because of this difference in morphology, the habitat adjacent to the clump edge is less shaded than it is closer to the larger fronds of the clump interior. Thus density-dependent facilitation may be greater in the clump center than at the edge, and one large clump with long central fronds would likely experience more self-shading than an amalgamation of many small clumps. To date, the growth rates within a clump and the rates of secondary frond attachment in different regions have not been measured.

Resilience of the upper limit following perturbation, however, is not perfect, and the upper limit would likely persist higher if an external trigger allowed it to be established. *Endocladia* transplanted into swaths survived for 33 months, 9.5 cm, on average, above the naturally occurring upper limit. This is substantial, when compared to the inter-annual stability over the last 35 years seen in the upper limit history of Chapter 1 (>6 S.E. of the inter-annual elevation change).

In general, density-dependent interactions are known to destabilize intermediate states and provide rapid switching between boundary conditions (Cannon 1967; Wilson and Agnew 1992). In particular the models of Wilson and Nisbet (1996; 1997) show that density-dependent facilitation, of the sort observed in the thinning experiment, can lead to sharp range limits even in a smoothly varying field of physical constraints.

For the case of *Endocladia*, the positive effects of neighbors (seen in the thinning experiment) act to increase the upper limit elevation and oppose the environmental limitations of

temperature and/or its correlates (also see Chapter 5). The relative strength of these opposing biological and physical factors determines the elevation of the range edge. In addition, because the range of *Endocladia* is not in equilibrium (seen in the transplant and swath transplant experiments), historical explanations, such as recruitment limitation or catastrophe, (when the "switch was last thrown") could play an important role in determining the position of the actual range limit at any given time.

To summarize, environmental constraints set the approximate elevation of *Endocladia's* upper range limit (to within 9.5 cm). However, the precise edge of the range is sharpened by pronounced density-dependent survival and increased within-clump growth. Interactions such as these are known to lead to both sharp borders and rapid range transitions (Chapter 2). Thus the same dynamics that cause the sharp upper limit, in this case, may also explain the discontinuity in the historical record.

Chapter 4

DESICCATION-COUPLED THERMOTOLERANCE: A SURVIVAL MECHANISM IN THE INTERTIDAL ALGA *ENDOCLADIA MURICATA*

4.1 Introduction

The ability of desiccation to increase thermal tolerance is widespread among taxonomic groups from insects to plants to microbes (Rothschild and Mancinelli 2001; Alpert and Oliver 2002). The protective role of desiccation is well appreciated for resting forms and for species that survive long periods of inactivity (see references in Leopold 1986), and there is an extensive literature on the physiological mechanisms by which organisms become more stress-resistant when they are desiccated (see reviews by Crowe et al. 1992; Gaff 1997; Crowe et al. 1998; Alpert 2000; Hoekstra et al. 2001; and Rascio and La Rocca 2005)

In contrast, the ecological importance of increased thermotolerance in marine plants (e.g., Kanwisher 1957; Biebl 1972; Smith and Berry 1986) is seldom appreciated. Many intertidal marine algae experience frequent desiccation during low-tide, and because low-tide conditions are both hotter and drier than high-tide periods of submersion, incidence of desiccation and high-temperature exposure usually coincide. The co-occurrence of hot and dried conditions suggests that increases in thermotolerance upon desiccation may be ecologically important for these organisms. However, experiments on the interaction between temperature and desiccation in intertidal plants have largely focused on the disruptive effects (sensu Davison and Pearson 1996) of desiccation (Hodgson 1981; Matta and Chapman 1995; Beach and Smith 1997). For example, the distributions of many intertidal algae are well predicted by the rate that photosynthesis recovers following desiccation stress (Dring and Brown 1982), and the literature abounds with experiments to test the many deleterious roles of desiccation (Schoenbeck and Norton 1978; Dromgoole 1980; Hodgson 1981; Oates and Murray 1983; Pena et al. 1999; Williams and Dethier 2005)). Despite the co-occurance of desiccation and temperature extremes in the intertidal zone, the perspective of intertidal ecologists is dominated by the perceived stresses associated with desiccation. The protective role of desiccation is largely overlooked in a ecological context.

Here I report on the ecological repercussions of enhanced thermotolerance during desiccation in the high-intertidal alga *Endocladia muricata* (Post. & Rupr.) J. Ag.

Endocladia grows as an aggregation of individuals into a thick mat or "turf" that blankets the substratum. The turf morphology is common among high-intertidal algal species worldwide (Stephenson and Stephenson 1972). Furthermore, the canopy formed by these turf species is an important component of the upper intertidal habitat. For example, in central California, more than 60 species shelter in the *Endocladia* turf (Glynn 1965).

But the turf also shelters itself. Competition and herbivory are intense in the intertidal zone, and the compacted growth form enables turfs to survive where isolated individuals cannot (Hay 1981; Taylor and Hay 1984). Enhanced survival results from positive interactions (such as increased water retention) between individuals and between fronds of one aggregated individual (Scrosati and DeWreede 1998). However, there is a tradeoff, as increased aggregation also results in lowered photosynthetic performance within the matrix, presumably due to self shading and nutrient limitation (Taylor and Hay 1984; Smith and Berry 1986).

An important aspect of the turf morphology is that the degree of aggregation is variable, and individuals may develop less-compact canopies when stresses due to temperature, desiccation, and herbivory are removed (Taylor and Hay 1984). In this sense, the turf morphology is a plastic mix of complementary ecological strategies. Under stressful conditions, increased aggregation results in a strategy of persistence but reduced growth (K-selected strategy). However, when environmental conditions permit, the turf may thin and become more opportunistic, increasing growth, while becoming less stress-resistant (r-selected strategy).

In addition to having the potential for changing strategies over time, many turf species are hereromorphic (possessing both a crustose and upright growth form) and different life history phases often employ contrasting strategies (Hay 1981). For instance, many species of algal turf have a perennial crust with "sacrificial" upright fronds, which grow rapidly and usually contain the reproductive structures. In contrast, the crust is slow-growing and

resistant to herbivory (Hay 1981; Taylor and Hay 1984). Therefore, if the fronds die, the crust may be preserved, and more fronds can re-grow from the crust.

Although most evident in heteromorphic species, this combination of fast- and slow-growing ecological strategies (within an individual) may apply more generally. For aggregated species, gradients exist between the clump interior and the edge, and the interaction between environmental gradients (e.g., temperature and desiccation) may create heterogeneity in life-history characteristics within a clump. For example, if rapid drying at the clump edge leads to increased thermotolerance in peripheral fronds but decreased rates of growth, the clump edge would be more K-selected than the clump center.

In this chapter, I propose that these contrasting ecological strategies (r- and K-selected types) arise directly within an isomorphic clump of *Endocladia* as the alga dries from the perimeter inwards. Therefore, contrasting morphologies are unnecessary for achieving multiple strategies within a single species. In turf species such as *Endocladia*, the magnitudes of both increased thermotolerance and the difference in desiccation rate between the clump interior and exterior determine whether desiccation-enhanced thermotolerance can be ecologically important. Here I compare the thermotolerance of saturated and dried *Endocladia* for both mature thalli and recently settled spores to evaluate the ecological importance of increased thermotolerance during desiccation.

4.2 Methods

4.2.1. Treatment of samples

All *Endocladia* samples were collected from the high intertidal zone (1-1.5 m above MLLW, NTDE 1983-2001) at Hopkins Marine Station, Pacific Grove, CA, (36.62°N, 121.91°W) and kept submerged in flowing seawater overnight. Samples collected on December 13 and 14, 2003, were heated for one hour in either a wet or dried state in a drying oven (Fischer Scientific IsoTemp 500). Wet samples were placed in a covered petri dish containing a small amount of water to ensure that the thallus remained hydrated without being submerged. "Dry" samples were dried at room temperature with a fan to 10-15% relative water content prior to treatment, and also placed in a covered petri dish during heat shock. Relative Water Content (RWC) is defined following Slayter (1967) as:

$$\text{RWC} = \frac{\text{fresh weight - dessicated weight}}{\text{fresh weight - dry weight}} \times 100\% = 100 - \% \text{ desiccation.}$$

During heat exposure, the oven temperature was recorded each minute with an iButton temperature logger (Thermochron, 0.5 ºC resolution, Dallas Semiconductor), and thallus temperature was measured with a small (40-gauge) thermocouple placed within the algal clump. The oven was pre-heated to the test temperature (between 25 and 65 ºC). Dried thalli reached oven temperature within 15 minutes, while wet thalli reached oven temperature within 10 minutes. The difference was presumably due to evaporative water loss, as "dried" thalli (10-15% RWC) continued to lose water until they equilibrated with the lowered humidity within the heated oven. Because they were contained at 100% relative humidity, wet thalli could not evaporatively cool. Following heat shock, the samples were allowed to recover for 36 hours in flowing seawater before survivorship was determined.

In addition, the survivorship of wet *Endocladia* heated for different lengths of time was determined for samples collected between October 20th and November 7th, 2005. These samples were held as above, except heat stress was applied to individual fronds using an aluminum heating block. The temperature of the block was kept constant at each end by a heater embedded at one end, and tubes cooled by a water bath at the other end. In this way, a temperature gradient was set up within the block and tubes could be held at various temperatures, depending on their placement within the gradient block. Fronds were heated in the block within 1.5 ml micro-centrifuge tubes that were capped, with a small amount of water in the bottom, and fronds were held at temperatures between 30°C and 45°C for 0.5, 1 , 2 , and 4 hours.

4.2.2. Vital Assay

Survival was determined by comparing relative rates of photosynthesis between fresh tissue and tissue after heat shock and 36-hour recovery. Relative rates of photosynthesis were measured using a Pulse Amplitude Modulated fluorometer (PAM).

The use of fluorescence to measure photosynthesis rates (Schreiber et al. 1986; Bolhàr-Nordenkampf and Öquist 1993) relies on the principle that fluorescence and ATP-synthesis

are competing pathways for transferring energy from a photon absorbed by photosystem II, the first photosystem in the photosynthetic pathway. When photosystem II absorbs a photon and becomes excited, the energy excited electron is either passed on to the electron acceptor plastoquinone, or if plastoquinone is already reduced (because it is involved in electron transport from a recent photon absorption), the electron loses energy through fluorescence (heat de-excitation is presumed constant with respect to the rate of photochemical de-excitation and is therefore ignored). Thus, if a photon is absorbed by photosystem II, it can either be used to generate ATP, or it will fluoresce. The probability that the photon will enter the photosynthetic pathway is the probability that it is absorbed by a non-fluorescing ("open") reaction center. This probability is termed the quantum yield. Yield is measured using a high intensity light pulse that saturates all photosystem II reaction centers, causing them to fluoresce. This maximal fluorescence, Fm, provides a "count" of the total number of reaction centers. Under ambient light, fluorescence is then lowered to a rate Ft, and the likelihood that an absorbed photon is used in photosynthesis (the yield) is calculated as the proportion of reaction centers that are open. Yield=(Fm-Ft)/Fm. The Electron Transport Rate (ETR) is the quantum yield times the number of photons in the photosynthetically active portion of the spectrum (PAR) that are absorbed by photosystem II (PAR x Absorbance x 0.5). The factor of 0.5 is used because roughly half of the absorbance is due to photosystem I and does not contribute to the measured fluorescence.

After heat exposure and subsequent recovery, rapid light curves were constructed for dark-adapted samples using a PAM fluorometer (Diviving PAM, Heinz Walz GmbH). Electron transport rates (ETR = quantum yield x PAR x 0.5 x absorbance) were averaged for 3 saturating, but not photoinhibitory light levels (Figure 4-1, PAR fluxes of 500, 650 and 1000 μmol photons/m^2). Absorbance was measured with a Li-Cor 1800 spectroradiometer and the PAR light source on the PAM was calibrated using a Li-Cor 190 PAR sensor. Samples were considered dead if ETR had not recovered above 25% of fresh sample ETR. Conclusions remain unchanged regardless of whether the discriminating percentage was chosen to be 25% or 60% of fresh-sample ETR because less than 4% of post-heat-shock samples were in the range of 25%-60% of fresh ETR. (Note that, because the assay is a

ratio, it is acceptable to measure only the relative ETR at a constant light intensity: absorbance and calibrated PAR values are not essential.)

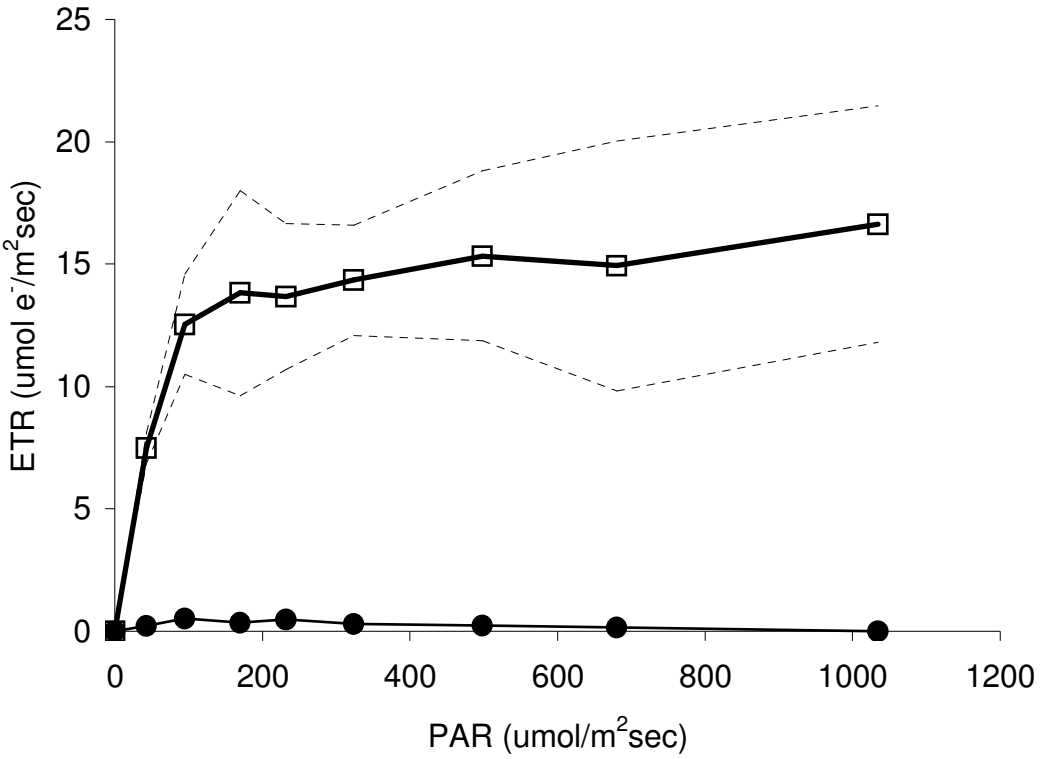

Figure 4-1. Rapid light response curves for dark-adapted, hydrated *Endocladia*. Open squares are values for pre-treatment samples. Dashed lines are 95% confidence intervals for the data, not the mean. Filled circles are a typical response curve for non-photosynthesizing *Endocladia* (e.g., either "dead" or desiccated).

To test for further recovery of ETR, 15 individuals classified as alive and 15 individuals classified as dead were assayed after an additional 24 hours submerged in seawater. In all 15 samples classified as dead, there was neither substantial recovery of ETR nor a change in survival classification. In contrast, ETR continued to approach fresh ETR in all 15 samples classified as alive.

Samples collected in 2005 were assayed with a PAM 210 at the single light level of approximately 750 μmol photons/m² PAR, and survival was determined as above.

4.2.3. Thermotolerance of Settled Spores

Spore thermotolerance was also determined in both wet and dried states. To induce sporulation, spore-bearing thalli of *Endocladia muricata* collected on August 8, 2005 were dried to less than 20 percent RWC at room temperature (20-23° C) in airflow from a fan. Thalli were then rehydrated in autoclaved filtered sea water in a large petri dish, and spores were soon released upon rehydration (Woodward [1984] reports tetraspore release within 1 minute and carpospore release within 5 minutes after a desiccated frond was resubmerged). During spore release, the dish was placed within a darkened incubator at 13°C (average ambient sea water temperature in Pacific Grove in August) and agitated every hour to keep the spores in suspension. After 8 hours numerous spores had been released and the suspension was swirled gently and distributed into petri dishes resulting in approximately equal numbers of spores in each dish from 8-10 parent thalli. Spores were incubated for 3 days at 13ºC under fluorescent light (G.E. 15W warm white bulb) with a daily light period of 14 hours. The water was changed daily, and the spores were allowed to dry at room temperature (~20 to 23ºC). Drying the cultures daily kept them free of ciliates, which otherwise would decimate the colonies.

After 3 days, the spores were subjected to heat within a drying oven as above. Prior to heat-stress, water in the dry-treatment petri dishes was poured out, and the spores (which adhered to the dish) were dried with the plate in a vertical orientation at room temperature with a fan. In wet spores, the water was poured off, and a film of water remained, which kept the spores moist. Both groups of spores were in a covered petri-dish during heating. Following heat-stress, the spores were allowed to recover in autoclaved seawater for 48 hours before survivorship was determined.

Individual groups of spores were marked, counted, and the group followed through treatment. Spores were classified as alive if they retained their reddish pigmentation [largely due to water-soluble phycobili proteins (Lee 1999) that could diffuse away when the enclosing membranes were damaged]. Spores that lost pigment were pronounced dead. A

pilot study determined that spores retaining their pigment for 48 hours continued to retain pigment for at least 4 days, while spores without pigment failed to recover and often deteriorated noticeably in this time (data not shown). The fraction of all spores surviving within a dish (n=87 to 150) was used as the estimate for survivorship.

4.2.4. Analysis

Survivorship curves were fit to the data using probit regression (Finney 1964) in MatLAB.

4.3 Results

4.3.1. Desiccation Increases Thermotolerance

The survivorship curves for both saturated (RWC~100%) and desiccated (RWC<15%) thalli collected at the upper limit of *Endocladia muricata* at Hopkins Marine Station are shown in Figure 4-2. The temperature where 50% mortality occurred (LT-50) was 35°C for wet thalli, while for dry thalli the LT-50 was substantially hotter: 47°C.

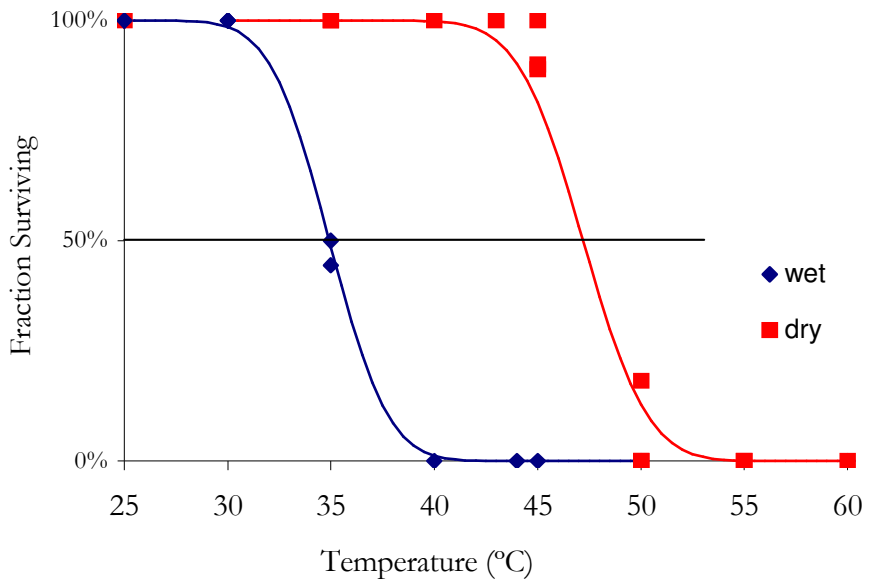

Figure 4-2. Survival curves for "dry" (<15% RWC) and wet (100% RWC) *Endocladia* following 1.5-hr temperature stress and 48 hours recovery. LT-50 for wet and dry *Endocladia* are 35ºC and 47ºC respectively. Note: wet survival curve is comparable to those shown with much better temperature resolution in Figure 4-3 for 1.5 and 2 hours of heat stress.

Endocladia can survive hotter temperatures for shorter amounts of time (Figure 4-3). This experiment was done to determine the actual shape of the relation between LT-50 and duration of heat stress, and this result will be elaborated upon in Chapter 5.

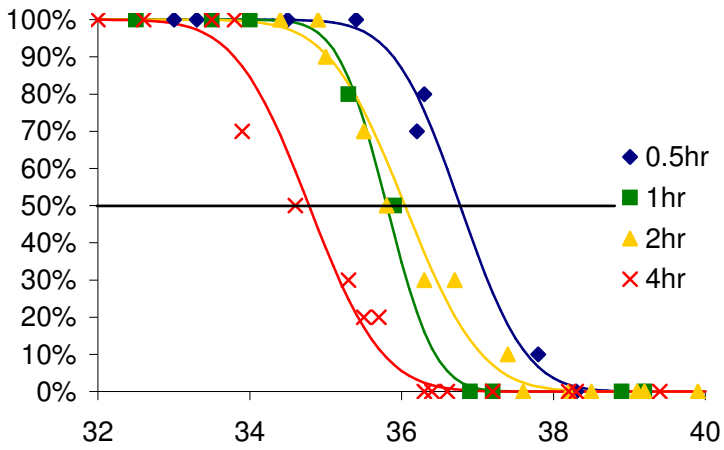

Duration of Heat Stress (hr)	LT-10	LT-50	LT-90
0.5	35.8	36.8	37.7
1	35.1	36.1	37.0
2	34.8	35.8	36.5
4	33.7	34.8	35.7

Figure 4-3. Survivor curves for "wet" *Endocladia* (100% RWC) for different durations of heat stress. Summary parameters are shown in the table.

The thermotolerance of 3-day-old spores showed a similar increase in survival when they were dehydrated, although the magnitude of the effect was less (Figure 4-4). The LT-50 of wet spores was 34ºC to 35°C, comparable to wet adult thalli, while the LT-50 of dry spores was 39°C, substantially below that of dry thalli (47ºC). The haploid tetraspores and the diploid carpospores showed similar patterns of thermotolerance.

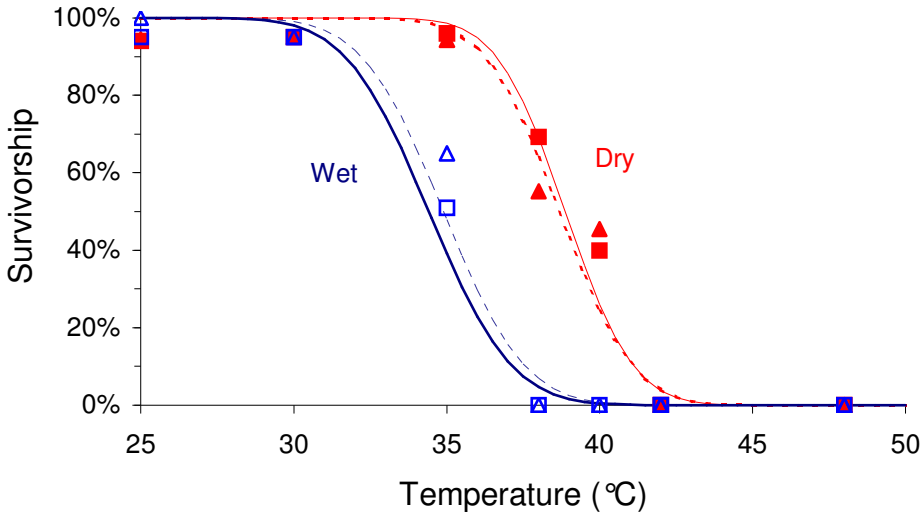

Figure 4-4. Survivorship for 3-day-old spores of *Endocladia muricata* after 1 hour exposure to heat stress and 48 hours of recovery. Carpospores (squares) are diploid and tetraspores (triangeles) are haploid; both are dispersal phases. Survivorship after desiccation is showed by filled symbols (▲,■). Hydrated survival is shown by outlined symbols (Δ,□) LT50 is approximately 35°C when wet and 39°C when dry regardless of phase.

4.3.2. Photosynthesis During Drying

The rate of photosynthesis is negligible when thalli are dehydrated below 30% RWC (Figure 4-5). This result corroborates the findings of Britting and Chapman (1993) for this species.

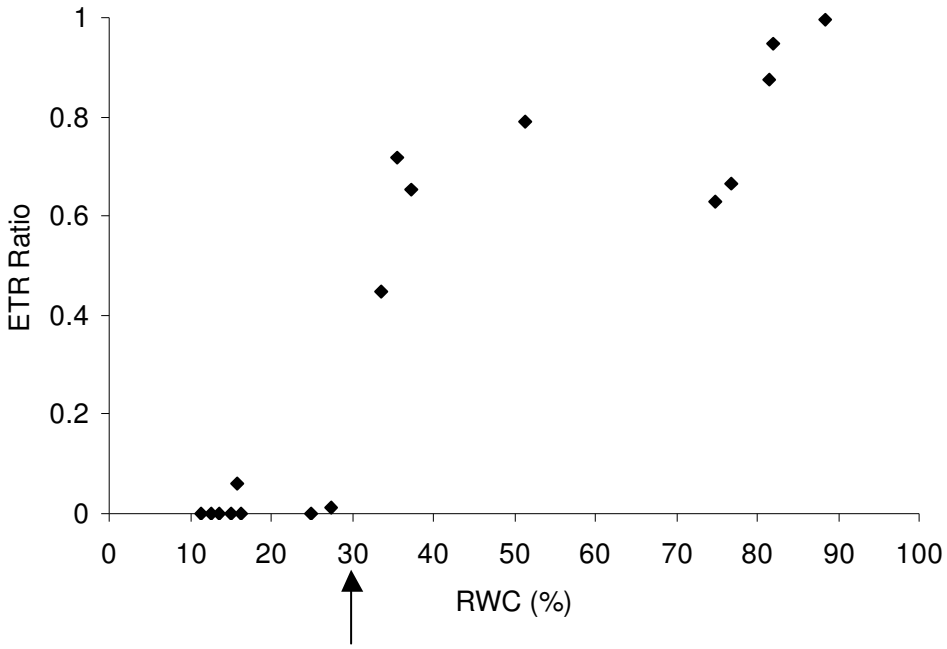

Figure 4-5. Ratio of Electron Transport Rate (ETR) during desiccation to ETR of fully-hydrated thalli for various states of desiccation. Thalli dried below 30% relative water content have negligible rates of photosynthesis, compared to fully hydrated thalli.

Within a 4-cm-diameter clump, the clump edge dries more quickly than the clump center (Figure 4-6), and for a moderate windspeed of 1 m/s the clump center is moist and capable of photosynthesis (RWC>30%) for approximately one hour longer than the clump edge. Under these conditions, the entire clump (both center and edge) is dried such that photosynthesis is stopped within 2 hours. This is the equilibrium state of *Endocladia* during emersion, which is seen as the long-term asymptote of the drying curve. The maximal possible desiccation (the equilibrium RWC) depends on ambient relative humidity (Figure 4-7). For typical conditions in Pacific Grove, CA, the relative humidity in the intertidal zone is between 40% and 60%, and this results in an equilibrium RWC of 5% to 15% (Figure 4-7). Thus *Endocladia* survives substantial desiccation, often on a daily basis.

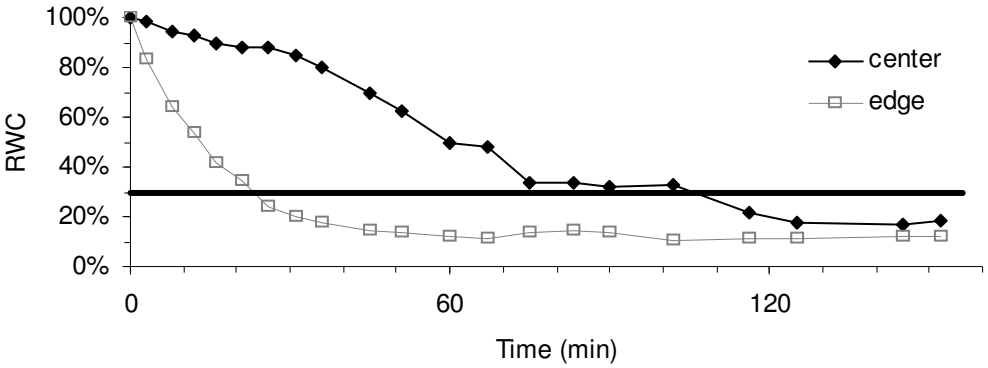

Figure 4-6. Drying curves for central (♦) and exterior (□) portions of an 8-cm-diameter clump of *Endocladia* measured in a wind tunnel under 1 m/s wind speed, and no solar irradiation. The clump edge dries faster than the clump center, and under such conditions, fronds near the clump center experience longer periods engaged in photosynthesis with RWC above 30% (horizontal line is shown at RWC=30%). Under these conditions, most of the clump is dried within 2 hours, although small basal portions of fronds may remain moist.

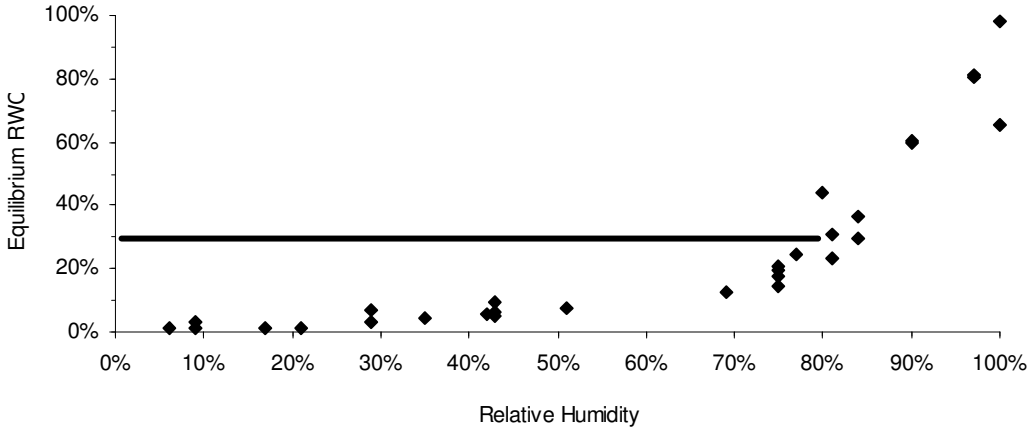

Figure 4-7. Equilibrium Relative Water Content (RWC) as a function of ambient Relative Humidity (RH). Humidity was controlled by saturated salt solutions, and the RWC was measured after 2 days equilibrating in a closed container above the solution. Photosynthesis is negligible below 30% RWC (line shown), and therefore below ~ 80% RH, *Endocladia* dries to photosynthetic dormancy.

4.4 Discussion

4.4.1. Survival and Growth: A Dessication-Mediated Tradeoff

The thermotolerance of *Endocladia muricata* markedly increases when thalli are dried, both for mature thalli and for recently settled spores, and photosynthesis stops when thalli are dried to 30% RWC. Thus, due to the dependence of thermotolerance on desiccation, there is a tradeoff between the potential for growth and survivorship. This tradeoff is manifest within an *Endocladia* clump: compared to interior fronds, the outer fronds dry more quickly and therefore experience both less time exposed to potentially-lethal temperatures, and less time hydrated and engaged in photosynthesis. The ecological importance of this trade-off relies on two conditions: first, increased survival of dry thalli, and second, enhanced growth of thalli that remain moist longer.

First, increased survival when dry: The maximum temperature of *Endocladia* I have measured in Pacific Grove, CA is 41 °C, on April 26th, 2004 (in this case the crispy-dry alga survived). This temperature exceeds the thermal limit (LT50=35°C) of both mature thalli and spores when they are hydrated. It is also above the thermal limit of dry spores (LT50=39°C), but well below the thermal limit of dry thalli (LT50=47°C). The maximum temperature of wet *Endocladia* I have measured is 37°C (on July 3rd, 2003. In this case there was widespread bleaching and the alga died; see Figure 4-9a). Thus, in Pacific Grove, CA, dried thalli appear to be at minimal risk of heat death, while hydrated thalli do experience lethal temperatures.

Second, increased growth when wet: Within a clump, central fronds remain moist longer (Figure 4-6), and they appear to grow faster than peripheral fronds. Outer fronds of high-intertidal *Endocladia* clumps do not bear sporangia, and they are often much shorter than the fronds of the clump interior. Within the clump centers, reproductive portions of the fronds are shed seasonally (personal observation), and this biomass must be regenerated. If growth rates (neglecting tissue loss) were the same at the clump edge and at the center, the seasonal loss of material from central fronds would cause these fronds to elongate more slowly. In clumps with minimal frond mortality (so frond age is not a dominant factor) the slower rate of elongation would lead to central fronds that are shorter than peripheral fronds. However,

the opposite size trend is observed: fronds are usually longer in the clump center, which suggests that these fronds may grow faster.

A notable pattern of bleaching within individual fronds also suggests that mortality is desiccation-dependent. During the widespread bleaching (and subsequent mortality) event of July 2003, I was perplexed to find that the middle of the fronds often bleached, while the tips and very base retained their pigment (Figure 4-8). These individuals later appeared to have healthy frond tips, but the fronds eventually broke below the bleached portion and re-grew from the unharmed basal portion. In light of the markedly differential thermotolerance between wet and dry thalli, I suggest that the frond tips may have been protected because they had dried. The clump center, close enough to the rock and shaded to the point that it remained cool enough, survived even when wet, but the central portion of the frond died because it was both wet and less shaded and therefore reached its lethal temperature.

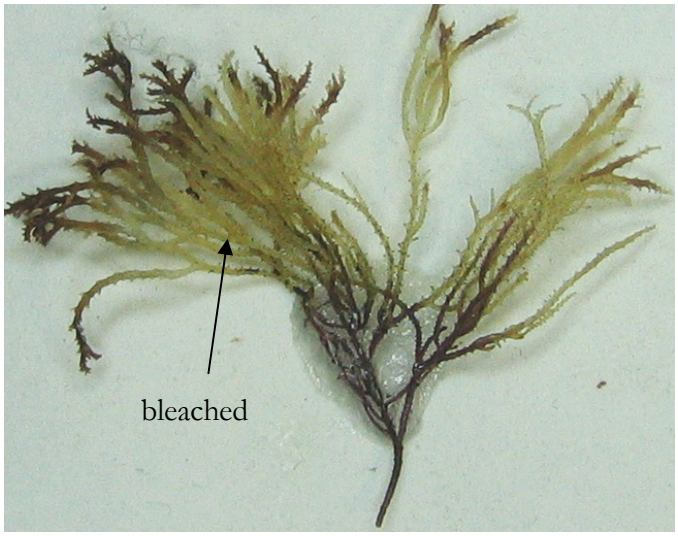

Figure 4-8. Bleaching pattern seen on fronds (July 3, 2003). The bleached portions subsequently died and broke off.

A second pattern of mortality also suggests that desiccation-enhanced thermotolerance may be ecologically important. Numerous events that prove lethal to interior fronds leave a fringe of *Endocladia* surviving— only the outermost fronds survive in a "fairy ring" (Figure

4-9). This matches the pattern in survival one would expect if the outer clump is protected by desiccation. However, it remains to be seen if this pattern in differential survival is due to desiccation protection of the outer fronds or if other causes (such as the clump center filling with trapped sediment) are more important.

(a)

(b)

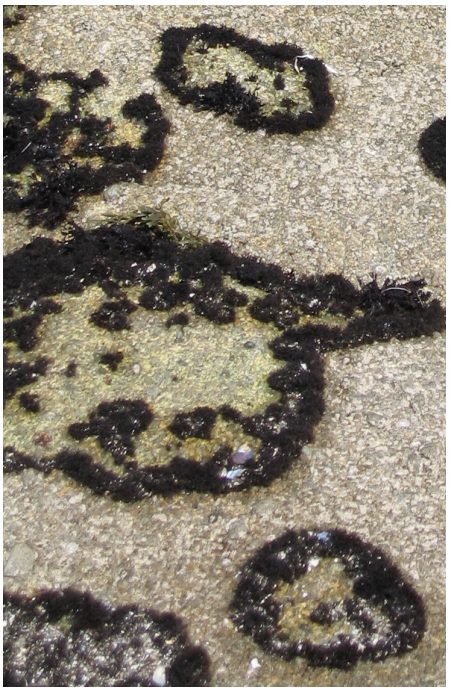

(c)

Figure 4-9. (a) *Endocladia* bleaching pattern during widespread bleaching event of July 3, 2003. (b,c) *Endocladia* "fairy rings", a common sight in the central California intertidal zone.

The surviving outer fronds in a fairy ring often are often the source for vegetative recolonization of the clump center. Thus, these outer fronds may serve a dual purpose: they may slow the drying rate of the inner, reproductive fronds (increasing the time hydrated and engaged in photosynthesis), as well as acting as a source for recolonization via vegetative growth in the event of a thermal catastrophe. In this light, the central clump is the more r-selected region, while the periphery is selected more for persistence than growth and reproduction (K-selected). The clump periphery therefore appears to have a similar ecological function as the basal crust of turf species (Hay 1981), and it may be a generally important function of the turf form in species that lack a prominent basal crust.

4.4.2. Duration of Natural Exposure: The Magnitude of the Tradeoff

Time spent drying out is a large portion of the total time *Endocladia* spends hydrated and potentially engaged in photosynthesis. Between August 1999 and August 2005, *Endocladia*'s average upper limit (at 1. 4 m above MLLW) was above the measured still water level for 87% of the time (data from Monterey Tidal Observations, NOAA). However, if splashing due to waves is considered, the amount of time spent high and dry is reduced considerably. If wavesplash is estimated from offshore waveheight (I will call this 0.2 m wave splash)[*] and added to still-water-level, the time *Endocladia* is dried is reduced to 75%, and if a constant wave splash of 0.5 m is assumed (likely an overestimate, see footnote), the fraction of time dry drops to 50%. Thus, even considering wave spash, the *Endocladia* upper limit spends a substantial fraction of the year above the water.

Furthermore, *Endocladia* at the upper limit is exposed to air for long uninterrupted periods. The duration of emergence is shown in Figure 4-10 as a frequency distribution. The frequency is the proportion of emergence events that last for a specified duration. For 0.2 m high waves, the distributions is bimodal. The bimodal distribution results because this

[*] I made the following assumptions to estimate the height of wave splash at this site: The average height of the wavesplash that first wets a site was measured in Chapter 5 as the average distance above the still water level when a site was first splashed (Harley and Helmuth (2003). At the elevation of the upper limit, this was 0.2 m (although as mentioned in Chapter 5, these measurements are biased toward hot days). I assumed the waves on a falling tide were the same size as on a rising tide. The average significant waveheight measured by a pressure-guage offshore of the rocks protecting this site was 0.9 m, and I scaled the continuous waveheight record for 1999-2005 by the ratio of the average measured wavesplash (0.2) and the offshore average significant wave height (0.9) to obtain a continuous estimate of wave splash at this site.

study site experiences mixed, semi-diurnal tides, and during some periods of the tidal cycle, every high tide wets the site, while at other times, only one high tide per day is high enough to wet the site. Emersion infrequently lasts longer than a day (1% of the periods of emergence with 0.2 m waves last longer than 24 hours, and the maximum continuous emergence, for 0.2m waves, was 4.6 days, in May 2002). The unimodal distribution of 0.5m waves indicates that under these conditions the upper limit is almost always splashed during both daily periods of high tide.

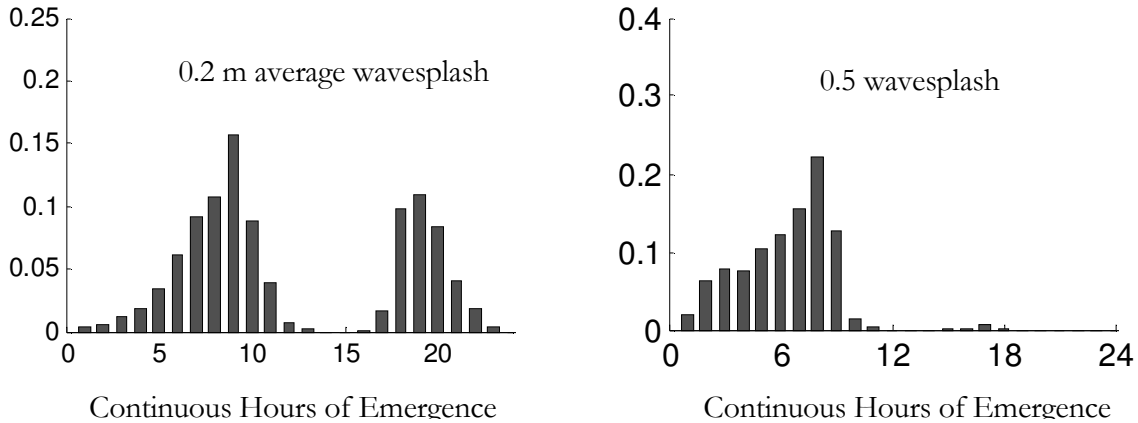

Figure 4-10 Frequency histograms for continuous emergence with wavesplash that reached 0.2 m (left) and 0.5 m (right) above the still water level. For example 15% of the emergence periods lasted for 9 hours when 0.2 m waves were considered.

During most periods of low-tide emergence, peripheral clumps are dried to a dormant state. That is, more than 98% of emergence events, considering 0.2 m waves, (or more than 90% for 0.5m waves) lasted more than 2 hours, which is roughly the time it takes for the periphal clumps of *Endocladia* to dry out in typical wind conditions (Figure 4-6). The central portions of large clumps, however, may remain wet for much longer, and this can greatly extend the time available for photosynthesis.

Considering only daylight hours (irradiance >100 w/m^2 measured at a nearby weather station ~100 m from the study site) approximately 10% of the year is spent drying during the 2 hours following emergence (10% for 0.2m waves, 13% for 0.5m waves). Considering that *Endocladia* is below the elevation of wave splash for only 25-50% of the year, this time spent drying represents a substantial fraction of the total time spent hydrated and potentially

engaged in photosynthesis (~30% for 0.2m waves and ~15% for 0.5m waves), and increasing this time by decreasing the drying rate would have a substantial impact on the time available for photosynthesis.

4.4.3. Summary

Endocladia is remarkable in that it experiences >90% desiccation [Alpert's (2005) criterion for "desiccation tolerant" or "anhydrobiotic" species], often on a daily basis. I have shown that when *Endocladia* is dry, thermotolerance increases and photosynthesis stops. Consequently, there is an ecological "tradeoff" between growth when wet and increased thermotolerance when dry. A substantial fraction of each year is spent "drying out". During these periods, the rate of drying determines how much of this time is spent hydrated, when *Endocladia* is potentially engaged in photosynthesis, but also more vulnerable to high temperature. Clumps dry from the edge, and this alone can result in a single clump adopting two contrasting ecological strategies: the clump center is poised for growth. In contrast the clump periphery sacrifices growth rate for increased thermotolerance. This may in turn give rise to interesting transient patterns ("fairy rings" and patterns of frond bleaching) within the *Endocladia* zone.

THERMAL TRACKING BY AN ECOSYSTEM ENGINEER: TEMPERATURES AT THE UPPER RANGE LIMIT OF *ENDOCLADIA MURICATA*

5.1 Introduction

Species' range limits have long fascinated biologists, and with recent concerns about climatic change, it is particularly important to understand the factors maintaining these borders. For decades the rocky intertidal zone has provided a model system for studying species' borders because of the prevalence of well-developed zones worldwide (Stephenson and Stephenson 1949). The long-standing hypothesis that the physical environment determines the upper limit of species' ranges (Connell 1961) continues to guide studies in intertidal ecology, and the thermal physiology of these organisms suggests that they may be poised for dramatic changes under a warming climate (Tomanek and Somero 1999; Stillman and Somero 2000; Stenseng et al. 2005). Despite widespread interest in thermal ecology and particular enthusiasm among intertidal ecologists, our knowledge of the thermal environment experienced by intertidal organisms remains rudimentary. Such basic knowledge as the frequency distribution of temperature (what is a "rare" body temperature?) and how this temperature distribution varies between sites remains poorly quantified.

5.1.1. A Case Study: Endocladia Muricata

Here I report a detailed look at the thermal environment surrounding the strikingly sharp ecotone and concomitant threshold in biodiversity that is formed by the upper limit of intertidal macroalgae at Hopkins Marine Station (Pacific Grove, CA). This upper limit has been called the "most conspicuous landmark" in this part of California (Stephenson and Stephenson 1972). This "landmark" often consists of a dense front of the turf-forming species *Endocladia muricata* that abruptly terminates into "bare" rock above. Within the *Endocladia* matrix, Glynn (1965) discovered a rich community of more than 60 species, and below the upper limit, *Endocladia* grades into an assemblage of turf algae that almost completely covers the substratum. This upper limit is therefore an important ecological

transition within the intertidal zone, below which small organisms can shelter within a dense canopy of seaweed, and above which the canopy is missing.

Although the upper limit is often sharply marked, the elevation at which it occurs is site specific and spatially variable. In the local area of this study, roughly 250 m of shoreline, the upper limit varied in elevation by about one meter, or 60% of the tidal range (Monterey diurnal range =1.62 m, NOAA). In addition, the elevation of this border was very stable over the 35 years preceding this study (see Chapter 1). Because of its spatial and temporal tractability, the *Endocladia* turf edge is appealing for study of the thermal environment near a well-defined and ecologically significant range boundary.

Indeed, temperature stress may be important in setting the upper limit of *Endocladia*. The work of Britting and Chapman (1993) indicates that *Endocladia* reaches temperatures that are high enough that, following exposure, a substantial period of recovery is needed before photosynthesis can be resumed. Recovery of photosynthesis upon low-tide stress has been shown to correlate with the upper limits of a number of intertidal algal species (Druehl and Green 1982; Hawkins and Hartnoll 1985). Thus high temperatures may limit the distribution of *Endocladia*.

If exposure to high temperature sets the elevation of *Endocladia's* upper range limit, two predictions follow. First, the upper limit of *Endocladia* would be positioned within the thermal habitat space such that high temperatures (for instance maximum temperatures or 99^{th} percentile temperatures) are less variable along the upper limit than one would predict by chance. That is, I hypothesize that departures of the upper limit from horizontal are due to *Endocladia* "choosing" a particular thermal regime and adjusting its elevation accordingly. Second, I hypothesize that at hot locations (e.g., southern exposures), the upper limit is lower than at cool locations.

To frame these hypotheses, horizontal transects are necessary for reference temperatures because these report measurements unaffected by biological response. In contrast, the upper limit may move up and down in response to the local temperature climate, and the expectation that higher upper limit sites will have higher temperatures may not hold, if the

range height is responding to temperature. By altering its range in this way, *Endocladia* may reduce the thermal variability between sites at the upper limit. I refer to this mitigating response of the range edge to temperature as "temperature compensation". In this light, the site-to-site temperature variability along the upper limit is akin to "residual" temperature differences; it is variability that remains unaccounted for by upper limit movement in response to local site temperature. Therefore, the biological temperature response can be assessed from the predictive power in the "residuals." If upper limit temperatures predict upper limit elevations, temperature compensation is incomplete because the putative elevational gradient in temperature still exists among upper limit sites. However, if there is no pattern to the "residuals," this means that the upper limit temperature is no longer correlated with elevation. In this case, the range is responding to eliminate the observed trend with elevation, and temperature compensation is substantial.

In summary, the hypothesis that the upper limit elevation responds to temperature (or a correlate thereof) leads to three test conditions:

(1) Limiting temperatures (e.g., 99th percentile or maximum temperatures) are less variable among sites at the upper limit than they are among sites along a horizontal transect. That is, the range edge is a limiting-temperature isotherm.

(2) Between sites, limiting temperatures measured along a horizontal transect are inversely correlated with upper limit elevations. In other words, hot sites have lowered upper limits.

(3) Limiting temperatures at the upper limit are uncorrelated with upper limit elevation. That is, there is no pattern to the "residual" upper limit temperatures (temperatures measured after biological response).

5.1.2. Temperature Compensation or "Hot Spots"?

The importance of biological temperature compensation, and our pressing need for small-scale temperature data, is highlighted by the pitfalls encountered in a recent and widely-influential study by Helmuth et al. (2002). Intertidal mussel (*Mytilus californianus*) body temperatures were compared across latitude from Washington State to Southern California,

with the expectation that body temperatures would be warmer at southern locations, due to warmer environmental temperatures. When no latitudinal trend in body temperature was evident, Helmuth et al. (2002) concluded that the body temperature variability among sites was the result of local "hot spots:" sites where mussels were at particular risk of localized extinction. However, without data on small-scale thermal heterogeneity for comparison, it is impossible to support a "hot spot" conclusion over one of sampling error, (i.e., is latitudinal variability significantly larger than the variability one would encounter sampling within a small neighborhood?). Furthermore, presupposing an environmental trend ignores the possibility of biological temperature compensation, which appears likely in this case. The mussel bed (and thus the position of the mussel loggers in the center of the bed) is generally lower at southern latitudes, possibly in response to a latitudinal gradient in temperature (Gislen 1943). In other words the mussel bed might adjust vertically to maintain a constant temperature (similar to the case I present for *Endocladia*). Given this mechanism for temperature compensation, it may be misleading to ignore biological response and expect mussel body temperatures simply to mimic environmental temperature gradients.

The purpose of this chapter is thus two-fold. First, in the context of the *Endocladia* range limit, I point out the importance of temperature (and/or its correlates) in setting the elevation of the upper limit within a small study site (~250 meters of shoreline). The upper limit is lower at hot sites than at cool sites, and this thermal tracking of the range limit leads to a controlled temperature among sites within the *Endocladia* community, and I discuss the ecological implications. Second, in a more generalized context, I explore in detail the thermal environment in this region of the intertidal zone and provide characterizations that will inform studies of the interaction between physiology and ecology.

5.2 Methods

5.2.1. Temperature Measurement

Temperatures within the *Endocladia* canopy were measured within artificial mimics equipped with iButton temperature loggers (Dallas-Maxxim Thermochron, 0.5ºC resolution). Loggers were placed at sites spanning the range of slopes and aspects found at Hopkins Marine Station, Pacific Grove, California. To mimic *Endocladia* temperatures, iButtons were glued to the rock (Z-spar Splash Zone Compound) and covered with a 5 cm x 6 cm swatch of

paint scrubber (3M) held in place by two stainless-steel screws set into plastic anchors in the rock. The algal canopy was cleared away for 5 cm around the loggers with a drill-mounted wire wheel. The paint scrubber mimicked living *Endocladia* in both light absorbance and drying time, and the temperatures recorded by iButtons within clumps of living *Endocladia* were well approximated by these thermal mimics (Figure 5-1).

Four iButtons were placed at different elevations within each site: one at the upper limit of *Endocladia*, (this elevation varied from site to site), one at the elevation of the average upper limit at Hopkins Marine Station (at approximately a constant elevation, 1.37 m above MLLW), and one each 20 cm above and 20 cm below the average upper limit elevation. This resulted in four transects, three at constant elevations, and one that followed the undulations in the upper limit (Figure 5-2). The elevation of each logger was surveyed from a nearby U. S. National Geodetic Survey Benchmark at known tidal elevation (PID GU3971, 6.81m above MLLW NTDE 1983-2001).

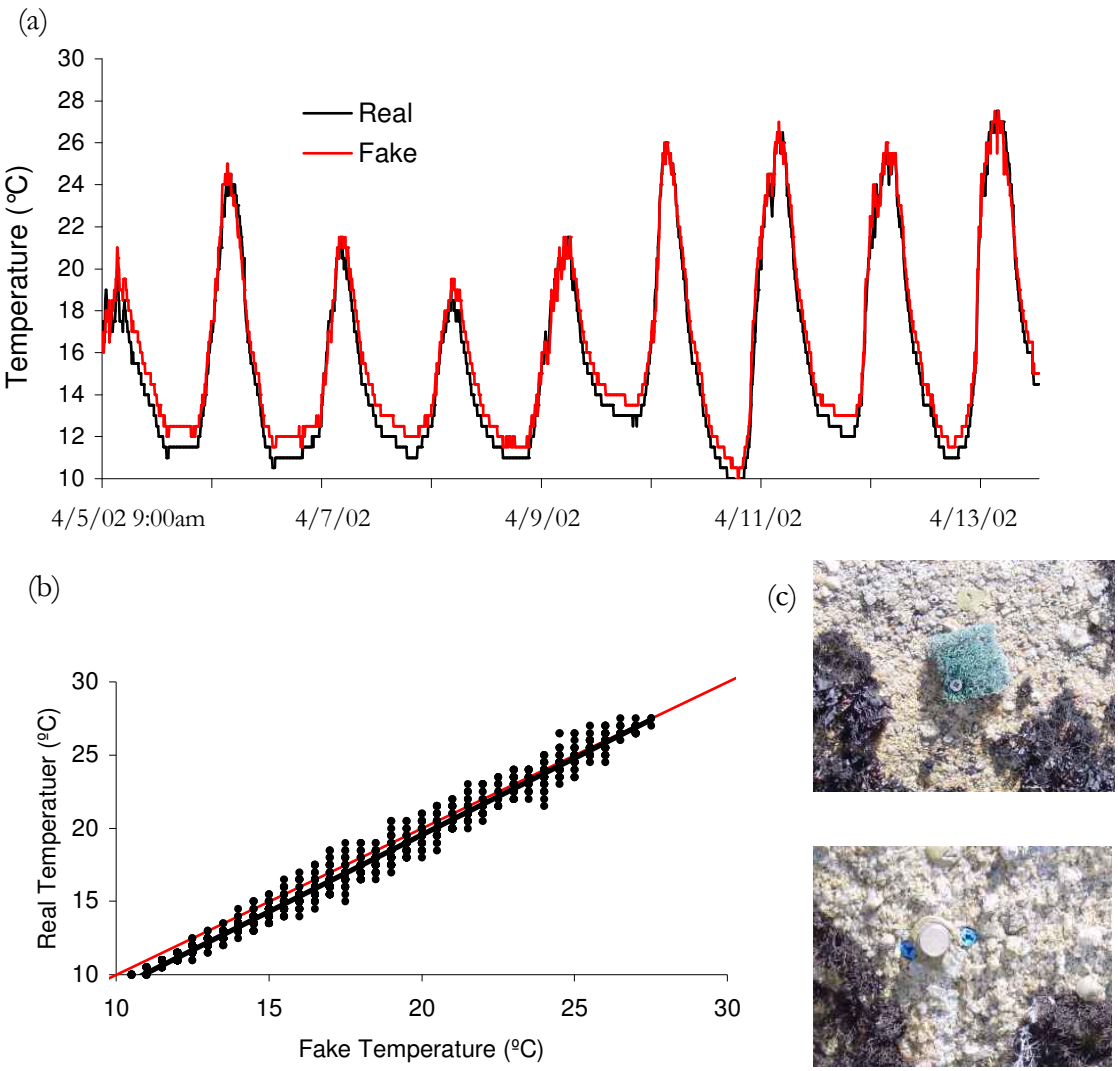

Figure 5-1. (a) Temperatures recorded within the *Endocladia* canopy and beneath an artificial thermal mimic. (b) The real and fake temperatures compared with the 1:1 line (light red line) and the heavy black trendline (Real=1.05 x Fake +1.43, R^2=0.99). An iButton temperature logger is shown glued in place (c, bottom) and covered by an *Endocladia*-like scouring pad (c, top).

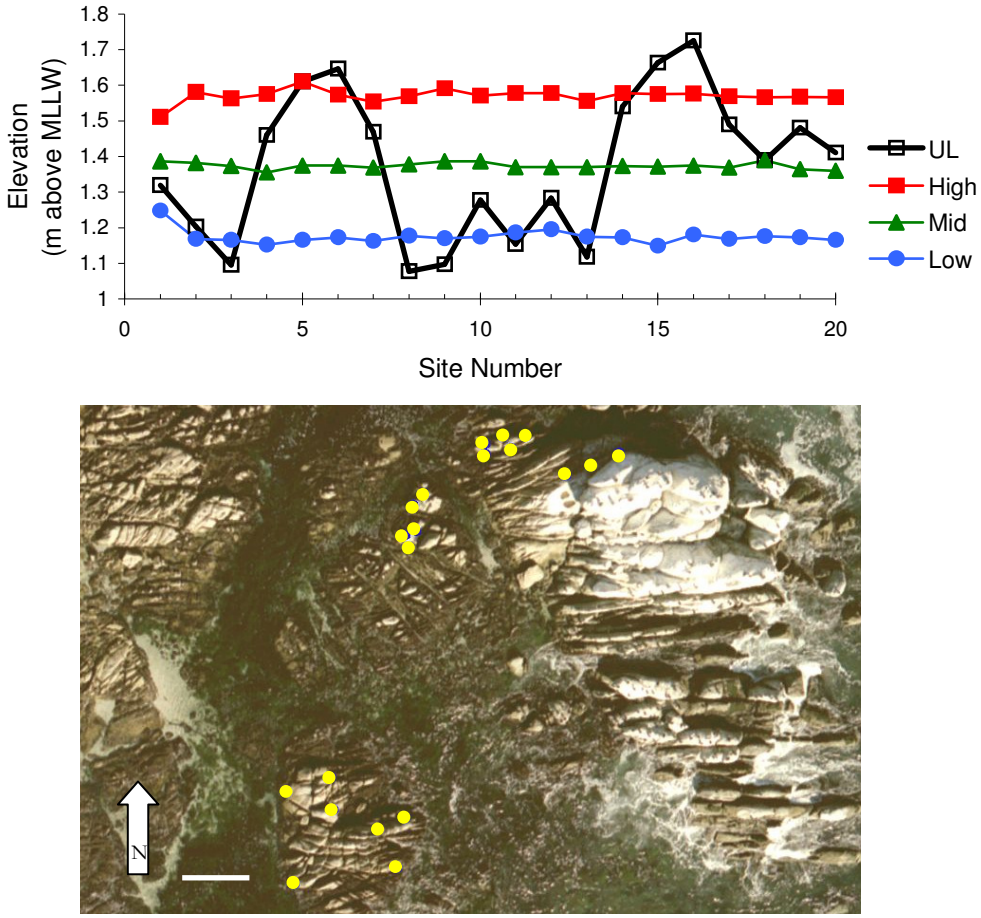

Figure 5-2. Elevations of temperature measurements (top). At each of 20 sites, temperatures were measured at 3 constant elevations (Low, Mid, High), and at the upper limit of *Endocladia* (UL). This results in 3 horizontal transects describing the thermal environment, as well as the actual temperatures experienced at the upper limit. Locations of sites are shown in the lower panel. Scale bar is 5 m.

The loggers were set to overwrite data after the memory was filled, so they would log continuously and all loggers were synchronized at the beginning of the experiment. Every 40 days, when the iButton memory was filled, data were downloaded in the field (without removing the loggers from the rock) using a Palm IIIxe and a Scanning Devices iConnection. The iButtons were first cleaned with a squirt of alcohol and dried with a cloth. A hexadecimal interpreter written in MatLAB greatly facilitated data extraction from the Palm IIIxe. The time stamping used by the iConnection was particularly prone to error

during the download process, so data were visually inspected on the Palm and re-downloaded from the iButton if an error was noted. Time errors were easily detected (seen as an error in the number of data points) and data could be re-aligned in time by matching overlapping temperature data in the new and previously downloaded files. In the final record, data were visually inspected to ensure that all loggers were aligned in time. Gaps in the record were filled by correlating with nearby loggers in the following manner: the temperature data for the seven days prior to the gap were correlated between the logger with missing data and all of the other loggers. The data from the logger with the highest correlation coefficient were extrapolated using the linear fit of these seven days to fill the gap in the following record. Approximately 2 % of the record was filled by interpolation, and the lowest R^2 was 0.87. Before deployment, loggers were calibrated in a controlled temperature bath, and a linear fit was used to correct iButton temperatures measured in the field.

Temperatures were measured at four elevations within 20 sites (Figure 5-2) every 30 minutes between July 4, 2002, and November 28, 2003. Measurements were continued at seven of these sites through October 2004, while the rest of the loggers were removed for use in other experiments.

5.2.2. Visualizing Temperature-Time Climates

A graphical method of visualizing the relationship between temperature, duration of heat exposure, and the frequency of occurrence (i.e., the physiologically-relevant aspects of temperature) is shown in Figure 5-3. At any temperature (along the X-axis), the duration (along the Y-axis) represents the period of uninterrupted time above that temperature. The number of times these conditions occurred in the 17 months of observation is the frequency (along the Z-axis), represented by contour lines of equal number of occurrences within the period of observation. Temperatures are in 0.5 °C bins, durations are in 30-minute bins, and contour lines are computed from this surface in MatLAB. Contour lines connect temperature-duration combinations that occurred with equal frequency. That is, these combinations were equally likely. The temperature-duration-frequency (TDF) plots shown are the average across all 20 locations of each transect.

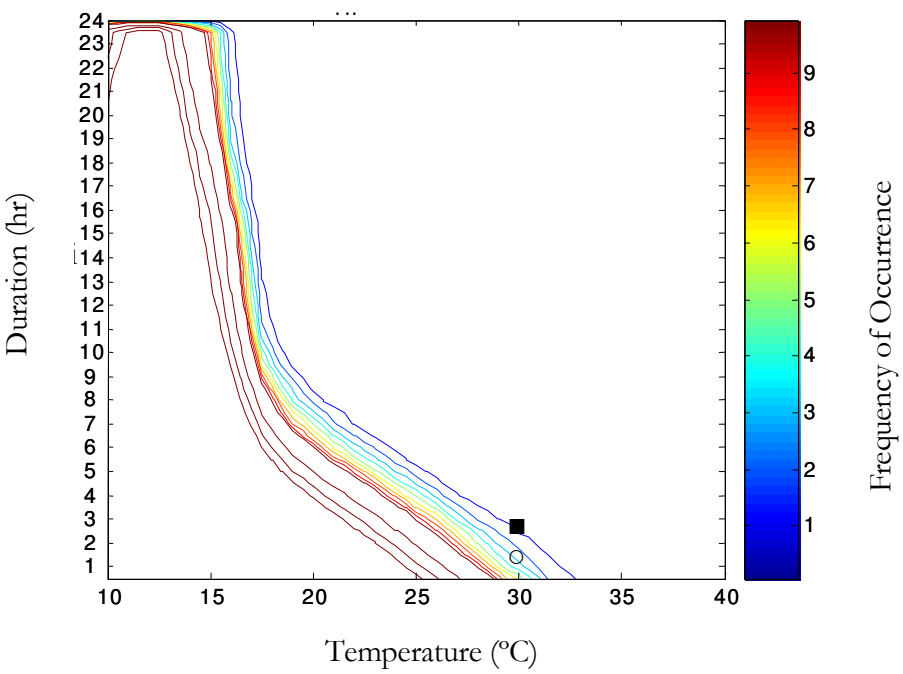

Figure 5-3. Contour plot of the temperature, duration and frequency (z-axis) surface for the average UL conditions between July 2002 and Nov 2003. Contours 1-10 (one to 10 occurrences in the record) are color coded, contours 20, 30 and 40 (wider spacing) are also shown. For example, averaged across sites, the upper limit exceeded 30ºC once for 3 hours (■) and 3 times for 1 hour (○). The inflection point between 15 and 20ºC corresponds to a typical Monterey evening air temperature: Temperatures do not exceed 20ºC overnight, but they often exceed 15ºC overnight. Steep slopes indicate that, for a given frequency, a small increase in temperature corresponds to a large decrease in the time spent above that temperature. The constant slope above 20ºC shows there is a constant temperature-duration trade off at these temperatures. Above 20ºC, 1 degree cooler corresponds to approximately 0.6 hours longer.

5.2.3. Wave-Splash and Effective Shore Level

Wave-splash increases the time *Endocladia* at a given elevation is wetted, and changes in wave exposure often change the elevation of intertidal zones (Ricketts et al. 1985). Harley and Helmuth (2003) introduced a convenient method by which the effect of wave splash can be quantified from temperature measurements. During an incoming tide, the first wave may rapidly cool a hot temperature logger. If the time is noted, the size of the wave splash can

be calculated as the difference between the actual height of the temperature logger and the height of the tide when the wave first doused the logger. Averaged over time, the sea level at first splash is called the Effective Shore Level, [ESL, Harley and Helmuth (2003)]. A crucial part of the analysis is choosing the size of the cooling step that indicates a wave splash. A larger value results in fewer erroneous data (for example, if the cooling were due to a cloud passing over the sun, it would not be interpreted as a wave splash if the critical step-size was larger than the cooling experienced under cloud cover). However, large critical step-sizes also skew the data so that only hot days are represented. I chose a 5ºC decline and a 7ºC decline in temperature as indications of wave-splash, and the results for both determinations of ESL were similar (see results and Figure 5-11).

5.3 Results

5.3.1. Upper Limit Elevation Approximates a High-Temperature Isotherm

Temperatures at the upper limit of *Endocladia* (UL) are notably different than along a horizontal transect. The elevation of the *Endocladia* upper limit is situated so that maximum temperatures approach 35°C at most sites, but exceed 35°C at only a few sites (Figure 5-4). Above 35°C, the UL and Low transects (20 cm below the average upper limit) are similar: few sites on either transect exceed 35°C. In contrast, at lower temperatures, less than a third of Low-transect sites exceed 30°C, and at these lower temperatures the UL transect is most similar to the High transect (20 cm above the average upper limit): most site maximum temperatures exceed 30°C. The aggregation of UL temperature maxima between 30ºC and 35°C leads to significantly less variability in maximum temperatures along the upper limit than along any of the horizontal transects (Table 5-1). This lowered among-site temperature variability at the upper limit is also seen when 99th percentiles are compared (Table 5-1), and while maximum temperatures are at most infrequent, temperatures exceeding the 99th percentile occur relatively commonly –for approximately 120 hours per year. In both cases, the upper limit of *Endocladia* is a better isotherm than is a horizontal transect, despite what might be predicted by its variation in elevation.

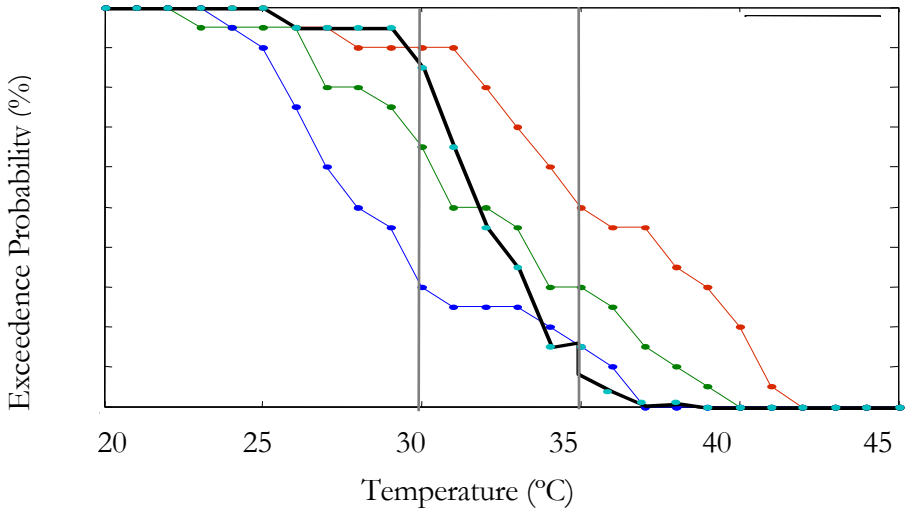

Figure 5-4. The probability that a site exceeds a given temperature is plotted relative to the temperature exceeded for all transects. High is red, Mid (at the average elevation of the UL) is green, Low is blue, and the UL transect is black. UL temperature maxima are clustered in the 30 to 35ºC range. Nearly all UL temperature maxima exceed 30º C (similar to the High horizontal transect, 20 cm higher), while few UL site maxima exceed 35º C (similar to the Low horizontal transect, 20 cm lower).

Temperatures	Low	Mid	High	UL
Max Temp (°C)	36.5	38.5	41.5	36.5
Range of Max Temp (°C)	16.5	14.5	16.0	9.5
σ^2 Max Temp (°C)	18.1	13.8	14.7	**5.2***
σ^2 99th percentile (°C)	11.7	11.4	11.7	**4.2***

Table 5-1. The variability in maximum temperature among sites is less at the UL than along a horizontal transect (Fmax test $p<0.05$). Similarly the range in maximum temperature is less at the UL, and the actual maximum temperature reached is the same as at a horizontal transect 20 cm lower. The pattern is the same for the 99th percentile (only the statistically tested result is shown).

5.3.2. The Upper Limit is Lowered at Hotter Sites

The elevation of the upper limit of *Endocladia* is predicted by site temperature. The elevation of the upper limit is lower at sites that experience higher maximum temperatures measured

along any of the three horizontal transects (Figure 5-5). This is also true if 99th percentiles are used instead of maximum temperatures, and the relations between upper limit elevation and 99th percentiles are even stronger (for Low, Mid and High Transects, R^2=0.78, 0.79, 0.69), probably because these temperatures are less variable than maximum temperatures.

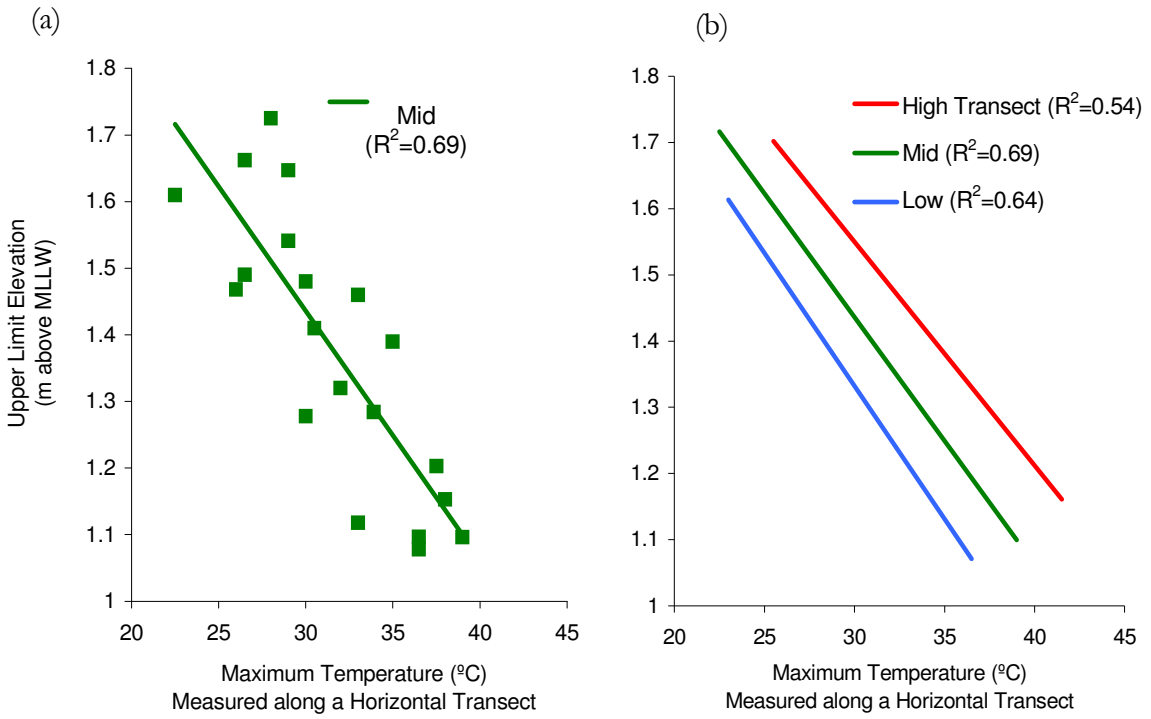

Figure 5-5. (a) The maximum temperature measured at a constant elevation (here, at the average UL elevation) predicts UL height. (b) Relations are similar for all 3 horizontal transects. The average slope is –0.037 m/ºC; a 1ºC increase in maximum temperature corresponds to a 3.7 cm decrease in the elevation of the UL.

The expected movement of the upper limit in response to an increase in maximum temperature is determined from the average slope in Figure 5-5, -0.037 m/ °C. Thus a 1°C rise in maximum temperature corresponds to a 3.7 cm lower upper limit. Note that this represents the expected *response* of the biological upper limit. To determine the thermal gradient across elevations in a manner unconfounded with biotic response, one can compare horizontal transects. Within the algal canopy, a 20 cm increase in elevation leads to an average increase in maximum temperature of 3 ± 1°C (95% C.I., n=40: 20 sites).

5.3.3. Residual Temperature Variability at the Upper Limit

In contrast to maximum temperatures measured along a horizontal transect, maximum temperatures measured along the upper limit (that is, those incorporating biological response) poorly predict the elevation of the upper limit (R^2=0.05). In the absence of a biological response to temperature, maximum temperatures at the upper limit would reflect the observed environmental gradient (3°C per 20 cm rise in elevation). Thus, the lack of correlation between maximum temperature and elevation indicates that biological response eliminates the environmental gradient in maximum temperatures. However, at lower percentiles the correlation between site-temperature and site-elevation substantially improves (i.e., there is a substantial pattern to the residuals; see Figure 5-6), which suggests that the degree of temperature compensation (via elevation change) is less at these more-commonly-occurring temperatures (Table 5-2).

Percentile	**100% (max)**	**99.95%**	**99.90%**	**99%**	**95%**	**70%**	**50% (median)**
Temperature value (average of all sites °C)	31.7	28.8	27.7	22.8	18.7	14.4	13.3
Hours per year exceeding given percentile	0	4	8	80	400	2500	4000
R^2 with UL Elevation	0.05	0.12	0.37	0.51	0.42	0.11	0.09

Table 5-2. Residual temperature variability at the UL (after biological response) at different percentiles. The average temperature and hours of exceedence are to help the reader interpret the frequency and temperature associated with a particular percentile. R^2 is calculated between UL temperature percentiles and UL elevation and indicates the predictive capacity of various percentiles.

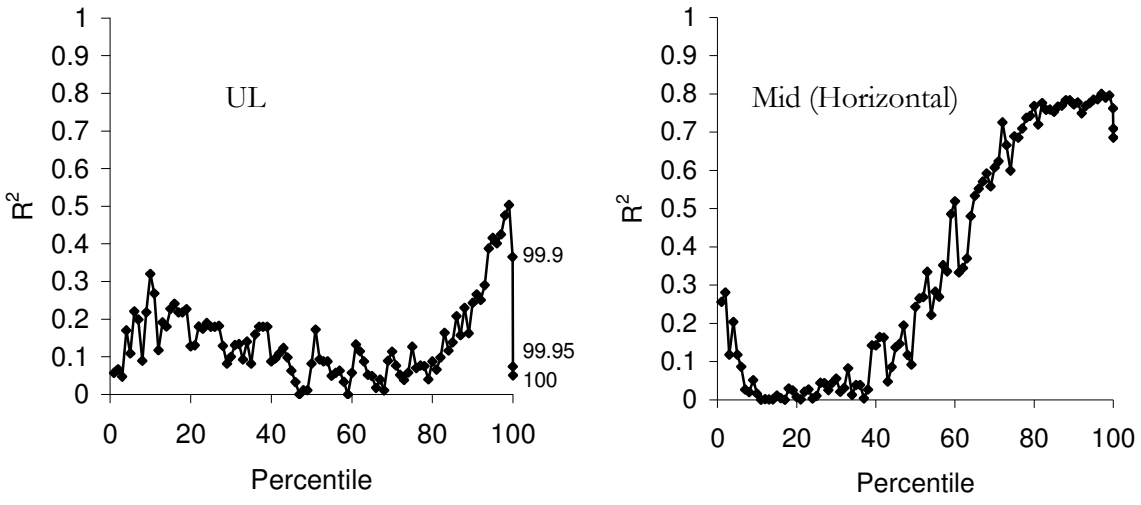

Figure 5-6. Squared correlation between temperature percentile and UL elevation for the UL transect (left) and the Mid (average UL elevation) transect (right). In these comparisons, the site-to-site variability in a given temperature percentile (along the x-axis) is correlated with the site-to-site pattern of upper limit elevation, and the resulting R^2 is plotted on the y-axis. For percentiles >80%, temperatures along the horizontal transect predict upper limit elevations better (higher R^2) than temperatures along the UL. UL temperatures between the 90th and 99.9th percentiles are predictive of the UL elevation, indicating an incomplete degree of temperature compensation at these percentiles. Data are every 1-percentile, except for the 99.9th , 99.95th and 100th (maximum) percentiles.

5.3.4. Probability Distributions of High-Intertidal Temperatures

The probability density function is a fundamental descriptor of an ecological variable, and when comparing temperatures between sites, it is important to quantify how the probability distribution of temperature varies at different locations. Among sites, the frequency distributions of temperature (Figure 5-7) are similarly shaped in their upper tails; therefore, correlations across sites made at a particular percentile are dependently linked to correlations made at other percentiles. That is, sites ordered by 99th percentile fall in nearly the same sequence as sites ordered by 90th percentile. In the previous section, 99th-percentile temperatures were correlated with upper limit elevations. Because nearly the same pattern exists in 90th percentiles, it is not surprising that the 90th percentiles also correlate with UL elevation. The correlations between percentiles are shown in Figure 5-8. Above the 99th

percentile, the correlation drops faster than below the 99th percentile, likely because there are few data at the highest percentiles (Table 5-2), and sampling error is therefore increased. However, at the upper limit, the drop in correlation is substantially larger than that seen in the horizontal transects, and this decorrelation at the upper limit is necessary for the pattern in residuals seen above: 99th percentiles predict upper-limit elevations, but the maximum temperatures do not (see Section 5.3.3.).

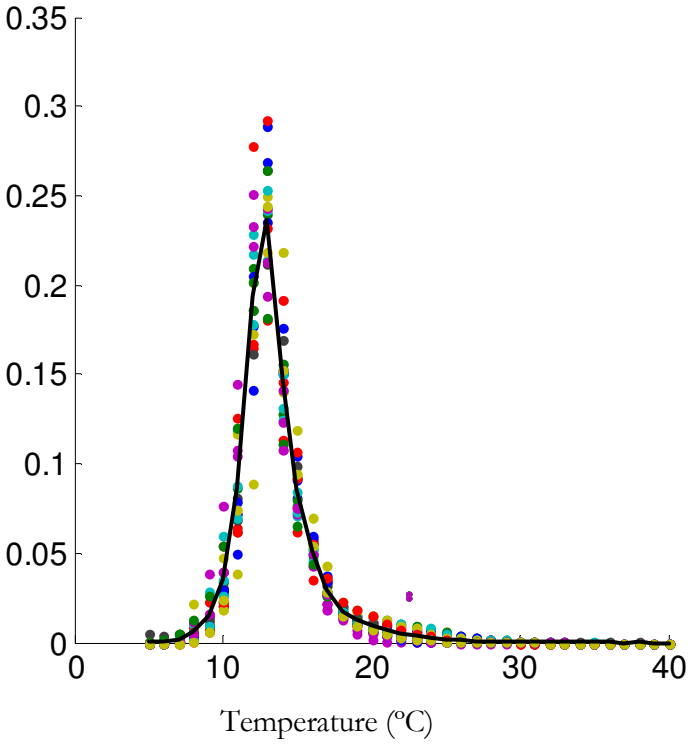

Figure 5-7. Probability density function of temperature for 20 UL sites (different colored dots) aligned at the median value (black line shows the average of all sites). Distributions are approximately exponential in the upper tail. For all transects the average exponent = 0.0093 ± 0.0022 (mean ± 95% C.I.)

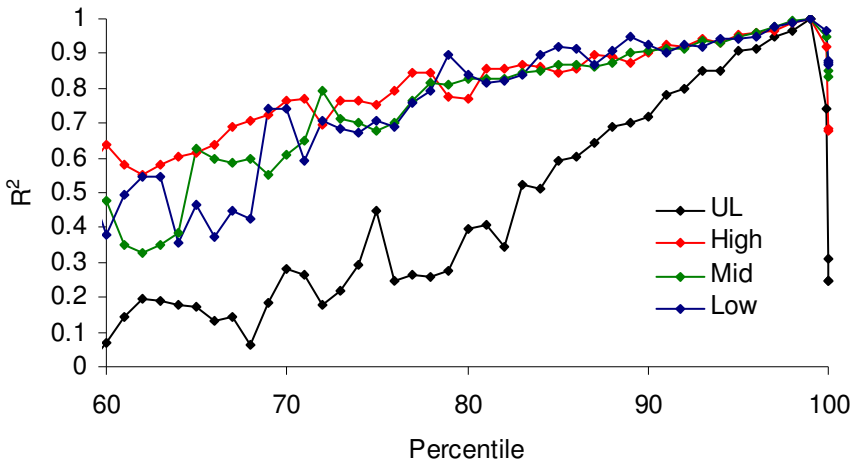

Figure 5-8. Squared correlation between particular percentiles (x-axis) and the 99th percentile showing the inter-relation among percentiles. The drop in correlation above the 99th percentile is likely due to the rarity of these highest percentiles (<8 hours per year exceeding the 99.9th percentile). Points are every 1 percentile, except the highest data are 99th, 99.9th, 99.95th, and 100th percentiles.

5.3.5. Enter Physiology: What Conditions are Riskiest?

The Temperature-Duration-Frequency (TDF) plot can be used to compare the thermal environment with an organism's physiology and determine which lethal conditions are most likely to occur. Figure 5-9 shows *Endocladia* thermotolerance for different durations of heat exposure overlaid atop the average TDF at the *Endocladia* upper limit (data from Figure 4-3). The riskiest temperature-time combination is the point where the lethal curve crosses the contour line of highest frequency. During the 17 months of observation, the temperatures (averaged across all sites) at the upper limit were never lethal (the lethal curve is always above any contour line). Along the High transect, 20 cm above the upper limit, short-hot lethal conditions were nearly reached, while longer-cooler lethal conditions appear less risky. If a member of the *Endocladia* community has a time survival curve shown by the dashed curve, the conditions of greatest risk (and potentially subject to the greatest selective pressure) is long-duration, lower-temperature survival. In this way, overlaying a TDF plot atop an organism's temperature-time tolerance can point out combinations of time and temperature that are most likely to cause mortality. If a lethal curve is approximately linear

(such as the ones shown here), a slope less than the slope of the TDF contour lines indicates longer-duration heat stress is more risky (the example in Figure 5-9), while if the slope of the lethal curve is steeper than the contour lines, short durations are more risky. A slope equal to the slope of the TDF contour lines indicates that risk is equally spread among temperature-duration conditions.

In addition, the slope of a TDF contour line indicates the "tradeoff" between temperature and time for an event with a given likelihood of occurrence. For example, the slopes for rare-to-moderately rare events (frequencies 1-40) are similar among transects (Table 5-3). At temperatures above 25°C the slope is -0.6 hr/degree, which indicates that a one-degree increase in critical temperature corresponds to 0.6 hours less time exceeding that temperature. Consequently, the similarity among slopes indicates that the temperature-duration tradeoff is constant throughout the habitat, from 20cm below the upper limit to 20 cm above the upper limit (if this higher habitat were covered with *Endocladia*). Increased elevations merely slide the TDF along the X-axis to higher temperatures. This means the TDF at a particular elevation is completely specified by a generalized TDF, and an x-intercept. (A convenient x-intercept measurement would be the maximum temperature achieved for half an hour.) The generality of this TDF and temperature-duration tradeoff remains to be seen.

Transect	**mean slope**	**slope S.E. (n=20)**
H	-0.642	-0.0489
M	-0.618	-.0567
L	-0.613	-.0401
UL	-0.655	-.0489

Table 5-3. Temperature-duration relationships ("tradeoffs") for all transects from the slope of the TDF contour lines at temperatures above 20ºC.

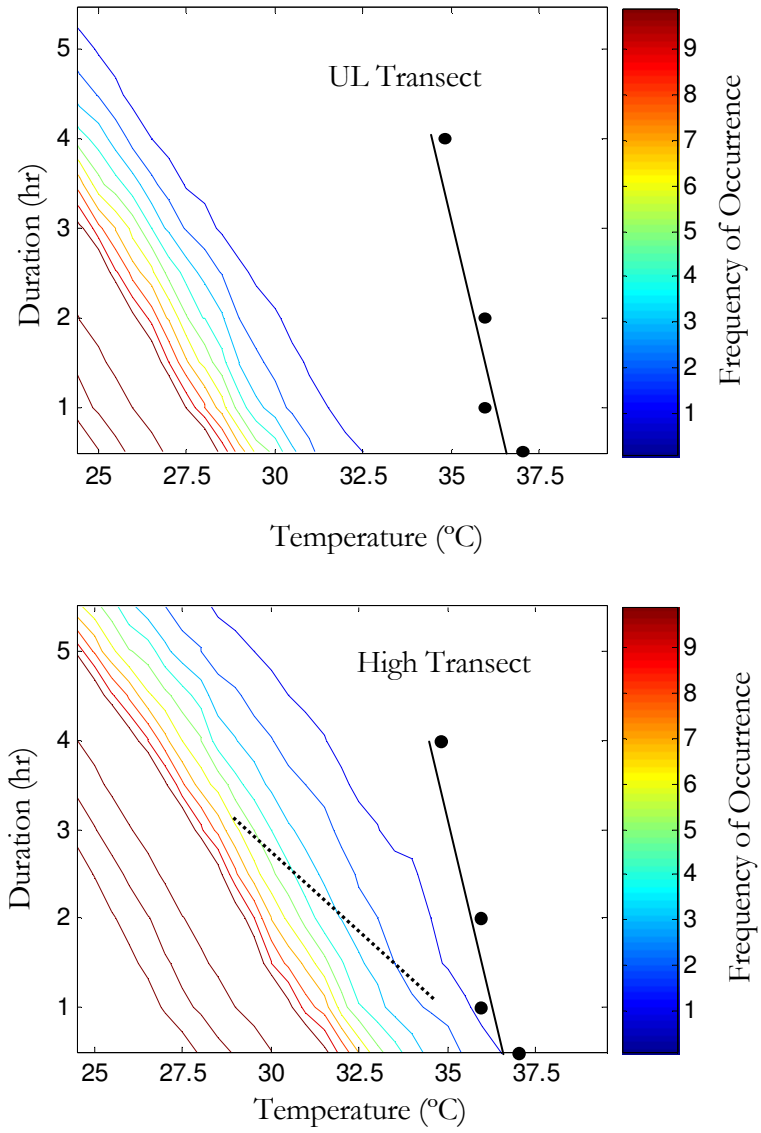

Figure 5-9. *Endocladia* LT-50 (temperature of 50% mortality) time-duration conditions (black line and points) overlaid atop the UL TDF (top) and the High transect TDF (bottom). Averaged across sites, time-durations conditions were never lethal at the UL. On the High horizontal transect, near-lethal conditions were reached for durations less than an hour, while longer durations are likely less risky. Dashed line is a hypothetical survivorship curve. See text for explanation.

5.3.6. Daily Temperature Time Courses

As physiologists seek more natural time histories for experiments on thermal performance, knowledge of the heating and cooling curves seen by organisms in the field is needed. The average temperature time course for a "hot" day is similar for all transects. However the shape of the time course changes, depending on the maximum temperature reached (Figure 5-10, Table 5-4). In, the average daily temperature trajectories are plotted for days with maximum temperatures within 1°C of 20ºC, 25ºC and 30ºC. The rate of heating is lower than the rate of cooling, and both rates depend on the temperature reached. Rate data appear in Table 5-4.

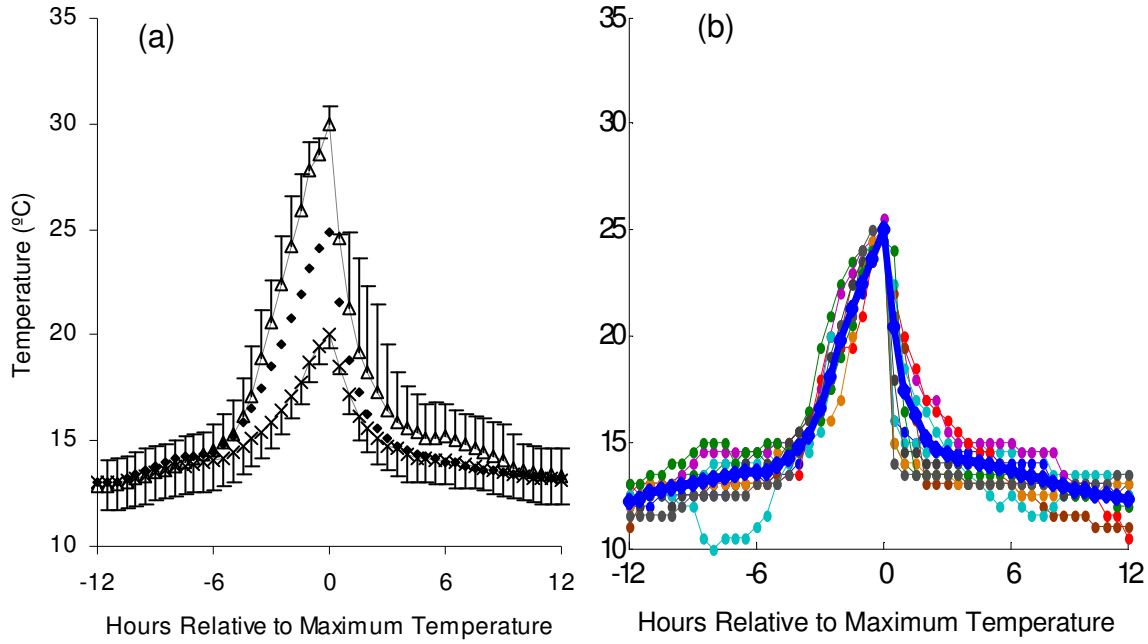

Figure 5-10. (a) Average heating-cooling curves for days reaching 20ºC (x), 25ºC (♦), and 30ºC (Δ) at the upper limit transect. Hotter days heat up at a faster rate. Error bars are 1 S.D. (no error bars shown for 25ºC. n=52, 31 and 17 days for 20ºC, 25ºC, and 30ºC, respectively). Rates for the 6 hours prior to max temperature and 2 hours following max temperature are given for all transects in Table 5-4. Individual days exceeding 25ºC are shown in (b), and the mean is seen to represent the data better during heating than during cooling.

(a) Heating Rates

	20ºC	25ºC	30ºC
UL	2.1	3.7	5.7
High	1.9	3.4	5.4
Mid	2.0	3.7	5.7
Low	2.0	3.8	5.6

(b) Cooling Rates

	20ºC	25ºC	30ºC
UL	-4.5	-8.6	-11.5
High	-3.8	-7.9	-11.8
Mid	-4.7	-8.5	-12.0
Low	-5.1	-9.3	-11.3

Table 5-4. (a) Average heating rates during the 6 hours before the maximum temperature for days reaching a maximum temperature (within a ± 1ºC window) of 20ºC, 25ºC, and 30ºC. (b) Cooling rates during the 2 hours following the time of maximum temperature (see Figure 5-10).

5.3.7. Effective Shore Level

Wave-splash is another important component of the intertidal environment (Fitzhenry et al. 2004). Effective Shore Level [ESL, after Harley and Helmuth(2003)] is plotted against absolute sea level (ASL) with the 1:1 line for reference in Figure 5-11. The three horizontal transects are plotted as points ± 95% C.I. because they occurred at a single elevation. The two values for each transect are different critical values of the cooling step that indicated a wavesplash (see Methods). The UL transect points span a range of elevations, and the importance of using horizontal transects for comparison is again seen: the elevation of the UL is correlated with ESL, but no biological response is indicated because the relation matches the abiotic relation between ESL and ASL among horizontal transects.

At higher tide levels, wave splash increases because the greater water depth allows larger waves to reach the site without breaking (personal observation). Therefore, the size of the wave that first wets a site is correlated with the site's absolute tidal elevation. This increase in wave-splash at higher tides can be seen as a slope less than 1 in Figure 5-11; at high ASL, the difference between ASL and ESL [a measure of wave-splash*, (Harley and Helmuth 2003)] increases. Because organisms at higher ASL are wetted by wave-splash from bigger waves, this effect acts to "expand" the intertidal zone for organisms that can take advantage of wave splash. The increase in wave-splash with tidal elevation is shown quantitatively in

* ESL is the height of the still water level at the time of the first wave splash, therefore the difference between the site elevation and still water level (ASL-ESL) equals the height the wave splashed up the shore. That is, the still water is raised up by the waves so that the water just reaches the elevation of the site. This distance is the height of the wavesplash.

Figure 5-12. However, in this study, the wave climate was similar among sites, and the effects of wave-splash on the *Endocladia* range were not detectable. That is, when measured along a horizontal transect, there is no significant relation between wavesplash (=ASL-ESL) and upper limit elevation (regression, $p>0.05$).

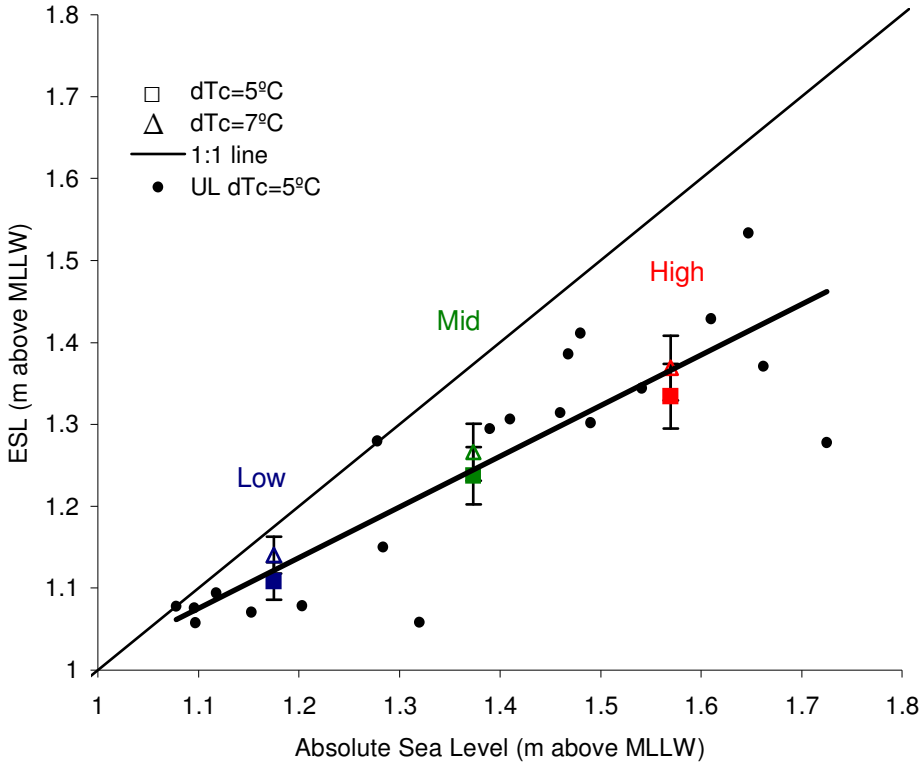

Figure 5-11. Effective Shore Level (ESL = the still-water level at the time of first wave splash) at the UL, a modified measure of elevation that includes local wave splash is plotted against absolute elevation (ASL) for all 4 transects. The horizontal transects (color-coded with error bars =95% C.I) show the same relation as the UL transect (• with regression line ESL= 0.62 x ASL+0.40, $R^2=0.73$). The slope <1 indicates that wave-splash increases at higher elevations. ESL is shown estimated using 2 different critical temperatures (dTc): 7ºC and 5ºC. See methods for further explanation.

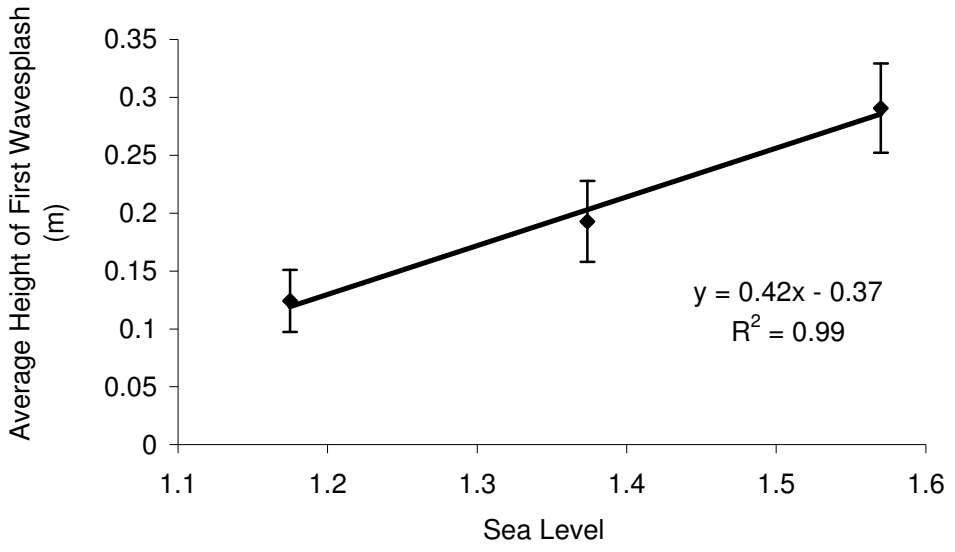

Figure 5-12. Average height of the wavesplash that first wets a site (±95% C.I.) increases with tidal height. Wavesplash is measured as ASL-ESL. See text for further description.

5.4 Discussion

I have shown that exposure to infrequent high temperature likely determines the elevation of the upper range limit of *Endocladia muricata* at Hopkins Marine Station. The site-to-site pattern in upper limit elevation can be used to predict thermal microhabitats because the upper limit is lower at hotter sites than at cooler sites (when temperatures are compared along a horizontal transect), and this range-truncation reduces high-temperature variability at the upper limit. Consequently, the environmental temperature gradient (3ºC increase in maximum temperature per 20 cm increase in elevation) is not seen when measuring biologically-modulated temperatures at the range edge.

Helmuth et al. (2002) also documented an environmental trend that was masked in the biologically relevant thermal record, but their conclusions were markedly different. Because their loggers were placed at unknown elevations that followed the elevation of the mussel bed (which is lower in the south [Gislen 1943]), the likelihood of biological temperature compensation appears likely. Helmuth et al. (2002) posited that variability in temperatures measured at a biologically determined height (what I called residual temperature variability)

was due to local "hotspots." Thus, the question arises: is the variability observed significant enough to warrant individual site-specific explanations? The temperature range that Helmuth et al. (2002) reports across the entire west coast of the United States (8°C for summer 99th percentiles) matches the *local* temperature variation I observed for the *Endocladia* upper limit along a 250 m transect (8°C for summer 99th percentiles).

Although a direct comparison is impossible (the two being different species), two further points suggest that the *Endocladia* temperature ranges are probably not exceptionally wide. First, *Endocladia* temperatures were all measured in a local area with consistent wave splash, and this would limit temperature variability with respect to the mussel study, which was much broader in extent and likely also covered a range of wave climates. Second, *Endocladia* temperatures were measured at the upper limit, a biological elevation that is more easily determined than mid-mussel bed, and thus there is likely less error due to logger placement in the current study. In this light, perhaps the most marked result of Helmuth et al (2002) is not the absence of a latitudinal trend, but rather the low variability observed over all, which suggests mussels are also "choosing" sites to effectively regulate high temperatures across a wide range of latitude.

Through changes in range, species such as mussels and *Endocladia* are capable of regulating temperatures for the entire community within the habitat they provide. The result is an "ecological homeostasis" where thermal heterogeneity among sites is muted by the behavior of the habitat-forming species. One might therefore expect the thermotolerances of these habitat-forming species to drive the thermal limits of associating organisms. A further observation of Gislen (1943) suggests that this possibility may be testable along the California coast. Gislen (1943) noted that the upper limit of *Endocladia* was exceptional because it is one of the few range limits with increased elevation further south. Other upper limits (including mussels') were consistently lower further south [Gislen (1943) suggested the possibility of a genetically driven change in thermotolerance]. If *Endocladia* inhabits different thermal zones across latitude, while mussels inhabit largely the same thermal zones, it would be possible to sample the thermotolerance of associated species and determine the extent to which the physiology of habitat-forming species drives thermotolerance community-wide.

5.4.1. Applications for Ecophysiology

The next generation of experiments to measure species' thermal tolerances will likely include time as an additional factor (Denny, Miller and Harley 2006). Using the data in Figure 5-10, it will be possible to challenge organisms (or suites of organisms within this turf) with environmentally realistic temperature histories.

In addition, the TDF graph prompts the questions: what shape are the temperature-time-mortality curves for species sheltering in the turf, and what temperature-time combination are most risky, given measured environmental conditions? The TDF predicts that, if these organisms experience equal risk of mortality at both extreme and moderately high temperatures, mortalities should be equal along a contour line. Glynn (1965) found high densities of the small bivalves *Lasea cistula* and *Musculus pygmaeus*, so it would be logistically opportune to determine the riskiest thermal conditions for these organisms.

5.4.2. Conclusion

Inexpensive and robust temperature loggers have the potential to greatly enhance our understanding of biologically-relevant intertidal temperatures (Helmuth and Hofmann 2001; Fitzhenry et al. 2004). However, it is important to recognize that even sessile ectotherms such as algae and mussels can "regulate" temperatures by adjusting their ranges to compensate for site-to-site temperature patterns, and therefore actual body temperatures may fall in a much narrower range than the scope of temperatures predicted from environmental data. When this sort of temperature compensation is done by a species that creates habitat, the effects of this thermal regulation likely propagate throughout the associated community.

PREDICTING THALLUS TEMPERATURES FROM WEATHER STATION DATA: A HEAT BUDGET FOR *ENDOCLADIA MURICATA*

6.1 Introduction

In Chapter 5, I presented measured temperature data from 80 loggers that thermally mimicked the central portion of a clump of the alga *Endocladia muricata*. However, temperatures experienced around the clump periphery are likely different because outer fronds dry faster and are less self-shaded than central fronds. In this chapter I develop a thermal model that uses local weather data (air temperature, solar irradiance and so on) to estimate temperatures of small isolated clumps of *Endocladia* and fronds on the periphery of larger clumps. In these cases, direct measurement is limited, because the fine-gauge temperature probes needed to measure the temperatures of small (<1mm diameter) fronds cannot survive field conditions during high tide, and therefore continuously recording temperature loggers are not an option. Consequently temperature data from exterior portions of the clump are sporadic, being limited to days when it appeared hot enough to warrant a trip into the intertidal zone to measure *Endocladia* thallus temperatures. In addition to providing estimates of organism temperatures when direct measurement is impractical, thermal models allow one to test the sensitivity with which physiological temperatures respond to environmental variables. For example, the model reveals that when the wind speed exceed 1.4 m/s (the average minimum day-time wind speed, measured at a nearby weather station) the *Endocladia* is never more than 3.5ºC above air temperature. So for many days, wind speed and air temperature alone are enough to show that thallus temperatures are non-lethal.

Predictive thermal models are widely used in crop micrometeorology and terrestrial physiology to predict the temperature of an organism from measured weather conditions (Monteith 1973; Gates 1980; Campbell and Norman 1998; Nobel 1999). In the intertidal zone, heat-budget models have been used to predict temperatures of mollusks (Helmuth

1998; Denny and Harley submitted), barnacles (Wethey 2002), and the red alga *Mastocarpus papillatus* (Bell 1995).

In the current context, the main use of this heat budget model is to estimate temperatures for portions of the thallus where an extensive record of direct measurements is impossible.

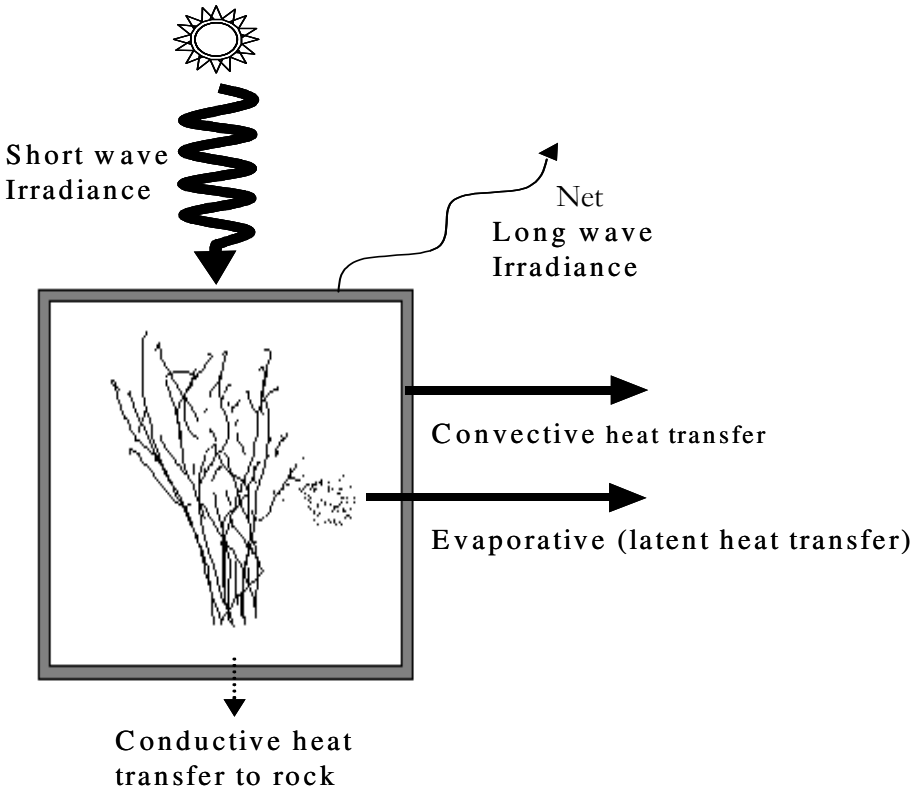

Figure 6-1. Heat fluxes in and out of the control volume (box) around the Endocladia clump. No spatial heterogeneity is considered within the control volume: parameter values are averaged over the entire clump and assumed to be uniform. The sum of the illustrated heat transfer modes equals the heat stored by changing the internal temperature of the alga. Arrow weights represent the relative magnitudes of the different heat fluxes. The arrows indicate the direction of heat transfer under usual conditions when the thallus is warmer than the surrounding environment.

6.2 Theory

The thermal model I used to predict the temperature and desiccation state of *Endocladia* is depicted in Figure 6-1. First, a hypothetical volume (the control volume) is defined around

the *Endocladia* thallus, and the equations governing heat and water flux into and out of this volume are derived by applying the laws of conservation of mass and conservation of energy[1]. The control volume in Figure 6-1 includes all the fronds of the thallus clump. Therefore I will derive *average* parameters for the clump, and within-clump variations are not considered within the framework of this type of lumped model.

Heat transfer can accurately be described as a combination of four independent heat transfer modes: (1) conduction, (2) radiation, (3) convection, and (4) latent heat transfer. The first three modes are termed "sensible heat" transfer because they can be felt or measured as a temperature difference. Latent (Latin: hidden) heat is aptly named because it cannot be measured with a thermometer. It is the heat associated with a change in phase, and is computed from the rate of evaporation or condensation. Below I consider each component of the heat transfer equation in turn. For a summary of notation, units, and how the parameters are treated in the model see Table 6-1.

(1) Conduction occurs where the rock and thallus are in direct contact. Because this area is miniscule for small-stiped Endocladia, conduction is negligible, in comparison to other heat transfer modes, and we will not consider it further.

(2) Radiation can be divided into two equations, one for short-wave (=solar) absorbance and one for long wave "blackbody" irradiance. Short-wave radiant energy is absorbed at the rate:

$$\dot{Q}_s = a_E S_{flux} A_s \qquad (1)$$

Here a_E is the absorbance, S_{flux} is the short-wave radiant power flux, and A_s is the projected area being illuminated.

[1] Because the control volume has been drawn around a mass source, the net mass flux through the volume is not zero. This complication adds two additional terms: the enthalpy of the water leaving the control volume, and the change in enthalpy of the volume due to net mass efflux. However, these terms exactly offset one another, and here I present the heat equations as they are typically described.

Constant Inputs		Functions of Inputs	
A_{IR}	Area for IR transfer (m^2)	$h_c(wind)$	heat transfer coefficient ($W/m^2 K$)
A_c	Area for convective transfer (m^2)	$h_m(wind)$	mass transfer coefficient (m/s)
A_m	Area for mass transfer (m^2)	$\varrho_E(T_E$, RWC)	water vapor density at thallus surface (kg/m^3)
A_s	Area for short wave transfer (m^2)	$\varrho_{vap}(T_{air}, RH_{air})$	water vapor density of air (kg/m^3)
σ	Stefan-Boltzmann constant ($5.67 \times 10^{-8} W/m^2K^4$)	ζ(RWC)	coefficient modifying h_c for high rates of mass transfer
λ	heat of vaporization of water ($2.3 \times 10^6 J/g$)	**Time-dependent Inputs**	
C_{pWater}	Specific heat capacity of water ($4.18 \times 10^3 J/kg K$)	$Wind$	Wind speed (m/s)
C_{pDry}	Specific heat of dry *Endocladia* assumed to be the same as wood ($1.40 \times 10^3 J/kg K$)	T_{air}	Air temperature (K)
C_{pAir}	Specific heat capacity of air ($1.01 \times 10^3 J/kg K$)	RH_{air}	Relative humidity (unitless)
ϱ_{Air}	density of air (1.2 kg/m^3 at 290-300K)	S_{flux}	Solar irradiance (W/m^2)
a_{air}	Thermal diffusivity of air ($22.5 \times 10^{-6} m^2/s$ at 298K)	**Initial Conditions**	
D_{wv}	diffusivity of water vapor in air ($2.6 \times 10^{-5} m^2/s$ at 298K)	$T_E(0)$	Inintial *Endocladia* temperature (K)
Δt	time step of model (5 seconds)	m_E (0)	Initial Mass of *Endocladia* (kg)
ε_E	emissivity of *Endocladia* (0.98 unitless)	RWC(0)	Initial Relative Water Content of *Endocladia*
ε_{env}	emissivity of the environment		

Table 6-1. Model inputs classified by type. Constant inputs are either measured for a given thallus, or, if a value is given, the parameter is constant for all *Endocladia* thalli. Time-dependent inputs are continuously varying and were measured every 5 seconds. Functions of inputs, except in the case of ϱ_{vap}, were determined empirically. ϱ_{vap} was determined from published values (Nobel 1999). Initial conditions were measured at the start of each run.

By the Stefan-Boltzmann equation, the rate of long-wave radiant emission equals $\sigma\varepsilon T^4$, where T is the absolute surface temperature; σ is the Stefan-Boltzmann constant (W/m^2K^4), and ε is the emissivity of the material. Emissivity is the ratio of the energy radiated by the material at a given temperature, to the energy a black body would emit at the same

temperature. By Kirchoff's law of thermal radiation, emissivity is also equal to the long-wave absorbance [see Robitaille (2003) for a recent review of the lasting controversy surrounding this law]. The net heat transfer through infrared radiation (IR) is the difference between the IR emitted by the alga, and IR absorbed from the surroundings:

$$\dot{Q}_{IR} = \sigma\varepsilon_{env}(T_{env})^4 \cdot A_{IR}\varepsilon_E - A_{IR}\sigma_E\varepsilon_E(T_E)^4, \qquad (2)$$

where ε_E and ε_{env} are the emissivities of *Endocladia* and the environment respectively, T_{env} is the absolute temperature of the environment, and A_{IR} is the area (m^2) that is radiating to the environment. Here the first term is the IR emitted by the environment and absorbed by the thallus: the environment emits $\sigma\varepsilon_{env}(T_{env})^4$ W/m^2, and of this only the fraction $A_{IR}\varepsilon_E$ is absorbed by the thallus. The second term is the IR emitted by the thallus.

(3) Convection is the process by which heat energy is transferred across the thermal gradient in the air near the thallus surface through inter-molecular collisions. In flow, molecules are transported both through diffusion (random motion) and advection (average net motion), and these transport processes are lumped together when computing the rate of convective heat transfer $\dot{Q}_c$. The resulting equation is known as Newton's law of cooling.

$$\dot{Q}_c = h_c(T_{air} - T_E)A_c \qquad (3)$$

The temperature difference between the air and the Endocladia surface ($T_{air} - T_E$) drives convective transfer at a rate proportional to the heat transfer coefficient h_c (W/m^2K). This heat flux occurs across the area for convective transfer A_c (m^2).

The thermal gradient for convective heat transfer is analogous to the velocity gradient associated with the velocity boundary layer near a surface. The analogy between the velocity gradient, temperature gradient, and concentration gradient (when mass transfer or nutrient flux is considered) is a powerful heuristic that was first recognized by Osborne Reynolds of

Reynolds Number renown (Jakob and Hawkins 1957), and I will return to this analogy in detail in the calculation of the coefficients of heat and mass transfer. A motivation for this elegant relation appears in Appendix 2.

(4) Latent heat flux is the product of the latent heat of water λ (J/kg), and $\dot{m}$ (kg/s), the rate of mass flow due to evaporation or condensation:

$$\dot{Q}_L = \lambda \dot{m} \qquad (4)$$

The equation governing mass transfer is similar to the equation of heat transfer, by the Reynolds analogy introduced above. Both are boundary layer processes driven by gradients close to the surface. The rate of mass transfer is, by analogy:

$$\dot{m} = h_m(\rho_{air} - \rho_E)A_m \qquad (5)$$

where h_m is the mass transfer coefficient (m/s), ρ_{air} is the ambient water vapor density (kg/m^3) computed from the temperature and relative humidity, ρ_E is the vapor density at the surface (g/m^3), and A_m is the area (m^2) over which mass transfer takes place.

The sum of these four heat transfer modes equals the rate of heat storage:

$$\dot{Q}_{stored} = C_p m \dot{T}_E \qquad (6)$$

where C_p is the specific heat capacity (J/kg K) of the water-*Endocladia* combination, m is the total mass (kg), and $\dot{T}_E$ is the rate at which the *Endocladia* temperature is changing (K/s).

The overall heat balance, neglecting conduction, can now be written:

$$\dot{Q}_{stored} = \dot{Q}_{conv} + \dot{Q}_{s} + \dot{Q}_{IR} + \dot{Q}_{L} \qquad (7)$$

With the model defined this way, the main problem is determining the coefficients particular to *Endocladia*. The model inputs are listed in Table 6-1. When a value is given for a parameter, this value applies for all conditions. The measurement details are given in the methods section.

6.3 Methods

All wind tunnel experiments were carried out in the tunnel described in Bell (1995). Thallus temperatures were measured with fine (40 gauge) thermocouples inserted into the thallus through a hole made with a 30-gauge hypodermic needle and then held in place with cyanoacrylate glue (Zap-A-Gap). These measurements were checked against temperatures measured with an infrared camera (Infrared Solutions IRSnapshot 525) and confirmed to be accurate during the entire drying period (data not shown). Different numbers of lights (Sylvania Capsylite 120W Spotlights) were used in combination to provide varying levels of short-wave irradiance. Vertical and horizontal wind speeds were measured 10 cm above the alga with Kurtz hot-film anemometers, and the vector sum is used as the wind speed. All data were collected every 5 seconds with a data logger (model 23X, Campbell Scientific).

The remainder of the methods will be split into measuring the coefficients involved in each mode of heat transfer.

6.3.1. Radiation

To calculate the short-wave energy flux absorbed by *Endocladia*, both the emission spectrum of the light source (lights or sun) and the spectral absorbance of *Endocladia* were measured with a Li-Cor 1800 spectroradiometer for wavelengths between 300 and 1100 nm. At each wavelength (1 nm bins) the net energy absorbed by the alga equals the product of the wavelength-specific incident flux and the absorbance. The energy absorbed at each wavelength was summed for all measured wavelengths and normalized to the total flux emitted. This resulted in a value for absorbance that was corrected for the two spectrally different light sources. In the laboratory, light passed through 2 cm of water, which was

assumed to absorb infrared and ultraviolet wavelengths outside the range measured by the Li-Cor 1800. For sunlight, irradiance values outside the measurement range of the Li-Cor 1800 are small. Regardless of the light source, irradiance values are reported as if the thallus were in sunlight, and irradiance was measured with a pyranometer (i.e., incident short-wave flux). The area for solar flux was taken as the plan-view area calculated from a digital photograph using Image J.

The emissivity of wet and dry *Endocladia* was calculated using a thermal camera (Infrared Solutions IRSnapshot 525). Material at known temperature (equilibrated within a covered dewar and the cover quickly removed prior to measurement) was photographed, and the emissivity value set on the camera was adjusted until the temperature of the image matched the temperature measured within the dewar. The emissivity of the environment within the wind tunnel (Plexiglas walls) was 0.83 (Bell 1995). For estimates in the field, the Swinbanks' empirical relation for clear skies was used for the emissivity of air (Gates 1980).

The area for long wave radiation was taken as the bounding surface area of the thallus clump, because this is the surface for net exchange with the environment. The bounding area was calculated as a conical frustum with diameters and height estimated with calipers (Figure 6-2).

6.3.2. Convection

The convective heat transfer coefficient can be determined by solving the energy budget equation for h_c when dry *Endocladia* is thermally equilibrated, so there are no storage or latent heat terms. Under such conditions the convective heat transfer coefficient is:

$$h_c = \frac{\dot{Q}_s + \dot{Q}_{IR}}{(T_{air} - T_E)A_c} \qquad (8)$$

The temperatures and radiant energy terms are measured as above, and the convective area is taken as the volume of the surface for IR irradiance (Figure 6-2) multiplied by 6.6. This area is equivalent to approximating the thallus area as its bounding volume (Figure 6-2) filled with vertical cylinders (fronds) the average diameter of a dry *Endocladia* frond and separated

by the average frond separation. The relation between h_c and wind speed is shown in Figure 6-3 for three different clumps.

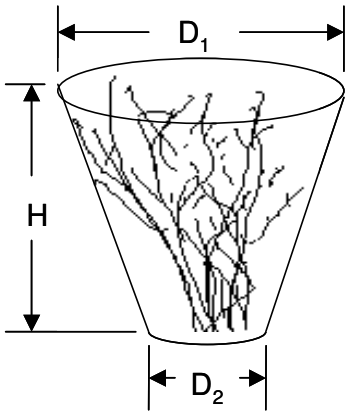

$$\text{Surface area} = \pi\left(\frac{D_1}{2}\right)^2 + \pi\left(\frac{D_2}{2}\right)^2 + \pi\left(\frac{D_1}{2} + \frac{D_2}{2}\right)\sqrt{\left(\frac{D_1}{2} - \frac{D_2}{2}\right)^2 + H^2}$$

$$\text{Volume} = \pi\frac{H}{3}\left[\left(\frac{D_1}{2}\right)^2 + \left(\frac{D_1}{2}\right)^2 + \left(\frac{D_1 D_2}{4}\right)\right]$$

Figure 6-2. Bounding surface for the *Endocladia* clump, used to calculate areas for heat and mass transfer.

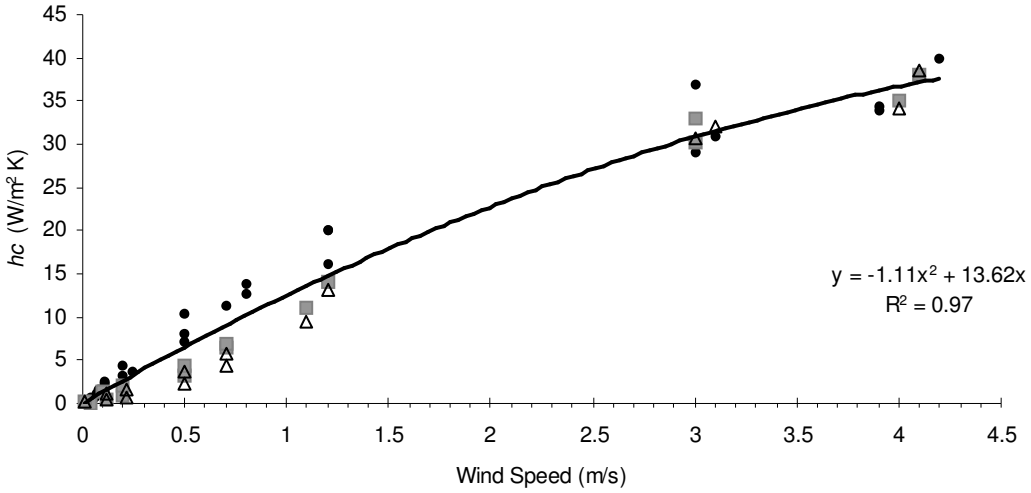

Figure 6-3. Convective heat transfer coefficient (*hc*) measured in the wind tunnel for 3 different clumps (•, ■, Δ) of dry *Endocladia muricata*. *Hc* is shown for isolated clumps, 1-2 cm in diameter (•, ■) and the upwind edge of a larger, 8-cm-diameter clump (Δ). Convective heat-transfer coefficients are similar in all cases. A quadratic fit was used in the model to compute *hc* from measured wind speed.

The heat transfer coefficient for dry *Endocladia* was also used for wet *Endocladia* because the shape stays similar during drying. However two modifications must be made: First, the convective area depends on the relative water content (RWC) because the frond diameter shrinks during drying (Figure 6-4).

Second, during high rates of mass transfer, water vapor moves rapidly through the boundary layer, and this alters flow conditions (and thus h_c) (Bird et al. 1960; Lebedev 1961; Geankoplis 1993). The effect of drying rate on heat transfer is usually measured experimentally on a case-by-case basis (Kondjoyan and Daudin 1993; Sun and Marrero 1996) as a function of desiccation state and wind speed, and in this study, h_c is scaled by the empirical factor ζ (=2.5 x RWC for RWC > 20). The resulting equation for convective heat transfer, modified from equation 3, is thus:

$$\dot{Q}_c = h_c \zeta (T_{air} - T_E) A_c \qquad (9)$$

This point warrants emphasis, because it is a source of confusion. The energy budget of Bell (1992; 1995) underestimated the temperatures of hydrated thalli (1992, p.158) because evaporative cooling overwhelmed convective heating when the thallus was drying. To account for this error, Bell doubled the heat-transfer coefficient at all water contents, without further explanation. This would be expected to introduce systematic errors at intermediate and low RWC and at low wind speeds, when drying rates are reduced. Introducing the factor ζ results in a transfer coefficient that depends on relative water content as well as wind speed.

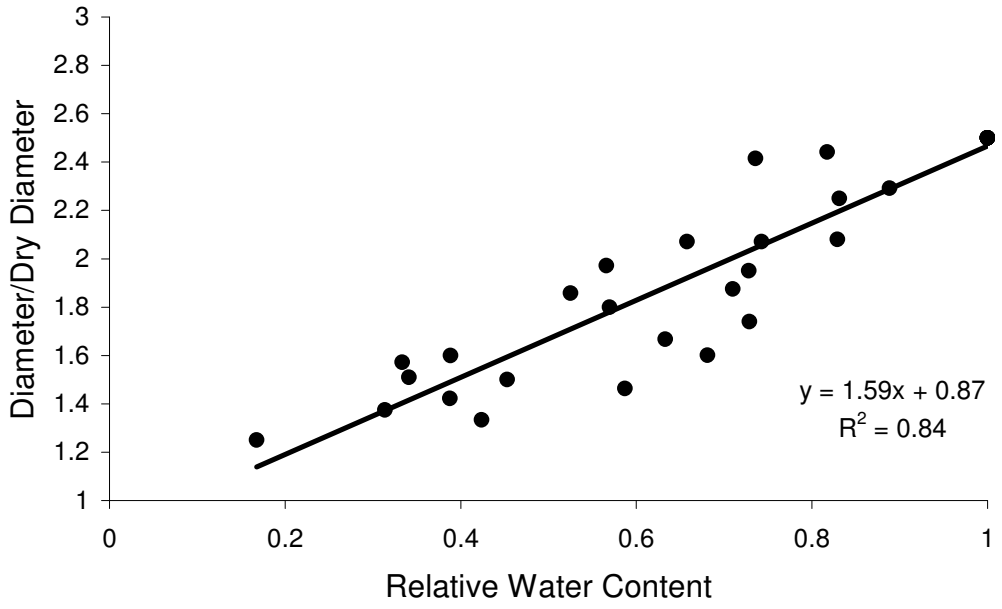

Figure 6-4. Frond diameters shrink as the thallus dries. Fully hydrated fronds are approximately 2.5 times thicker in diameter than fronds dried to 10% relative water content.

6.3.3. Mass Transfer and Latent Heat

The mass transfer coefficient was calculated from the heat transfer coefficient using a modified Reynolds analogy called the Chilton-Colburn analogy (Incropera and DeWitt 2002).

$$h_m = h_c \rho_{air} C_p Le^{\frac{2}{3}} \qquad (10)$$

Here h_m and h_c are the heat and mass transfer coefficients respectively, ρ_{air} is the density of air, C_p is the specific heat capacity of air, and Le is the dimensionless quantity known as the Lewis number, which is the ratio of thermal diffusivity, a (m^2/s) and mass diffusivity, D_{wv} (m^2/s) of water vapor in air (See appendix 2 for a more complete motivation). The rate of mass transfer, from equation 5 is

$$\dot{m} = h_m(\rho_{air} - \rho_E)A_m \qquad \text{(5, repeated)}$$

From the definition of relative humidity, ambient vapor density (ρ_{air}) can be computed as the product of the relative humidity and the saturated vapor density. Relative humidity was measured and saturated vapor density was computed from air temperature using a fourth-order polynomial fit to the data in Nobel (1999, p. 443).

$$\rho_{sat} = 3.32 \times 10^{-6} T_{air}^4 + 9.17 \times 10^{-5} T_{air}^3 + 0.0121 T_{air}^2 + 0.315 T_{air} + 4.92 \qquad (11)$$

Relative humidity (converted to vapor density using the above relations) at the thallus surface is a crucial element driving mass-transfer (equation 5) that has rarely (if ever) been possible to measure, and therefore the air in contact with a plant surface is usually assumed to be saturated (Nobel 1999). I did not assume saturation; rather I assumed that the surface relative humidity was equal to the relative humidity under equilibrium conditions. As the *Endocladia* dries out, the relative humidity at the surface decreases (Figure 6-5), and thus the surface relative humidity depends on thallus water content. To determine the relationship, I took the reverse approach: instead of manipulating water content and measuring relative humidity at the interface (difficult), I manipulated the ambient relative humidity and measured the water content at equilibrium. Relative humidity was manipulated by placing fronds in closed chambers above saturated solutions of different salts. The salt solutions maintained a constant, known, relative humidity (Weast et al. 1978), and within 24 hours, the frond stopped losing water and came to equilibrium. The relative water content was measured after 3 days equilibrating at room temperature, and the relation plotted as relative humidity versus relative water content (Figure 6-5). At equilibrium, the relative humidity at the thallus surface approximates the relative humidity within the chamber, and if one

assumes that time-dependent resistances to water flowing through the thallus are negligible (so the surface is always in equilibrium), the relationship between thallus RWC and thallus-surface relative humidity can be applied under dynamic conditions.

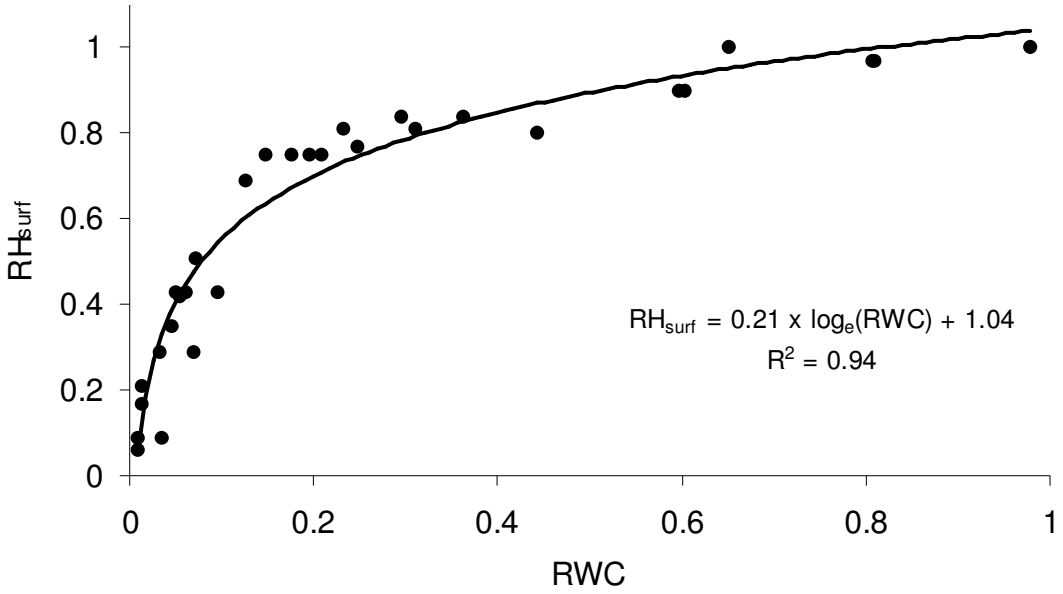

Figure 6-5. Surface relative humidity under steady state conditions (RH_{surf}) versus Relative Water Content (RWC). The fit shown was used in the model to calculate RH_{surf} from RWC. The fit shown adequately represents the data, and maintains a smooth transition, however the actual mechanism of drying may better be described as two distinct processes (i.e., two lines).

6.3.4. Heat Storage

At each time in the model, the mass of water in the thallus was calculated from the initial relative water content and weight, and the cumulative mass loss. The mass of water and the mass of dry *Endocladia* were multiplied by their respective specific heat capacities (Table 6-1). The result was divided by the model time step to yield the rate of heat storage.

6.4 Results

6.4.1. Model Verification

The model's accuracy was assessed by comparing model predictions (thallus temperature and RWC) with values measured for thalli in the wind tunnel under varying environmental

conditions. These results present the best possible scenario, and measurements in the field are expected to have additional errors, due to the imprecision with which micro-site environmental conditions are measured. For example, in the wind tunnel, all long-wave radiation is exchanged with the wind tunnel sides, with known temperatures and emissivity, but in the field, the thallus radiates to the rock, air and ocean, and all are different temperatures. Therefore the amount of energy exchanged will differ from site to site, depending on the site geometry (e.g., "how much sky is seen," quantified by the so-called "view factor" [Incropera and DeWitt, 2002]). I did not determine the magnitudes of these errors, and further field-calibration is required before the model can be applied to a particular site.

Figure 6-6 shows the model errors for equilibrated dry thalli. Under conditions leading to high-temperature stress, the equilibrium temperature is the maximum temperature *Endocladia* can reach, and Figure 6-6 shows the errors in predicting this maximum temperature.

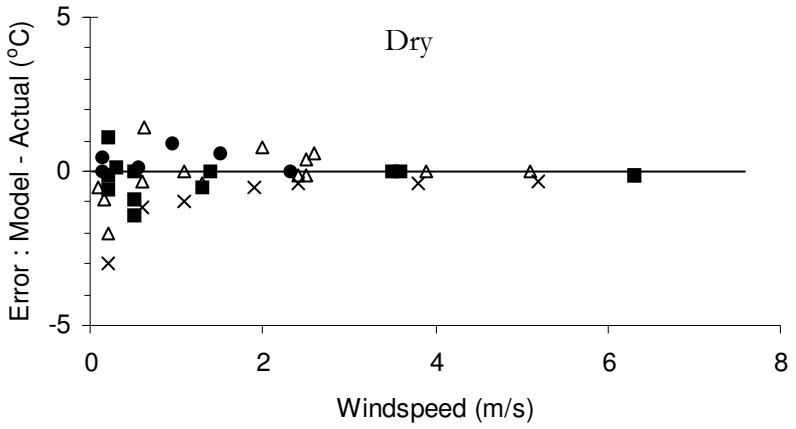

Figure 6-6. Model errors in predicting equilibrium temperature of dry *Endocladia* for 4 light levels: 200 (●), 250 (■), 350 (x) and 500 (Δ) W/m². Equilibrium temperatures are the maximum temperatures reached under these conditions. Model errors are greatest at low wind speeds.

Additionally, the model errors are shown in Figure 6-7 for *Endocladia* at two points on the drying curve. The runs started with saturated *Endocladia.* 90% RWC occurred 1 to 7 minutes after the run started, and 30% RWC was reached between 10 and 120 minutes later,

depending on the wind speed and light conditions. 30% RWC was chosen as the cut-off separating "wet" from "dry" thalli because photosynthesis is negligible when the alga is dried below 30% RWC (Chapter 4). Wet and dry are convenient categories, given the detail with which physiological responses to temperature are known, but a continuum of desiccation states exists, and it is a first approximation to lump thalli into wet and dry categories.

Model errors are within 4º C for both wet and dry thalli (Figure 6-7). For dried thalli, the model performs better at higher wind speeds.

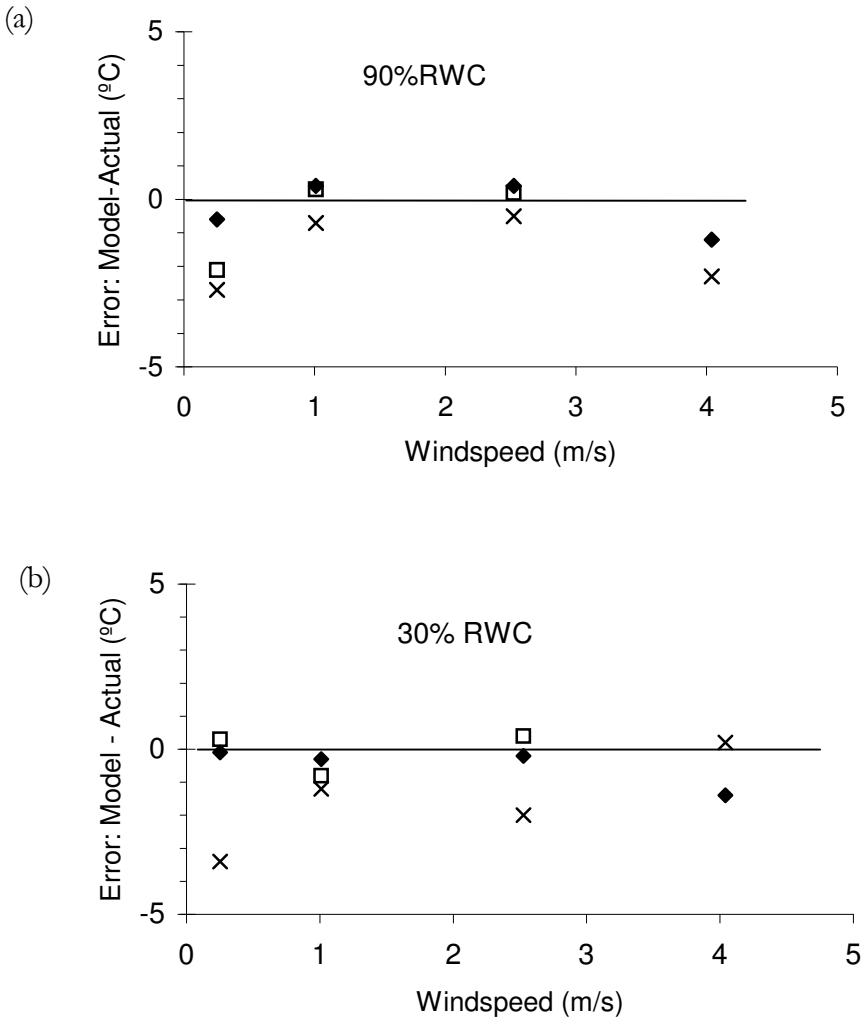

Figure 6-7. Model errors (predicted minus measured temperatures) in the wind tunnel at two points on the drying curve: (a) 90% Relative Water Content (RWC) and (b) 30% RWC. Short-wave irradiance values are 660 W/m^2 (x), 330 W/m^2 (□), and 0 W/m^2 (♦, room lights only).

6.4.2. Lethal Combinations

Because the thermotolerance of *Endocladia* depends on whether the alga is wet or dry (Chapter 4), predicting lethal conditions requires simultaneously predicting the RWC and temperature of the alga. Drying curves for 2 wind speeds are shown in Figure 6-8. The black portion of the lines indicate where the alga exceeded the temperature causing 50% mortality (LT50) in either a wet (RWC >30%, LT50=36 ºC) or dried (RWC< 30%,

LT50=47 ºC) state. The maximum temperature reached depends strongly on wind speed, and this temperature persists as long as environmental conditions last. The equilibrium water content also depends on wind speed because at low wind the thallus becomes hotter, and the surface relative humidity is increased, which leads to increased desiccation (a household example is that a hot wash-cloth steams at room temperature; a cold one does not).

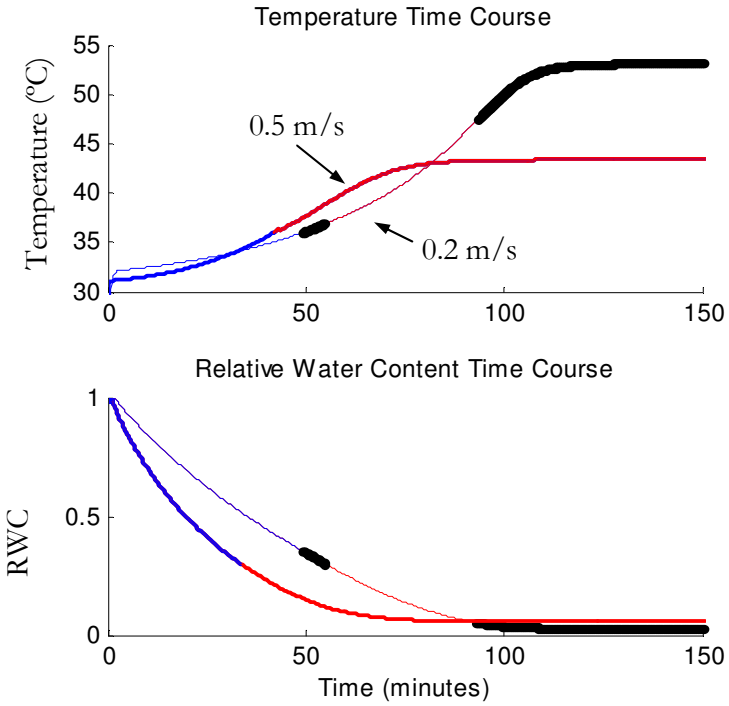

Figure 6-8. The temperature (top) and Relative Water Content (bottom) time courses are shown for two different wind speeds, with other environmental conditions held constant. Wind speeds are 0.2 m/s (thin line) and 0.5 m/s (thick line). The lines are colored as follows: In upper panel, red denotes temperatures above 36ºC, the wet-LT50 temperature (causing 50% mortality for 1 hour exposure); blue are lower temperatures. In the lower panel, red marks RWC < 30%, when the alga is not photosynthesizing, and blue marks wetter thallus conditions. Black marks conditions reaching wet-lethal (>36ºC) and dry lethal (>47ºC) temperatures. Lethal conditions are only reached for the lower wind speed, and the duration of wet-lethal conditions is likely too short (due to the drying rate) to cause mortality. The air temperature is 35ºC, solar flux is 1000 W/m², relative humidity is 60%.

LT50s were reached at a wind speed of 0.2 m/s, but not 0.5 m/s (Figure 6-8). However the exposure above wet LT50 temperatures (the lower black portion) is for a much shorter duration than the 1-hour exposure that causes 50% mortality. Mortality resulting from these conditions is likely less than 50%, and perhaps these brief conditions are entirely non-lethal. Therefore, concluding that these conditions (0.2 m/s wind, air temperature of 35ºC, solar flux of 1000 W/m², relative humidity of 60%) cause mortality is a lower bound or conservative estimate of the conditions causing mortality.

Figure 6-8 considers only one air temperature and one level of solar irradiance. These conditions in combination with a 0.2 m/s wind lead to lethal thallus temperatures, but if the wind is 0.5 m/s the combination is non-lethal. The next step is to determine the suite of environmental combinations that cause the alga to reach lethal temperatures. The lethal combinations from a number of wind speeds, solar irradiances and air temperatures are shown in Figure 6-9. The lethal temperatures are again taken as LT50 for one-hour exposures. However, wet *Endocladia* spends considerably less than one hour at these temperatures before it dries below 30% RWC (see Figure 6-8). Therefore the combinations indicated are also lower bounds, or the most benign conditions that may cause mortality in wet *Endocladia*. For example, if only durations longer than 30 min are considered lethal, the air temperature must exceed 34ºC before wet *Endocladia* dies, even under the harshest wind and irradiance conditions considered (0.1 m/s wind, and 1200 W/m² irradiance). If the wind is increased to 0.2 m/s, the air temperature must exceed 39ºC in order to maintain wet-lethal temperatures for 30 minutes.

6.4.3. Environmental Conditions: Are These Lethal Combinations Likely to Occur?

Irradiance, wind speed and air temperature have been measured continuously at a weather station on a bluff above the intertidal zone at Hopkins Marine Station. The combinations of irradiance, wind speed and air temperature are shown in Table 6-2. In computing this table I assumed that the wind speed at the weather station was 10 times as fast at the weather station as in the intertidal zone. Therefore 0.1 m/s in Table 6-2 equals 1.0 m/s at the weather station. This was based on measurements taken on March 24, 2006 when the wind speed at the weather station was 2.5 m/s, *Endocladia* was 25-30ºC, and the minimal sustained wind speeds in the intertidal zone were about 0.2 m/s. Other scaling factors can be applied

and read off the table as well. For example, if the wind speed in the intertidal zone is half as fast as the wind at the weather station, multiply the wind values in the table by 0.5/0.1 to convert the table to this new wind-scaling factor.

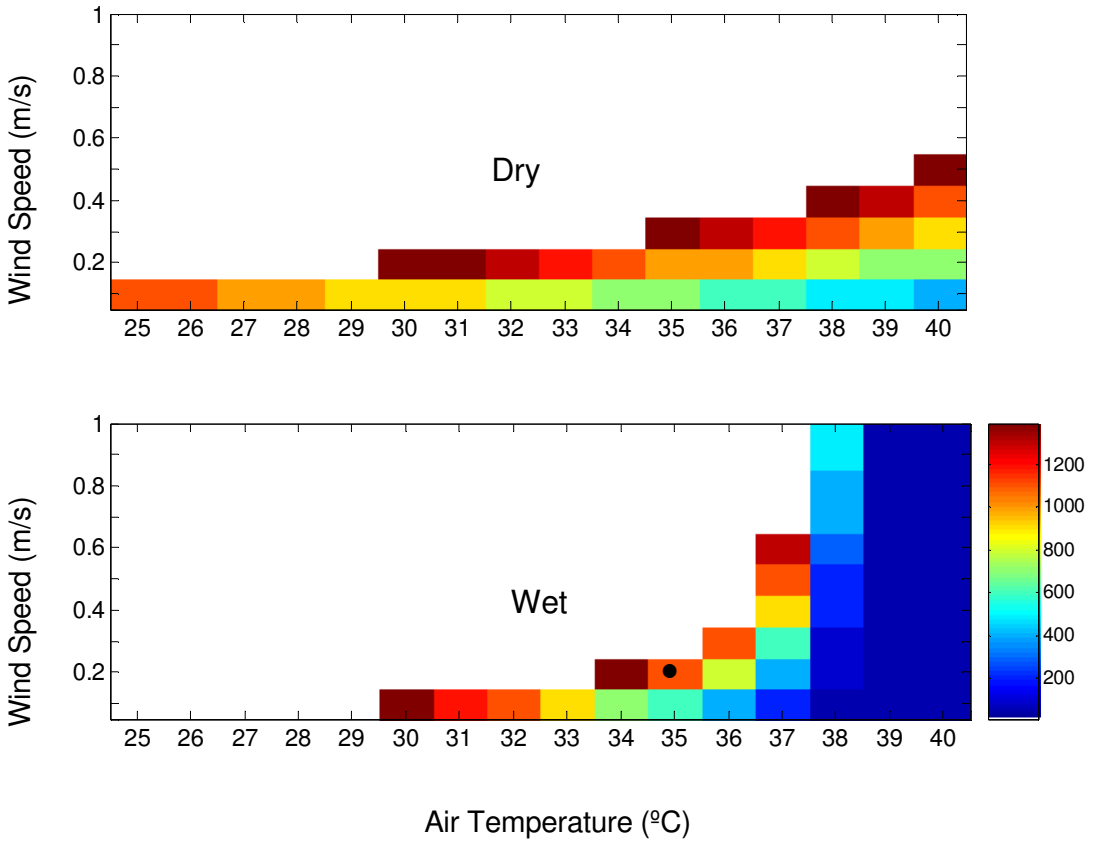

Figure 6-9. Combinations of temperature, wind speed and solar irradiance (color coded W/m²) that lead to lethal thallus temperatures. For example, the lethal conditions in Figure 6-8 are shown (●): Air temperature of 35 ºC, wind speed of 0.2 m/s and solar irradiance of 1000 w/m². Lethal temperatures are taken as LT50 for 1-hour duration of heat exposure, and exposure times shown for wet *Endocladia* may be substantially less (see Figure 6-8), therefore the "lethal" conditions shown are low estimates on the likely conditions for mortality. See text for further discussion.

Even with this low-wind speed scaling, environmental conditions that would lead to mortality of isolated clumps (and peripheral fronds of large clumps) were never seen in the 6-year period of weather observations. For dry clumps, this corroborates field

measurements taken on especially hot, windless days: thallus temperatures never exceeded 41ºC, while the LT50 for dry *Endocladia* is 47 ºC (Chapter 4). Relative water content measurements were not taken for isolated clumps, and therefore the wet-lethal conditions were not assessed directly in the field. However Chapter 4 suggest that wet-lethal conditions were only reached at the clump center, while the clump peripheries survived.

Tair (ºC)	Irradiance (W/ m²)	Wind speed 0.1 (m/s)	Wind 0.2 m/s	Wind 0.3 m/s	Tair (ºC)	Irradiance (W/ m²)	Wind speed 0.1 (m/s)	Wind 0.2 m/s	Wind 0.3 m/s
25	**700**	6.2	30.8	87.3	**29**	**700**	0.0	1.0	31.8
25	**800**	2.1	13.4	63.7	**29**	**800**	0.0	0.0	29.8
25	**900**	0.0	6.2	43.1	**29**	**900**	0.0	0.0	27.7
25	**1000**	0.0	0.0	19.5	**29**	**1000**	0.0	0.0	17.5
25	**1100**	0.0	0.0	0.0	**29**	**1100**	0.0	0.0	0.0
26	**700**	3.1	19.5	66.8	**30**	**700**	0.0	1.0	18.5
26	**800**	1.0	8.2	50.3	**30**	**800**	0.0	0.0	17.5
26	**900**	0.0	3.1	36.0	**30**	**900**	0.0	0.0	16.4
26	**1000**	0.0	0.0	18.5	**30**	**1000**	0.0	0.0	12.3
26	**1100**	0.0	0.0	0.0	**30**	**1100**	0.0	0.0	0.0
27	**700**	1.0	12.3	53.4	**31**	**700**	0.0	0.0	11.3
27	**800**	0.0	4.1	44.2	**31**	**800**	0.0	0.0	11.3
27	**900**	0.0	3.1	33.9	**31**	**900**	0.0	0.0	11.3
27	**1000**	0.0	0.0	18.5	**31**	**1000**	0.0	0.0	7.2
27	**1100**	0.0	0.0	0.0	**31**	**1100**	0.0	0.0	0.0
28	**700**	0.0	3.1	39.0	**32**	**700**	0.0	0.0	8.2
28	**800**	0.0	2.1	37.0	**32**	**800**	0.0	0.0	8.2
28	**900**	0.0	2.1	30.8	**32**	**900**	0.0	0.0	8.2
28	**1000**	0.0	0.0	18.5	**32**	**1000**	0.0	0.0	6.2
28	**1100**	0.0	0.0	0.0	**32**	**1100**	0.0	0.0	0.0

Table 6-2. The number of hours that various combinations of wind, temperature and irradiance occurred between August 1, 1999 and August 1, 2005. For example, the boxed value indicates that there were 3.1 hours when the air temperature exceeded 27ºC, the irradiance exceeded 800 W/m², and the wind was less than 0.2 m/s. Wind speed is assumed to be 10% of the value at a nearby weather station. In no cases were conditions lethal for isolated clumps of *Endocladia.*

Tair (ºC)	Irradiance (W/ m²)	Wind speed 0.1 (m/s)	Wind 0.2 m/s	Wind 0.3 m/s
27	900	6.2	30.8	87.3
27	1000	2.1	13.4	63.7
27	1100	0.0	6.2	43.1
27	1200	0.0	0.0	19.5
27	1300	0.0	0.0	0.0
28	900	3.1	19.5	66.8
28	1000	1.0	8.2	50.3
28	1100	0.0	3.1	36.0
28	1200	0.0	0.0	18.5
28	1300	0.0	0.0	0.0
29	900	1.0	12.3	53.4
29	1000	0.0	4.1	44.2
29	1100	0.0	3.1	33.9
29	1200	0.0	0.0	18.5
29	1300	0.0	0.0	0.0
30	900	0.0	3.1	39.0
30	1000	0.0	2.1	37.0
30	1100	0.0	2.1	30.8
30	1200	0.0	0.0	18.5
30	1300	0.0	0.0	0.0

Tair (ºC)	Irradiance (W/ m²)	Wind speed 0.1 (m/s)	Wind 0.2 m/s	Wind 0.3 m/s
31	900	0.0	1.0	31.8
31	1000	0.0	0.0	29.8
31	1100	0.0	0.0	27.7
31	1200	0.0	0.0	17.5
31	1300	0.0	0.0	0.0
32	900	0.0	1.0	18.5
32	1000	0.0	0.0	17.5
32	1100	0.0	0.0	16.4
32	1200	0.0	0.0	12.3
32	1300	0.0	0.0	0.0
33	900	0.0	0.0	11.3
33	1000	0.0	0.0	11.3
33	1100	0.0	0.0	11.3
33	1200	0.0	0.0	7.2
33	1300	0.0	0.0	0.0
34	900	0.0	0.0	8.2
34	1000	0.0	0.0	8.2
34	1100	0.0	0.0	8.2
34	1200	0.0	0.0	6.2
34	1300	0.0	0.0	0.0

Table 6-3. The worst-case scenarios are incorporated here. Lethal combinations are shaded. The table is the same as Table 6-2, but air temperatures are increased 2ºC (due to local heating of the air), and irradiance values are increased by 200 W/m² (due to reflected sunlight). For example, the boxed value (see Table 6-2) now indicates that there were 3.1 hours when the air temperature exceeded 29ºC, the irradiance exceeded 1100 W/m², and the wind was less than 0.2 m/s.

6.4.4. Worst-Case Scenario

Two further effects may cause local conditions to be more severe than those measured at the weather station.

Reflected irradiance from the granite surface is potentially significant for fronds at the clump edge, because these fronds are exposed to irradiance from both the top and the bottom surfaces (Figure 6-2). Vertical reflected irradiance measured on March 27, 2006 was 100-300

W/m², when incident irradiance was 950 W/m² (measured at the angle of maximum incident irradiance, perpendicular to the sun's rays).

Furthermore, in the field, rock temperatures as high as 41 ºC have been measured (on April 26th, 2004), and under these conditions it is likely that the local air temperature is higher than the air temperature at the weather station, (which only reached 25.5ºC on April 26th, 2004). This effect was demonstrated in the wind tunnel by measuring air temperatures before and after air had flowed over a heated plate (Figure 6-10). For wind blowing at 0.25 m/s over a smooth heating plate 0.6 m square, the air temperature 5 cm above the downstream edge was 1 to 2 ºC hotter than air in the free stream.

The effects of reflected irradiance and locally increased air temperatures are shown in Table 6-3. This table is the same as Table 6-2, but air temperatures are increased 2 ºC, and irradiance values are increased by 200 W/m². Under these conditions, lethal temperatures were reached for a total of 4.1 hours during the 6 years of weather station data.

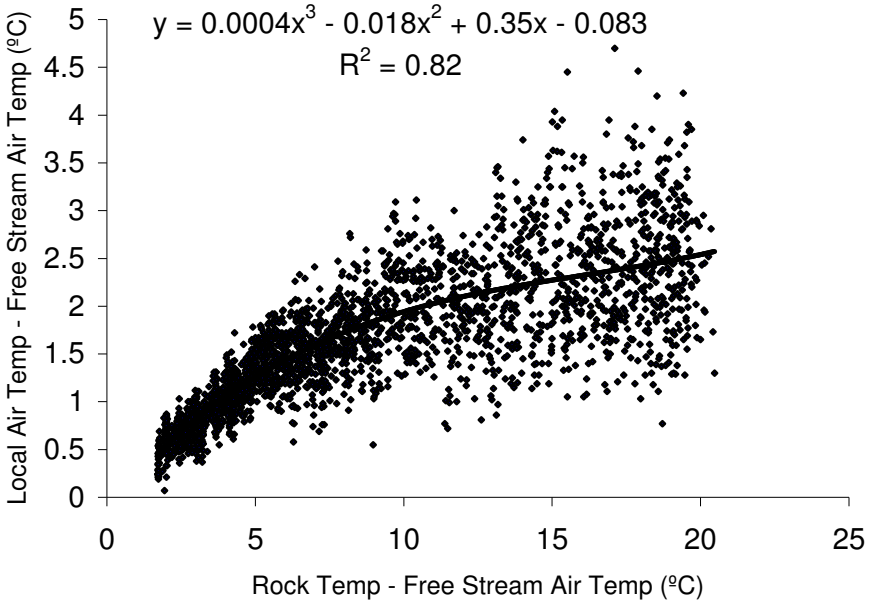

Figure 6-10. Local air temperature 5 cm above a heated plate is warmer than free stream air temperatures for a wind speed of 0.25 m/s. A cubic fit is shown.

6.5 Discussion

Both this model and the model of Bell (1995) indicate that wind speed is a primary determinant of thallus temperature. When the wind speed exceeds 1.4 m/s *Endocladia* never heats more than 3.5 ºC above the air temperature. For wind speeds greater than 1 m/s *Endocladia* remains cooler than air temperature until it is dried to a RWC of less than 25%, even under intense sunlight (S_{flux}=1000 W/m², RH=60%, Tair= 20 to 40 ºC).

Local relative humidity is also crucial, because RH is important in determining the drying rate, and therefore the amount of time that *Endocladia* is both wet and hot. This is likely a factor in the mortality seen in the center of larger clumps, because as air passes through the moist outer fronds it is humidified before it reaches the central fronds. Therefore the central portions of large clumps dry more slowly. This, in turn, potentially increases the time spent both wet and hot (Figure 6-8, Chapter 4).

The heat budget model indicates that small isolated clumps seldom reach lethal temperatures. This is the result of two conditions. First, when *Endocladia* is dry, its thermotolerance is higher than the equilibrium temperatures that thalli reach under the environmental conditions measured at Hopkins Marine Station. Second, during the time that thalli are at risk of experiencing wet-lethal temperatures, evaporative cooling prevents the thalli from heating. These results are perplexing. If small isolated clumps seldom reach lethal temperatures, then what causes the high mortality of small clumps (seen in Chapter 3), and why are these small clumps "rescued" by artificial shades?

One possibility is that the assumptions I made in correcting weather station data so that it represented intertidal weather conditions were inadequate. For example, if intertidal temperatures were 5ºC hotter than weather station temperatures (instead of the 2 ºC used in Table 6-3), lethal conditions would be much more frequent. However, the weather station data I used are some of the best available. Here the weather station was less than 100 m away from the field site, yet under crucial conditions of low wind speeds, the environmental data do not seem to represent conditions near the surface of intertidal rocks (e.g., wind speed is much greater at the weather station and weather station temperatures are likely cooler than air temperatures near hot intertidal rocks). Therefore, the next step in modeling

the temperatures of intertidal algae will require estimating local conditions from environmental data taken a substantial distance away.

Local calibration of weather station data is a simple solution in principle: A local weather station could be set-up in the intertidal zone at low tide, and the results correlated to the weather station on the bluff. Although this is a feasible project for commonly occurring environmental conditions, for rare environmental conditions (i.e., those likely to cause mortality), the calibration must take place on the same exceptional days when the model estimates lethal temperatures. In this case, the modeling approach would not provide any logistical advantage because if one could be in the field calibrating the weather station for local measurements, one could simply measure thallus temperatures directly and forego the model altogether.

A more generalizable solution would be to model how environmental conditions change near the rock surface under conditions of low wind speed. The low wind speed simplification is applicable because thalli do not heat substantially when it is windy, and at higher wind speeds the heated rock likely has less of an effect on local air temperatures as the air becomes more mixed.

In conclusion, this heat budget model predicts that isolated clumps will seldom experience thermally lethal conditions. Yet small clumps have been observed to bleach and die within a few months of thinning (Chapter 3). Perhaps high temperature is not the cause of mortality. On the other hand, the local conditions expected to induce mortality (very low wind speeds) are conditions when wind-driven mixing is low, and therefore site-specific heterogeneity is expected to be greatest. Under these conditions, local environmental variables in the *Endocladia* zone do not coincide with conditions estimated from a nearby weather station. This in turn severely limits the utility of this model. Further study of how conditions vary between the intertidal zone and nearby terrestrial weather stations is required.

COMPARING GLYNN'S SURVEYS WITH PHOTOGRAPHIC DATA

Peter Glynn's study of the *Endocladia-Balanus* association (1965) includes two lines of evidence which conflict with the photographic history I present in Figure 1-6. This is a problem for which there is no apparent solution, and the deeper one looks, the more perplexing the mystery becomes.

The facts:

1) Between 1959 and 1961 Glynn (figure 8 in Glynn 1965) surveyed the *Endocladia-Balanus* association 30 cm higher than I surveyed it in 2001 [and 30 cm higher than I surveyed it in 2005; I will refer to this level as the current elevation of the *Endocladia* upper limit. This change in upper limit was originally pointed out by Hopkins undergraduates Ashley Simons and Erin Leydig (1995.)] However, photographs taken by Glynn and others between 1959 and 1961 show that *Endocladia* was actually 30 cm *lower* than its current elevation (Figure 1-6.) Thus, there is an approximately 60 cm discrepancy between the change indicated by comparing surveyed elevations and the change shown in photographs.

2) All surveys were conducted from the same reference peg, so there has been no change in baseline elevation. Furthermore, In December, 2003, Glynn visited HMS, and confirmed that his definition of the upper limit of the *Endocladia-Balanus* association is similar to the upper limit of *Endocladia* I have measured. The upper limit of the association is not the highest *Balanus,* nor is it the highest absolute *Endocladia* clump. To re-create Glynn's measure of the upper limit of the *Endocladia-Balanus* association, one traces an imaginary line through the uppermost clumps of *Endocladia* within an arm's reach (~ 2 meters) of his permantly-marked pegs. This line marks the upper limit of the association at a particular site. I recreated Glynn's measure for 11 of his surveyed sites (Figure A1-1) and at all sites, his survey indicates the upper limit of *Endocladia* was higher circa 1959-1961 than it is currently.

This contradicts the photographic history in Figure 1-6, and again there is an approximately 60 cm discrepancy between the survey comparison and the photographic comparison.

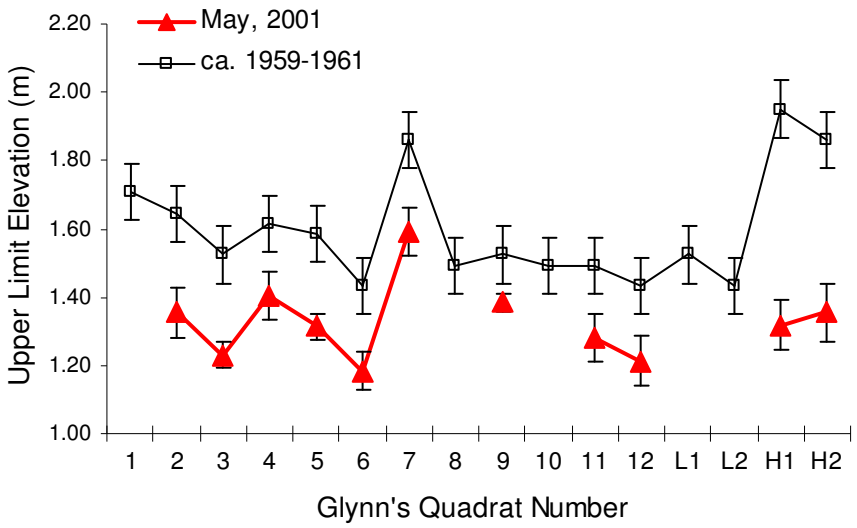

Figure A1-1. Surveys of the upper limit of *Endocladia* in 2001 and circa 1959-1961 (Glynn 1965) at the same locations. Elevations are relative to the peg in Glynn (1965) reported as 3.82 feet above MLLW. 2001 error bars are 1 SEM of the elevations of 10 of the highest clumps of *Endocladia* within 2 m of Glynn's pegs.

3) Glynn's sites were located below the upper limit of *Endocladia*, and he sampled substantial quantities of *Endocladia* from these sites. I have found 11 of the pegs marking Glynn's sites, and many of these pegs are currently above the upper limit of *Endocladia* (and therefore contain no *Endocladia*). Furthermore, many of these pegs were also above the upper limit as shown in Glynn's 1962 photograph. In 1962, Glynn precisely marked the location of his sites on an index photograph, and it is this carefully-marked photograph that shows the lack of *Endocladia* at the sampled sites. This is the crux of the mystery. Did the range shift downward 60 cm during the latter period of Glynn's study (between 1961 and 1962) and yet this range shift went unnoticed? Moreover Glynn's index sheet (figure 7 in Glynn 1965, see Figure

A1-2, below) is meticulously constructed, and it shows precisely marked sites that visibly lack *Endocladia*. Would the range shift not have been noticed during the construction of this figure?

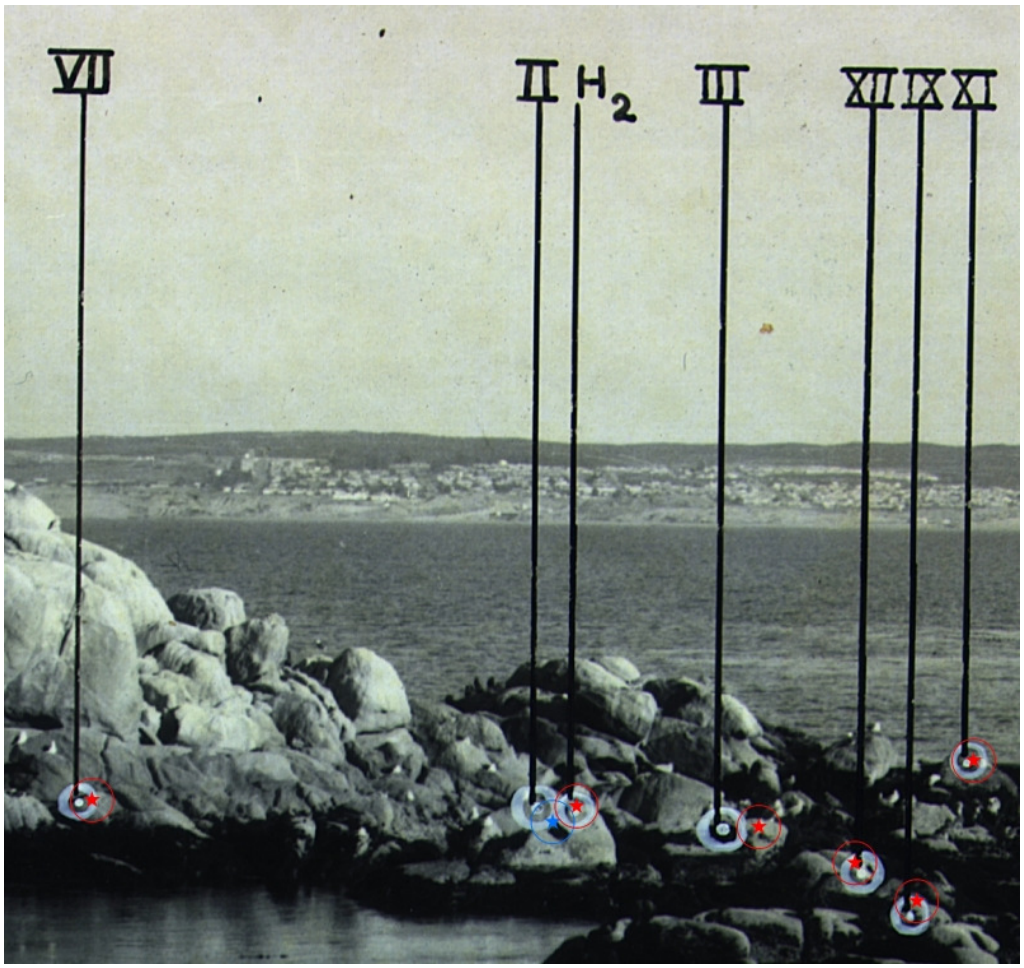

Figure A1-2. Detail from Glynn (1965) figure 7. Peg locations visible in the photographs are marked with a red star. Those that are not visible are marked in blue. Glynn's tracing of peg locations is quite accurate, and in many cases, the peg locations are above the upper limit. Did Glynn, who meticulously traced the locations of his quadrats onto this photograph overlook a 60 range shift that occurred during his study?

4) To make sure Glynn's site were actually visible in his index sheet (vs. the site being eclipsed behind a foreground rock), I re-created Glynn's photograph with people

placing their fingers atop Glynn's pegs. If I could see a person's fingertips, I knew the photograph showed Glynn's peg. Figure A1-2 shows Glynn's index photograph. The pegs that are visible in the photograph are indicated in red. The pegs were not in the center of the site. However, they were situated as close as possible to the sampling site, and at approximately the same elevation as the quadrat center (Peter Glynn pers. comm.) Figure A1-3 shows a re-survey of Glynn's pegs, compared to the published quadrat elevations. The consistency between the peg elevations and the quadrat elevations indicates that the pegs do indeed mark the elevation of the center of Glynn's sites.

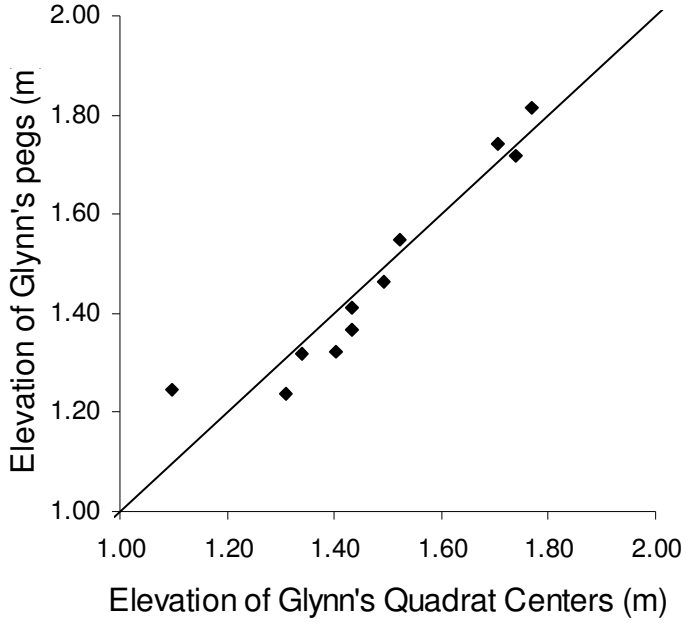

Figure A1-3. The elevations of Glynn's pegs surveyed in 2001 are plotted relative to the published elevations of the quadrat centers. Elevations are relative to the peg referenced in Glynn (1965) with a reported elevation of 3.82 feet above MLLW.

The conclusion:

Reconciling Glynn's survey with the photographic record requires a 60 cm upward shift in *Endocladia's* range, before the period of Glynn's sampling (1959-1961). Furthermore, an identical 60 cm downward shift is required between 1961 (the end of sampling) and 1962, when Glynn took the index photograph that marks his study sites. Neither of these shifts appear in the photographic record. And neither was noticed by Glynn. Is this possible?

Peter Glynn began a job in Puerto Rico in 1960, before he finished his dissertation, and between 1960 and 1962, friends sent samples to him in Puerto Rico. Glynn returned to Hopkins Marine Station in 1962 and defended in 1963. Glynn was not absolutely certain that he would have noticed a range shift that occurred during his absence. Thus it may be possible that 2 equal and opposite range shifts bracketed Glynn's study period. But Glynn and I both feel this is unlikely, given the photographic evidence. How then did Glynn sample *Endocladia,* if his quadrats were above the upper limit? That is the crux of this unsolved mystery. Because of these irreconcilable inconsistencies, I have chosen to rely solely on photographic evidence in reconstructing the history of *Endocladia's* upper limit.

REYNOLDS' ANALOGY

The Reynolds analogy quantitatively links convective heat and mass transfer for organisms in flowing fluid. The analogy is based on the similarity in form between the general equations governing heat and mass transfer, Fourier's law and Fick's law:

Fourier's Law $\frac{\dot{Q}_c}{A_c} = -B_c \frac{dT}{dx}$ (1)

Fick's Law $\frac{\dot{Q}_m}{A_m} = -B_m \frac{dM}{dx}$ (2)

Subscripts *c* and *m* denote convective heat transfer and mass transfer respectively. Heat flux is driven by the gradient in temperature $\frac{dT}{dx}$, and mass flux is driven by an analogous gradient in mass concentration $\frac{dM}{dx}$. Flux occurs at a rate proportional to the gradient, and proportionality constants B_c and B_m are termed the thermal conductance and the mass diffusivity, respectively. In discrete form Fourier's law is

$$\frac{\dot{Q}_c}{A_c} = B_c \frac{\Delta T}{\Delta x} \quad (3)$$

or, rearranging terms: $\dot{Q}_c = \frac{B_c}{\Delta x}(T_{air} - T_E)A_c$. (4)

When the length Δx is incorporated into a new transfer coefficient $h_c = \frac{B_c}{\Delta x}$, Fourier's law becomes Newton's Law of Cooling, presented earlier as the equation governing convective heat transfer:

$$\dot{Q}_c = h_c(T_{air} - T_E)A_c \quad . \qquad (5)$$

Similarly, in discrete form, Fick's law becomes the equation for mass transfer presented earlier:

$$\dot{m} = h_m(\rho_{air} - \rho_E)A_m \quad . \qquad (6)$$

Because h_c is the thermal conductance (B_c) divided by the length Δx, the thermal conductance in flow equals $h_c \Delta x$. The arbitrary length Δx is usually taken to be a characteristic length L of the object (such as its diameter, if spherical). The thermal conductance in flow, $h_c L$, divided by the thermal conductance in still air is the dimensionless number known as the Nusselt number.

$$Nu = \frac{h_c L}{k_{air}} . \qquad (7)$$

Similarly, the mass diffusivity in flow ($B_m = h_m L$) divided by the mass diffusivity in still air is known as the Sherwood number.

$$Sh = \frac{h_m L}{D_{wv}} . \qquad (8)$$

Thus the Nusselt and Sherwood numbers represent dimensionless rate ratios. That is, they indicate how much transfer rates are increased by flow, beyond what occurs in still air. Reynold's analogy asserts that, since these processes proceed via the same mechanism of molecular collisions, the increases due to flow should be the same. That is, the Nusselt and Sherwood numbers should be *the same*. Equating *Nu* and *Sh* results in an equation that relates the heat an mass transfer coefficients:

$$\frac{h_c}{h_m} = \frac{k_{air}}{D_{wv}} \quad . \qquad (9)$$

Defining the thermal diffusivity as the thermal conductance divided by the rate of thermal storage $\alpha_{air} = \frac{k_{air}}{\rho_{air} C_{pAir}}$, and substituting for k_{air}, noting that $\frac{\alpha_{air}}{D_{wv}}$ is the Lewis number encountered earlier,

$$\frac{h_c}{h_m} = \rho_{air} C_{pAir} \frac{\alpha_{air}}{D_{wv}} = \rho_{air} C_{pAir} Le . \qquad (10)$$

This is Reynolds' analogy.

Up until now we have assumed that the distance scales over which heat and mass transfer occur are equal. However, this is not always the case. Heat and mass transfer are boundary layer processes. Therefore the thickness of the associated boundary layer (the thermal boundary layer for heat transfer, the concentration boundary layer for mass transfer) defines the proper distance scale. Reynolds was unaware of this scale inequality because his work predated Prandtl's boundary layer concept (Jakob and Hawkins 1957), and a significant improvement to Reynolds' analogy is possible once it is recognized that the concentration boundary layer and the thermal boundary layer are not always of equal thickness. Before the dimensionless rate ratios can be equated (eq. 9) they must be normalized, so they operate at the same scales, across the same distance.

Two dimensionless numbers are important for describing relative boundary layer thicknesses. The Prandtl number represents the relative thicknesses of the velocity boundary layer and the thermal boundary layer:

$$Pr = \frac{\upsilon}{\alpha}, \qquad (11)$$

where υ equals the kinematic viscosity.

Similarly the Schmidt number represents the relative thicknesses of the velocity boundary layer and the concentration boundary layer:

$$Sc = \frac{\upsilon}{D_{wv}}. \qquad (12)$$

Again, we see the importance of the Lewis number: $Le = \frac{Sc}{Pr}$; that is, *Le* is a measure of the relative thermal and concentration boundary layer thicknesses.

If *Nu* and *Sh* are normalized to their relative boundary thicknesses [raised to a power *n* for generality, see a text on dimensional analysis such as Bridgman's (1963) classic], the result is a modified Reynold's analogy:

$$\frac{Nu}{Pr^n} = \frac{Sh}{Sc^n} \qquad (13)$$

which after substitution becomes $\frac{h_c}{h_m} = \frac{k_{air}}{D_{wv} Le^n}$ or upon further substituting of α_{air} for k_{air}:

$$\frac{h_c}{h_m} = \rho_{air} C_{pAir} Le^{1-n} \qquad (14)$$

under most conditions $n = \frac{1}{3}$ (Incropera and DeWitt 2002) and this becomes the Chilton-Colburn analogy:

$$\frac{h_c}{h_m} = \rho_{air} C_{pAir} Le^{\frac{2}{3}} \qquad (15)$$

which I used to determine the mass transfer coefficient from the easily-measured heat transfer coefficient.

REFERENCES

Abbott, I. A., and G. J. Hollenberg. 1976. *Marine Algae of California*. Stanford Univesity Press, Stanford.

Alpert, P. 2000. The discovery, scope, and puzzle of desiccation tolerance in plants. *Plant Ecology* 151: 5-17.

Alpert, P. 2005. The limits and frontiers of desiccation-tolerant life. *Integrative and Comparative Biology* 45: 685-695.

Alpert, P., and M. J. Oliver. 2002. Drying without dying. Pages 3-43 in M. Black and H. Pritchard, eds. CAB International, Wallingford, UK.

Barry, J. P., C. H. Baxter, R. D. Sagarin, and S. E. Gilman. 1995. Climate-Related, Long-Term Faunal Changes in a California Rocky Intertidal Community. *Science* 267: 672-675.

Beach, K. S., and C. M. Smith. 1997. Ecophysiology of a tropical rhodophyte III: Recovery from emersion stresses in *Ahnfeltiopsis concinna* (J. Ag.) Silva et DeCew. *Journal of Experimental Marine Biology and Ecology* 211: 151-167.

Bell, E. C. 1992. Consequences of morphological variation in an intertidal macroalga: physical constraints on growth and survival of *Mastocarpus papillatus*. Ph.D. Stanford University, Stanford.

Bell, E. C. 1995. Environmental and morphological influences on thallus temperature and desiccation of the intertidal alga Mastocarpus papillatus Kutzing. *Journal of Experimental Marine Biology and Ecology* 191: 29-55.

Bella, D. A., R. Jacobs, and H. Li. 1994. Ecological indicators of global climate change: A research framework. *Environmental Management* 18: 489-500.

Biebl, R. 1972. Temperature resistance of marine algae. Pages 23-28 in K. Nisizawa, ed. *Proceedings of the Seventh International Seaweed Symposium. Sapporo Japan*. Halstead Press, New York.

Bird, R. B., W. E. Stewart, and E. N. Lightfoot. 1960. *Transport Phenomena*. John Wiley and Sons, Inc., New York.

Bolhàr-Nordenkampf, H. R., and Öquist. 1993. Chlorophyll fluorescence as a tool in photosynthesis research. Pages 193-206 in D. O. Hall, H. R. Scurlock, H. R. Bolhàr-

Nordenkampf, R. C. Leegood, and L. S.P., eds. *Photosynthesis and Production in a Changing Environment: a field and laboratory manual*. Chapman and Hall, London.

Bridgman, P. W. 1963. *Dimensional analysis*. Yale University Press, New Haven,.

Britting, S. A. 1992. Effects of Emergence on the Physiology and Biochemistry of a High Intertidal Alga, *Endocladia muricata*. Ph.D. University of California, Los Angeles, Los Angeles.

Britting, S. A., and D. J. Chapman. 1993. Physiological comparison of the isomorphic life history phases of the high intertidal alga *Endocladia muricata* (Rhodophyta). *Journal of Phycology* 29: 739-745.

Brown, J. H., G. C. Stevens, and D. M. Kaufman. 1996. The geographic range: size, shape, boundaries and internal structure. *Annual Review of Ecology and Systematics* 27: 597-623.

Caffey, H. M. 1985. Spatial and Temporal Variation in settlement and recruitment of intertidal barnacles. *Ecological Monographs* 55: 313-332.

Campbell, G. S., and J. M. Norman. 1998. *An Introduction to Environmental Biophysics*. Springer, New York.

Cannon, R. H. 1967. *Dynamics of Physical Systems*. McGraw-Hill, New York.

Carefoot , T. 1977. *Pacific Seashores*. University of Washington Press, North Vancouver.

Caughley, G., D. Grice, R. Barker, and B. Brown. 1988. The edge of the range. *Journal of Animal Ecology* 57: 771-786.

Connell, J. H. 1961. The Influence of interspecific competition and other factors on the distribution of the barnacle *Chthamalus stellatus*. *Ecology* 42: 710-723.

Connell, J. H. 1985. The consequences of variation in initial settlement vs. postsettlement mortality in rocky intertidal communities. *Journal of Experimental Marine Biology and Ecology* 93: 11-45.

Connell, J. H., T. P. Hughes, C. C. Wallace, J. E. Tanner, K. E. Harms, and A. M. Kerr. 2004. A long-term study of competition and diversity of corals. *Ecological Monographs* 74:179-210

Crowe, J. H., J. F. Carpenter, and L. M. Crowe. 1998. The role of vitrification in anhydrobiosis. *Annual Review of Physiology;* v.60; p.73-103.

Crowe, J. H., F. A. Hoekstra, and L. M. Crowe. 1992. Anhydrobiosis. *Annual Review of Phsiology* 54: 579-599.

Davis, A. J., L. S. Jenkinson, J. H. Lawton, B. Shorrocks, and S. Wood. 1998. Making mistakes when predicting shifts in species range in response to global warming. *Nature* 391: 783-786.

Davison, I. R., and G. A. Pearson. 1996. Stress tolerance in intertidal seaweeds. *Journal of Phycology*: 197-211.

Dayton, P. K. 1971. Competition disturbance and community organization the provision and subsequent utilization of space in a rocky intertidal community. *Ecological Monographs* 41: 351-389.

Dennis, B. 2002. Allee effects in stochastic populations. *Oikos* 96: 389-401.

Denny, M. W., and C. D. G. Harley. in press. Hot limpets: predicting body temperature in a conductance-mediated thermal system. *Journal of Experimental Biology 209*.

Denny, M.W., L.P. Miller and C. D. G. Harley. in press. Thermal stress on intertidal limpets: long-term hindcasts and lethal limits. *Journal of Experimental Biology 209*.

Denny, M. W., and R. T. Paine. 1998. Celestial mechanics, sea-level changes and intertidal ecology. *Biological Bulletin* 194: 108-115.

Doty, M. S. 1946. Critical tide factors that are correlated with the vertical distributions of marine algae and other organisms along the pacific coast. *Ecology* 27: 315-328.

Dring, M. J., and F. A. Brown. 1982. Photosynthesis of intertidal brown algae during and after periods of emersion: a renewed search fo physiological causes of zonation. *Marine Ecology Progress Series* 8: 301-308.

Dromgoole, F. I. 1980. Desiccation resistance in inter-tidal and subtidal algae. *Botanica Marina* 23: 149-159.

Druehl, L. D., and J. M. Green. 1982. Vertical distribution of intertidal seaweeds as related to patterns of submersion and emersion. *Marine Ecology Progress Series* 9: 163-170.

Dye, A. H. 1998. Community-level analyses of long-term changes in rocky littoral fauna from South Africa. *Marine Ecology Progress Series* 164: 47-57.

Estes, J. A., and D. O. Duggins. 1995. Sea otters and kelp forests in Alaska: Generality and variation in a community ecological paradigm. *Ecological Monographs* 65: 75-100.

Estes, J. A., and J. F. Palmisan. 1974. Sea Otters: Their role in structuring nearshore communities. *Science* 185: 1058-1060.

Farrell, T. M. 1991. Models and mechanisms of succession: an example from a rocky intertidal community. *Ecological Monographs* 61: 95-113.

Finney, D. J. 1964. *Probit Analysis*. Cambridge University Press, Cambridge.

Fitzhenry, T., P. M. Halpin, and B. Helmuth. 2004. Testing the effects of wave exposure, site, and behavior on intertidal mussel body temperatures: applications and limits of temperature logger design. *Marine Biology* 145: 339-349.

Foster, M. S., E. W. Nigg, L. M. Kiguchi, D. D. Hardin, and J. S. Pearse. 2003. Temporal variation and succession in an algal-dominated high intertidal assemblage. *Journal of Experimental Marine Biology and Ecology* 289: 15-39.

Francis, R. C., S. R. Hare, A. B. Hollowed, and W. S. Wooster. 1998. Effects of interdecadal climate variability on the oceanic ecosystems of the NE Pacific. *Fisheries Oceanography* 7: 1-21.

Gaff, J. L. 1997. Mechanisms of desiccation tolerance in ressurection vascular plants. Pages 43-58 in A. S. Basra and R. K. Basra, eds. *Mechanisms of environmental stress resistance in plants*. Harwood Academic Publishers, London.

Gardner, M. 1970. Mathematical games: the fantastic combinations of John Conway's new solitare game "life". *Scientific American* 223: 120-123.

Gaston, K. J., and S. L. Chown. 1999. Elevation and climatic tolerance: A test using dung beetles. *Oikos* 86: 584-590.

Gates, D. M. 1980. *Biophysical ecology*. Springer-Verlag, New York.

Geankoplis, C. J. 1993. *Transport processes and unit operations*. Prentice Hall, Englewood Cliffs, N.J.

Gislen, T. 1943. *Physiographical and ecological investigations concerning the littoral of the northern Pacific*. Hakan Ohlssons Boktryckeri, Lund.

Glynn, P. 1965. Ecological studies on the *Endocladia muricata-Balanus glandula* association in the intertidal zone in Monterey Bay, California. *Beaufortia* 12: 1-198.

Gurney, W. S. C., and J. H. Lawton. 1996. The population dynamics of ecosystem engineers. *Oikos* 76: 273-283.

Hanski, I. 1998. Metapopulation dynamics. *Nature (London)* 396: 41-49.

Harley, C. D. G., and B. S. Helmuth. 2003. Local- and regional-scale effects of wave exposure, thermal stress, and absolute versus effective shore level on patterns of intertidal zonation. *Limnology and Oceanography* 48: 1498-1508.

Hawkins, S. J., and R. G. Hartnoll. 1985. Factors determining the upper limits of intertidal canopy-forming algae. *Marine Ecology Progress Series* 20: 265-272.

Hay, M. E. 1981. The functional morphology of turf forming seaweeds: persistence in stressful marine habitats. *Ecology* 62: 739-750.

Helmuth, B., C. D. G. Harley, P. M. Halpin, M. O'Donnell, G. E. Hofmann, and C. A. Blanchette. 2002. Climate change and latitudinal patterns of intertidal thermal stress. *Science* 298: 1015-17.

Helmuth, B. S. T. 1998. Intertidal mussel microclimates: Predicting the body temperature of a sessile invertebrate. *Ecological Monographs* 68: 51-74.

Helmuth, B. S. T., and G. E. Hofmann. 2001. Microhabitats, thermal heterogeneity, and patterns of physiological stress in the rocky intertidal zone. *Biological Bulletin* 201: 374-384.

Hodgson, L. M. 1981. Photosynthesis of the red alga *Gastroclonium coulteri* (Rhodophyta) in response to changes in temperature, light intensity and desiccation. *Journal of Phycology* 17: 37-42.

Hoekstra, F. A., E. A. Golovina, and J. Buitink. 2001. Mechanisms of plant desiccation tolerance. *Trends in Plant Science* 6: 431-438.

Holling, C. S. 1973. Resilience and stability of ecological systems. *Annual Review of Ecology and Systematics*. 4:1-23.

Holt, R. D., and T. H. Keitt. 2005. Species' borders: a unifying theme in ecology. *Oikos* 108: 3-6.

Holt, R. D., T. H. Keitt, M. A. Lewis, B. A. Maurer, and M. L. Taper. 2005. Theoretical models of species' borders: single species approaches. *Oikos* 108: 18-27.

Incropera, F. P., and D. P. DeWitt. 2002. *Fundamentals of Heat and Mass Transfer*. John Wiley and Sons, New York.

Jakob, M., and G. A. Hawkins. 1957. *Elements of Heat Transfer*. Wiley, New York,.

Kanwisher, J. 1957. Freezing and drying in intertidal algae. *Biological Bulletin* 113: 275-285.

Keener, J. P. 1987. Propagation and its failure in coupled systems of discrete excitable elements. *SIAM Journal of Applied Mathematics* 47: 556-572.

Keitt, T. H., M. A. Lewis, and R. D. Holt. 2001. Allee effects, invasion pinning, and species' borders. *American Naturalist* 157: 203-216.

Kenyon, K. W. 1969. *The Sea Otter in the Eastern Pacific Ocean*. U.S. Bureau of Sport Fisheries and Wildlife; Washington, D.C.

Keough, M. J. 1983. Patterns of recruitment of sessile invertebrates in two subtidal habitats. *Journal of Experimental Marine Biology and Ecology* 66: 213-246.

Kimura, M., and G. H. Weiss. 1964. The Stepping Stone Model of Population Structure and the Decrease of Genetic Correlation with Distance. *Genetics* 49: 561-576.

Kinlan, B. P., and A. Hastings. 2005. Rates of population spread and geographic range expansion: what exotic species tell us. Pages 381-419 in D. F. Sax, J. J. Stachowicz, and S. D. Gaines, eds. *Species invasions: insights into ecology, evolution and biogeography*. Sinauer Associates, Sunderland, MA.

Kondjoyan, A., and J. D. Daudin. 1993. Determination of transfer coefficients by psychrometry. *International Journal of Heat and Mass Transfer* 36: 1807-1818.

Kovnat, G. D. 1982. *Intertidal foraging by the southern sea otter, Enhydra lutris*. M.Sc. Stanford University, Stanford.

Laurance, W. F., R. K. Didham, and M. E. Power. 2001. Ecological boundaries: a search for synthesis. *Trends in Ecology and Evolution* 16: 70-71.

Lebedev, P. D. 1961. Heat and mass transfer between moist solids and air. *International Journal of Heat and Mass Transfer* 1: 302-305.

Lee, R. E. 1999. *Phycology*. Cambridge University Press, Cambridge.

Leopold, A. C. 1986. *Membranes, metabolism, and dry organisms*. Comstock Pub. Associates, Ithaca.

Levin, S. A. 1974. Dispersion and population interactions. *American Naturalist* 108: 207-228.

Levine, J. D., P. Funes, H. B. Dowse, and J. C. Hall. 2002. Signal analysis of behavioral and molecular cycles. *BMC Neuroscience* 3: 1-25.

Lewis, M. A., and P. Kareiva. 1993. Allee dynamics and the spread of invading organisms. *Theoretical Population Biology* 43: 141-158.

Luning, K. 1990. *Seaweeds: Their Environment, Biogeography and Ecophysiology*. Wiley, New York.

Matta, J. L., and D. J. Chapman. 1995. Effects of light, temperature and desiccation on the net emersed productivity of the intertidal macroalga *Colpomenia peregrina* Sauv. (Hamel). *Journal of Experimental Marine Biology and Ecology* 189: 13-27.

May, R. M. 1977. Thresholds and breakpoints in ecosystems with a multiplicity of stable states. *Nature* 269: 471-7.

Menconi, M., L. Benedetti-Cecchi, and F. Cinelli. 1999. Spatial and temporal variability in the distribution of algae and invertebrates on rocky shores in the northwest Mediterranean. *Journal of Experimental Marine Biology and Ecology* 233: 1-23.

Monteith, J. L. 1973. *Principles of Environmental Physics*. Edward Arnold, London.

Munda, I. M. 2000. Long-term marine floristic changes around Rovinj (Istrian coast, North Adriatic) estimated on the basis of historical data from Paul Kuckuck's field diaries from the end of the 19th century. *Nova Hedwigia* 71: 1-36.

Nobel, P. S. 1999. *Physicochemical & environmental plant physiology*. Academic Press, San Diego.

Northcraft, R. D. 1946. Colonization of Bare Rock Surfaces by Marine Algae. Ph.D. Stanford University, Stanford.

Oates, B. R., and S. N. Murray. 1983. Photosynthesis dark respiration and desiccation resistance of the intertidal seaweeds *Hesperophycus-harveyanus and Pelvetia fastigiatia F-gracilis*. *Journal of Phycology* 19: 371-380.

Okubo, A. 1980. *Diffusion and ecological problems : mathematical models*. Springer-Verlag, Berlin ; New York.

Paine, R. T., and S. A. Levin. 1981. Intertidal landscapes: Disturbance and the dynamics of pattern. *Ecological Monographs* 51: 145-178.

Parmesan, C., S. Gaines, L. Gonzalez, D. M. Kaufman, J. Kingsolver, A. Townsend Peterson, and R. Sagarin. 2005. Empirical perspectives on species borders: from traditional biogeography to global change. *Oikos* 108: 58-75.

Pena, E. J., R. Zingmark, and C. Nietch. 1999. Comparative photosynthesis of two species of intertidal epiphytic macroalgae on mangrove roots during submersion and emersion. *Journal of Phycology* 35: 1206-1214.

Rascio, N., and N. La Rocca. 2005. Resurrection plants: The puzzle of surviving extreme vegetative desiccation. *Critical Reviews in Plant Sciences* 24: 209-225.

Reed, D. C., D. R. Laur, and A. W. Ebeling. 1988. Variation in algal dispersal and recruitment: the importance of episodic events. *Ecological Monographs* 58: 321-336.

Ricketts, E. F., J. Calvin, J. W. Hedgpeth, and D. W. Phillips. 1985. *Between Pacific Tides.* Stanford University Press, Stanford, CA.

Robitaille, P. M. 2003. On the validity of Kirchhoff's law of thermal emission. *IEEE Transactions on Plasma Science* 31: 1263- 1267.

Rothschild, L. J., and R. L. Mancinelli. 2001. Life in extreme environments. *Nature* 409: 1092-101.

Roughgarden, J., S. Gaines, and H. Possingham. 1988. Recruitment dynamics in complex life cycles. *Science* 241: 1460-1466.

Sagarin, R. D., J. P. Barry, S. E. Gilman, and C. H. Baxter. 1999. Climate-related change in an intertidal community over short and long time scales. *Ecological Monographs* 69: 465-490.

Sakai, A. K., F. W. Allendorf, J. S. Holt, D. M. Lodge, J. Molofsky, K. A. With, S. Baughman, R. J. Cabin, J. E. Cohen, N. C. Ellstrand, D. E. McCauley, P. O'Neil, I. M. Parker, J. N. Thompson, and S. G. Weller. 2001. The population biology of invasive species. *Annual Review of Ecology and Systematics* 32: 305-332.

Schoenbeck, M., and T. A. Norton. 1978. Factors controlling the upper limits of fucoid algae on the shore. *Journal of Experimental Marine Biology and Ecology* 31: 303-314.

Schreiber, U., W. Schliwa, and U. Bilger. 1986. Continuour recording of photochemical and quenching with a new type of modulation fluorimeter. *Photosynthesis Research* 10: 51-62.

Schroder, A., L. Persson, and A. M. De Roos. 2005. Direct experimental evidence for alternative stable states: a review. *Oikos* 110: 3-19.

Scrosati, R., and R. E. DeWreede. 1998. The impact of frond crowding on frond bleaching in the clonal intertidal alga *Mazzaella cornucopiae* (Rhodophyta, Gigartinaceae) from British Columbia, Canada. *Journal of Phycology* 34: 228-232.

Simons, A., and E. Leydig. 1996. Long term changes in the *Endocladia-Balanus* community at Hopkins Marine Station, Pacific Grove,CA. Pages 1-24. Unpublished manuscripts on file at Hopkins Marine Station Library.

Slayter, R. D. 1967. *Plant-Water Relationships.* Academic Press, London.

Smith, C. M., and J. A. Berry. 1986. Recovery of photosynthesis after exposure of intertidal algae to osmotic and temperature stresses: Comparative studies of species with differing distributional limits. *Oecologia* 70: 6-12.

Stenseng, E., C. E. Braby, and G. N. Somero. 2005. Evolutionary and acclimation-induced variation in the thermal limits of heart function in congeneric marine snails (genus *Tegula*): implications for vertical zonation. *Biological Bulletin* 208: 138-144.

Stephenson, T. A., and A. Stephenson. 1949. The universal features of zonation between tidemarks on rocky coasts. *Journal of Ecology* 37: 289-&.

Stephenson, T. A., and A. Stephenson. 1972. *Life Between Tidemarks on Rocky Shores*. W.H. Freeman and Co, San Francisco.

Stillman, J. H., and G. N. Somero. 2000. A comparative analysis of the upper thermal tolerance limits of eastern Pacific porcelain crabs, genus *Petrolisthes*: Influences of latitude, vertical zonation, acclimation, and phylogeny. *Physiological and Biochemical Zoology* 73: 200-208.

Sun, S.-H., and T. R. Marrero. 1996. Experimental study of simultaneous heat and moisture transfer around single short porous cylinders during convection drying by a psychrometry method. *International Journal of Heat and Mass Transfer* 39: 3559-3565.

Tait, R. V., and F. Dipper. 1998. *Elements of Marine Ecology*. Butterworth Heinemann, Oxford.

Taylor, C. M., H. G. Davis, J. C. Civille, F. S. Grevstad, and A. Hastings. 2004. Consequences of an Allee effect in the invasion of a pacific estuary by Spartina alterniflora. *Ecology* 85: 3254-3266.

Taylor, P. R., and M. E. Hay. 1984. Functional morphology of intertidal seaweeds: Adaptive significance of aggregate vs. solitary forms. *Marine Ecology Progress Series* 18: 295-302.

Terborgh, J. 1971. Distribution on Environmental Gradients Theory and a Preliminary Interpretation of Distributional Patterns in the Avi Fauna of the Cordillera Vilcabamba Peru. *Ecology* 52: 23-40.

Thom, R. 1975. *Structural stability and morphogensis; an outline of a general theory of models*. W. A. Benjamin, Reading, Mass.

Tirado, R., and F. I. Pugnaire. 2005. Community structure and positive interactions in constraining environments. *Oikos* 111: 437-444.

Tomanek, L., and B. Helmuth. 2002. Physiological ecology of rocky intertidal organisms: A synergy of concepts. *Integrative and Comparative Biology* 42: 771-775.

Tomanek, L., and G. N. Somero. 1999. Evolutionary and acclimation-induced variation in the heat-shock responses of congeneric marine snails (genus *Tegula*) from different thermal habitats: Implications for limits of thermotolerance and biogeography. *Journal of Experimental Biology* 202: 2925-2936.

Tomanek, L., and G. N. Somero. 2002. Interspecific- and acclimation-induced variation in levels of heat-shock proteins 70 (hsp70) and 90 (hsp90) and heat-shock transcription factor-1 (HSF1) in congeneric marine snails (genus Tegula): Implications for regulation of hsp gene expression. *Journal of Experimental Biology* 205: 677-685.

Underwood, A. J. 1978. A refutation of critical tidal levels as determinants of the structure of intertidal communities on British shores. *Journal of Experimental Marine Biology and Ecology* 33: 261-276.

Via, S. 2001. Sympatric speciation in animals: The ugly duckling grows up. *Trends in Ecology and Evolution* 16: 381-390.

Walker, B., and J. A. Meyers. 2004. Thresholds in ecological and social-ecological systems: a developing database. *Ecology and Society* 9.

Walther, G.-R., E. Post, P. Convey, A. Menzel, C. Parmesan, T. J. C. Beebee, J.-M. Fromentin, O. Hoegh-Guldberg, and F. Bairlein. 2002. Ecological responses to recent climate change. *Nature (London)* 416: 389-395.

Warren, M. S., J. K. Hill, J. A. Thomas, J. Asher, R. Fox, B. Huntley, D. B. Roy, M. G. Telfer, S. Jeffcoate, P. Harding, G. Jeffcoate, S. G. Willis, J. N. Greatorex-Davies, D. Moss, and C. D. Thomas. 2001. Rapid responses of British butterflies to opposing forces of climate and habitat change. *Nature* 414: 65-69.

Weast, R. C., D. R. Lide, and Chemical Rubber Company. 1978. *CRC Handbook of Chemistry and Physics*. CRC Press, Boca Raton, Fl.

Wethey, D. S. 2002. Biogeography, competition, and microclimate: The barnacle *Chthamalus fragilis* in New England. *Integrative and Comparative Biology* 42: 872-880.

Williams, S. L., and M. N. Dethier. 2005. High and dry: Variation in net photosynthesis of the intertidal seaweed Fucus gardneri. *Ecology* 86: 2373-2379.

Wilson, J. B., and A. D. Q. Agnew. 1992. Positive feedback switches in plant communities. *Advances in Ecological Research* 23: 263-336.

Wilson, W. G., and R. M. Nisbet. 1997. Cooperation and competition along smooth environmental gradients. *Ecology* 78: 2004-2017.

Wilson, W. G., R. M. Nisbet, A. H. Ross, C. Robles, and R. A. Desharnais. 1996. Abrupt population changes along smooth environmental gradients. *Bulletin of Mathematical Biology* 58: 907-922.

Woodward, D. L. 1988. Unbalanced gametophyte:sporophyte ratios in populations of the intertidal red alga *Endocladia muricata* in central California. Ph. D. UCLA, Los Angeles.

Woolfenden, J. 1979. *The California Sea Otter, Saved or Doomed?* Boxwood Press, Pacific Grove, CA.

Zar, J. H. 1999. *Biostatistical Analysis*. Prentice Hall, Upper Saddle River, NJ.